Quantifying the Effectiveness of Infectious Disease Interventions in Heterogeneous Populations

by

Kate Bubar

M.S., University of Colorado Boulder, 2022

B.S., Colorado School of Mines, 2019

A thesis submitted to the

Faculty of the Graduate School of the

University of Colorado in partial fulfillment

of the requirements for the degree of

Doctor of Philosophy

Department of Computer Science

2024

Committee Members:

Prof. Daniel Larremore, Chair

Prof. Elizabeth Bradley

Dr. Katelyn Gostic

Prof. Stephen Kissler

Prof. Nathan Lo

Bubar, Kate (Ph.D., Computer Science)

Quantifying the Effectiveness of Infectious Disease Interventions
in Heterogeneous Populations

Thesis directed by Prof. Daniel Larremore

During the COVID-19 pandemic, many questions arose about the effectiveness, necessity, and duration of interventions implemented to mitigate the transmission of SARS-CoV-2. For instance, limited initial supply of SARS-CoV-2 vaccine raised the question of how to prioritize available doses. In this thesis, I quantify the effectiveness of vaccination and testing policies using mathematical models to address these types of questions. Using SEIR-type mechanistic models, I investigate SARS-CoV-2 transmission dynamics in terms of age and immune status. By analyzing the cumulative number of simulated infections and deaths under different vaccination prioritization strategies, I demonstrate that prioritizing adults aged 60+ for initial COVID-19 vaccine doses minimizes mortality, and this strategy is robust across countries, transmission rates, vaccination rollout speeds, and estimates of infection-acquired immunity. I use a similar modeling approach to evaluate the effectiveness of unvaccinated-only testing programs in mixed-immunity populations, finding their effectiveness generally limited and dependent on population immunity, non-pharmaceutical interventions, and participation. Lastly, using a probabilistic model that incorporates within-host viral kinetics and theory from stochastic processes, I evaluate the potential effectiveness of screening travelers with molecular tests. This project considers screening for SARS-CoV-2 as well as influenza A, SARS-CoV-1, and Ebola to evaluate the potential effectiveness of these screening programs in general. I demonstrate how, for any pathogen or test, traveler screening is fundamentally limited by the amount of time before infection and detectability. The overarching goals for this thesis are to further our understanding of transmission dynamics and the role of targeted interventions in light of individual variation in susceptibility and infectiousness, and to evaluate and inform relevant public health policies.

Dedication

To my parents.

Acknowledgements

I would like to thank my thesis committee—Liz Bradley, Stephen Kissler, Katie Gostic, Nathan Lo, and Dan Larremore—for their invaluable support and mentorship. Special thanks to my advisor Dan, who has taught me so much about science and what it means to be a good scientist. Thank you for always advocating for me and opening so many doors for me over the past five years. Thanks also to Dan, Stephen, and Katie for the countless hours of thoughtful and interesting discussions, mixed with lightheartedness and laughter. You all made research fun and exciting, and that is a beautiful thing.

To my other academic mentors and friends: Scott Strong, for sparking my initial passion for applied math; Cecilia Diniz Behn, Karin Leiderman, and Deb Carney, for being wonderful and caring role models who inspired me to pursue graduate school; and the Larremore lab members, for making the lab such a fun and friendly space. Special thanks to Casey Middleton, my academic sister, whose strength, wit, creativity, and resilience constantly inspire me. Thank you for teaching me how to stand for myself. To everyone in the IQ Biology program and SFI's CSSS, for showing me the beauty of interdisciplinary research.

There are many loved ones whose support has been invaluable to me throughout this journey. I would like to especially thank Meag for teaching me how to reach my fullest potential, Will for believing in me even when I didn't believe in myself, the Oasis volleyball community for being a much-needed outlet away from everything that is grad school, and my grandma for her steadfast love. To my best friends—Julia, Olivia, Corey, Kianna, Dani, Erica, and Allegra—and my siblings, Max and Sara, thank you for always being there for me through all the craziness. Lastly, to my parents, thank you for always encouraging me to dream big and offering unwavering support through this, and every, endeavor.

Contents

Chapter

Tables

Table

Figures

Figure

Chapter 1

Introduction

The ongoing COVID-19 pandemic has profoundly impacted global public health, economies, and daily life, prompting unprecedented interventions and adaptations worldwide. Quick, clear, and well-motivated decision-making on the policies shaping these interventions has been of the utmost importance, particularly in the initial phases when resources were extremely limited. To inform such decision-making, mathematical models of infectious disease dynamics have been commonly used, along with economic analyses and ethical reasoning. The use of such models in this context is not new: mechanistic models have been used for decades to make predictions about the effectiveness of possible disease control measures and "bridge the gap between clinical trials and population-level use" [1]. However, the modern contexts, emerging pathogen, and sophisticated new technologies have required new models and analysis that are appropriately calibrated, validated, and communicated [2]. This thesis delves into the effectiveness of different interventions using mathematical modeling to address a variety of policy-related questions that arose during the pandemic. Not only was this work motivated by the pressing questions of the times that are interesting scientific questions per se, but it was also completed in a timely manner in order to inform the policies put into practice.

1.1 Chronicle of the COVID-19 pandemic

1.1.1 Timeline

The first documented cases of COVID-19 trace back to Wuhan, China at the end of 2019. The virus spread quickly in the beginning of 2020, first around China and neighboring countries, and then around the world. By March, there were over 100,000 confirmed global cases in over 100 countries, and, on March 11, 2020, the World Health Organization officially declared COVID-19 a pandemic. In the U.S., cases initially peaked in late March and early April, then started to rise once again in July and August. The number of cases of COVID-19 worldwide peaked in January 2021 following holiday gatherings and the emergence of more transmissible variants like Alpha. Following the cyclical patterns like that of many other respiratory viruses, global case counts have subsequently peaked thus far in April 2021, August 2021, January 2022, July 2022, and December 2022 [3]. On May 5, 2023, the WHO declared that COVID-19 is no longer a public health emergency of international concern, given that the disease was by then well established and trending downward [4]. However, as of June 2024, the WHO has not yet declared the pandemic officially over . Cases continue to occur widely, and, according to the CDC, there were nearly as many hospitalizations in the U.S. in January 2024 from COVID-19 as in January 2023 [5]. According to the WHO COVID-19 dashboard, there have been 776 million cases of COVID and 7.1 million deaths due to COVID-19 worldwide to date [3].

1.1.2 Interventions

While many different interventions have been implemented to control the spread of SARS-CoV-2 during the COVID-19 pandemic, I will focus this section on the interventions that pertain to Chapters 2-4: vaccines, vaccinate-or-test policies, and traveler screening programs.

1.1.2.1 Vaccines

On January 11, 2020, just two days after the sequence of SARS-CoV-2 became available, the NIH and Moderna began collaborating on the design of a vaccine. By April 2020, there were over 100 vaccines

in development worldwide [6]. In December 2020, within a year since the identification of this novel virus, the Pfizer/BioNTech and Moderna vaccines were among the first to receive emergency use authorization (EUA) by regulatory agenecies like the FDA in the U.S. and the EMA in Europe [7]. Vaccination programs promptly began worldwide, often prioritizing healthcare workers, the elderly, and those with underlying health conditions first. In the U.S., by June 2021 57% of people in the U.S. over 18 had received 1 or more COVID-19 vaccine doses, significantly reducing severe illness, hospitalizations and deaths [8]. Although there were significant disparities in the distribution of initial vaccines worldwide, the COVAX initiative played a critical role in facilitating access to COVID-19 vaccines around the world, especially in low- and middle-income nations. Variants of concern, such as Delta and Omicron, challenged the effectiveness of vaccination and follow up booster campaigns began in September 2021.

1.1.2.2 Vaccinate-or-test Policies

In the U.S., following the widespread availability of vaccines, different vaccination requirements were implemented by local governments, companies, and universities to enable the safe return to in-person activities. One such policy, referred to as vaccinate-or-test, required individuals to either be fully vaccinated or undergo testing, often once per week. In September 2021, the Biden administration announced that this type of policy would be federally mandated for companies with over 100 employees, but it ended up being blocked by the U.S. Supreme Court in January 2022 [9]. However, different institutions continued to implement this type of requirement, with the duration and implementation details varying widely between settings.

1.1.2.3 Traveler Screening Programs

Several countries, including the U.S., began screening travelers from Wuhan and other parts of China in January 2020, shortly after cases were reported outside of China. Screenings early in the pandemic often included temperature checks and health questionnaires. By April 2020, many countries had implemented more comprehensive traveler screening programs, in addition to mandatory quarantine, testing upon arrival, and tracking systems for incoming travelers. In the summer of 2020, some countries began requiring proof

of a negative COVID-19 test before departure or upon arrival. By the end of 2020, more countries adopted pre-travel testing requirements, either via rapid or PCR tests. Generally, either PCR testing was required within 24 to 74 hours days of before departure or rapid test at departure or upon arrival from October 2021 to June 2022 [10].

1.2 Goals

I have two overarching goals for this thesis. First, I aim to deepen scientific knowledge of the role of individual variation in infectious disease transmission, with a strong focus on SARS-CoV-2, and targeted interventions based on such variation. Some of the heterogeneities considered in this thesis include differences in susceptibility and infectiousness due to age, immune status, behavior, and pathogen load. The second goal of this thesis is to use the results from the first goal to identify specific and realistic recommendations for public health policy. Additionally, I hope this thesis demonstrates the importance and applicability of interdisciplinary science. My work relies on ideas from a plethora of fields, including complex systems, statistics, probability, scientific computing, virology, immunology, and epidemiology. I believe training in different disciplines enables creative research projects, and is necessary to achieve my two goals.

1.3 Outline

In **Chapter 2**, I explore how best to prioritize the initial doses of COVID-19 vaccines using a deterministic, age-stratified, SEIR-type model, that was developed during the summer and fall of 2020 before the approval of the first COVID-19 vaccine. At the time, it was unknown how efficacious the vaccine would be against infection, transmission, and severe disease, or how many doses would initially be available. With light of these unknown parameters, as well as ongoing questions about SARS-CoV-2 transmission and immunity, I explore how sensitive the best vaccine prioritization is to different population, vaccine, disease, and distribution parameters as well as different objective functions (e.g., minimizing mortality versus cumulative infections).

In the summer and fall of 2021, these vaccinate-or-test policies were considered by many govern-

ments, companies, and schools to safely return to in-person activities. However, the decision to implement these policies rarely considered the degree of population immunity. In **Chapter 3**, I introduce a model to demonstrate how transmission dynamics change under different assumptions of population immunity, depending on the circulating variant and the amount of vaccine-derived or infection-acquired immunity. I then use this model to evaluate the effectiveness of unvaccinated-only testing programs for COVID-19 under different outbreak and testing scenarios.

Throughout the first two years of the pandemic, different types of traveler screening programs were implemented in countries around the world. The use of molecular testing in screening programs seemed to offer better performance than symptom- or questionnaire-based screening due to the increased sensitivity and ability to detect asymptomatic infections with no known exposure. In **Chapter 4**, I explore the potential effectiveness of using molecular tests to screen people at airports during emerging infectious disease outbreaks for various pathogens.

Chapter 2

Model-informed COVID-19 vaccine prioritization strategies by age and serostatus

Portions of this chapter are adapted from:

K.M. Bubar, K. Reinholt, S. M. Kissler, M. Lipsitch, S. Cobey, Y. Grad, and D.B. Larremore. *Model-informed COVID-19 vaccine prioritization strategies by age and serostatus.* Science. 371: 916-921, 2021.

2.1 Introduction

SARS-CoV-2 has caused a public health and economic crisis worldwide. As of January 2021, there have been over 85 million cases and 1.8 million deaths reported [11]. To combat this crisis, a variety of non-pharmaceutical interventions have been implemented, including shelter-in-place orders, limited travel, and remote schooling. While these efforts are essential to slowing transmission in the short term, long-term solutions—such as vaccines that protect from SARS-CoV-2 infection—remain urgently needed. The benefits of an effective vaccine for individuals and their communities have resulted in widespread demand, so it is critical that decision-making on vaccine distribution is well motivated, particularly in the initial phases when vaccine availability is limited [12].

Here, we employ a model-informed approach to quantify the impact of COVID-19 vaccine prioritization strategies on cumulative incidence, mortality, and years of life lost. Our approach explicitly addresses variation in three areas that can influence the outcome of vaccine distribution decisions. First, we consider variation in the performance of the vaccine, including its overall efficacy, a hypothetical decrease in efficacy

by age, and the vaccine's ability to block transmission. Second, we consider variation in both susceptibility to infection and the infection fatality rate by age. Third, we consider variation in the population and policy, including the age distribution, age-stratified contact rates, and initial fraction of seropositive individuals by age, and the speed and timing of the vaccine's rollout relative to transmission. While the earliest doses of vaccines will be given to front-line health care workers under plans such as those from the COVAX initiative and the US NASEM recommendations [13], our work is focused on informing the prioritization of the doses that follow. Based on regulatory approvals and initial vaccine rollout speeds of early 2021, our investigation focuses generally on scenarios with a partially mitigated pandemic (R between 1.1 and 2.0), vaccines with protective efficacy of 90%, and rollout speeds of 0.2% of the population per day.

There are two main approaches to vaccine prioritization: (1) directly vaccinate those at highest risk for severe outcomes and (2) protect them indirectly by vaccinating those who do the most transmitting. Model-based investigations of the tradeoffs between these strategies for influenza vaccination have led to recommendations that children be vaccinated due to their critical role in transmission [14, 15] and have shown that direct protection is superior when reproduction numbers are high but indirect protection is superior when transmission is low [16]. Similar modeling for COVID-19 vaccination has found that the optimal balance between direct and indirect protection depends on both vaccine efficacy and supply, recommending direct vaccination of older adults for low-efficacy vaccines and for high-efficacy but supply-limited vaccines [17]. Rather than comparing prioritization strategies, others have compared hypothetical vaccines, showing that even those with lower efficacy for direct protection may be more valuable if they also provide better indirect protection by blocking transmission [18]. Prioritization of transmission-blocking vaccines can also be dynamically updated based on the current state of the epidemic, shifting prioritization to avoid decreasing marginal returns [19]. These efforts to prioritize and optimize doses complement other work showing that, under different vaccine efficacy and durability of immunity, the economic and health benefits of COVID-19 vaccines will be large in the short and medium terms [20]. The problem of vaccine prioritization also parallels the more general problem of optimal resource allocation to reduce transmission, e.g. with masks [21].

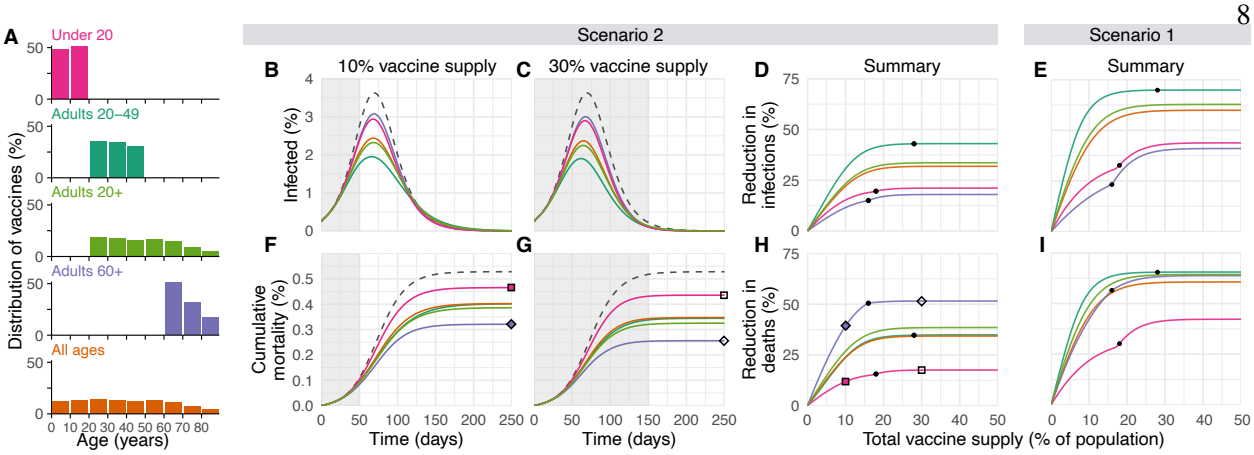

Figure 2.1: **Impacts of vaccine prioritization strategies on mortality and infections.** (A) Distribution of vaccines for five prioritization strategies: under 20, adults 20-49, adults 20+, adults 60+ and all ages. (B, C) Example simulation curves show percentage of the total population infected over time and (F, G) cumulative mortality for no vaccines (grey dashed lines) and for five different prioritization strategies (colored lines matching panel A), with 10% (B, F) and 30% (C, G) vaccine supply. Summary curves show percent reductions in (D, E) infections and (H, I) deaths in comparison to an unmitigated outbreak for vaccine supplies between 1% and 50% after 365 days of simulation. Squares and diamonds show how the outputs from single simulations (F, G) correspond to points in summary curves (H). Grey shading indicates period during which vaccine is being rolled out at 0.2% of total population per day. Black dots indicate breakpoints at which prioritized demographic groups have been 70% vaccinated, after which vaccines are distributed without prioritization. These simulations assume contact patterns and demographics of the United States [32,33] and an all-or-nothing, transmission-blocking vaccine with 90% vaccine efficacy and $R_0 = 1.5$ (Scenario 2) and $R_0 = 1.15$ (Scenario 1).

2.2 Results

2.2.1 Evaluation of vaccine prioritization strategies

We evaluated the impact of vaccine prioritization strategies using an age-stratified SEIR model, because age has been shown to be an important correlate of susceptibility [22–24], seroprevalence [22, 25], severity [26–28], and mortality [29,30]. This model includes an age-dependent contact matrix, susceptibility to infection, and infection fatality rate (IFR), allowing us to estimate cumulative incidence of SARS-CoV-2 infections, mortality due to infection, and years of life lost (YLL; see Methods) via forward simulations of one year of disease dynamics. Cumulative incidence, mortality, and YLL were then used as outcomes by which to compare vaccine prioritization strategies. These comparisons may be explored using accompanying open-source and interactive calculation tools that accompany this study [31].

We first examined the impact of five vaccine prioritization strategies for a hypothetical infection- and transmission-blocking vaccine of varying efficacy. The strategies prioritized vaccines to (1) children and teenagers, (2) adults between ages 20 and 49 years, (3) adults 20 years or older, (4) adults 60 years or older, and (5) all individuals (Fig. 3.1A). In all strategies, once the prioritized population was vaccinated, vaccines were allocated irrespective of age, i.e. in proportion to their numbers in the population. To incorporate vaccine hesitancy, at most 70% of any age group was eligible to be vaccinated [34].

We measured reductions in cumulative incidence, mortality, and YLL achieved by each strategy, varying the vaccine supply between 1% and 50% of the total population, under two scenarios. In Scenario 1, vaccines were administered to 0.2% of the population per day until supply was exhausted, with $R_0 = 1.15$, representing highly mitigated spread during vaccine rollout. In Scenario 2, vaccines were administered to 0.2% of the population per day until supply was exhausted, but with $R_0 = 1.5$, representing substantial viral growth during vaccine rollout (see Fig. 3.1 for example model outputs). Results for additional scenarios in which vaccines were administered before transmission began are described in the Online Supplementary Text, corresponding to countries without ongoing community spread such as South Korea and New Zealand. We considered two ways in which vaccine efficacy (ve) could be below 100%: an all-or-nothing vaccine, where the vaccine provides perfect protection to a fraction ve of individuals who receive it, or as a leaky vaccine, where all vaccinated individuals have reduced probability ve of infection after vaccination (see Methods).

Of the five strategies, direct vaccination of adults over 60 years (60+) always reduced mortality and YLL more than the alternative strategies when transmission was high ($R_0 = 1.5$; Scenario 2; 90% efficacy, Fig. 3.1; 30%-100% efficacy, Online Supp. Fig. S5). For lower transmission ($R_0 = 1.15$; Scenario 1), vaccination of adults 20-49 reduced mortality and YLL more than the alternative strategies, but differences between prioritization of adults 20-49, adults 20+, and adults 60+ were small for vaccine supplies above 25% (Figs. 3.1 and Online Supp. Fig. S5). Prioritizing adults 20-49 minimized cumulative incidence in both scenarios for all vaccine efficacies (Figs. 3.1 and Online Supp. Fig. S5). Prioritizing adults 20-49 also minimized cumulative incidence in both scenarios under alternative rollout speeds (0.05% to 1% vaccinated

per day; Online Supp. Fig. S6 When rollout speeds were at least 0.3% per day and vaccine supply covered at least 25% of the population, the mortality minimizing strategy shifted from prioritization of ages 20-49 to adults 20+ or adults 60+ for Scenario 1; when rollout speeds were at least 0.75% per day and covered at least 24% of the population, the mortality minimizing strategy shifted from prioritization of adults 60+ to adults 20+ or 20-49 for Scenario 2 (Online Supp. Fig. S6). Findings for mortality and YLL were only slightly changed by modeling vaccine efficacy as all-or-nothing (Online Supp. Fig. S5) or leaky (Online Supplemental Figure S7).

2.2.2 Impact of transmission rates, age demographics, and contact structure

To evaluate the impact of transmission rates on the strategy that most reduced mortality, we varied the basic reproductive number R_0 from 1.1 to 2.0 when considering a hypothetical infection- and transmission-blocking vaccine with 90% vaccine efficacy. We found that prioritizing adults 60+ remained the best way to reduce mortality and YLL for $R_0 \geq 1.3$, but prioritizing adults 20-49 was superior for $R_0 \leq 1.2$ (Fig. 3.3A, B and Online Supp. Fig. S8). Prioritizing adults 20-49 minimized infections for all values of R_0 investigated (Online Supp. Fig. S8).

To determine whether our findings were robust across countries, we analyzed the ranking of prioritization strategies for populations with the age distributions and modeled contact structures of the United States, Belgium, Brazil, China, India, Poland, South Africa, and Spain. Across these countries, direct vaccination of adults 60+ minimized mortality for all levels of vaccine supply when transmission was high ($R_0 = 1.5$, Scenario 2; Fig. 3.3E), but in only some cases when transmission was lower ($R_0 = 1.15$, rollout 0.2% per day, Scenario 1; Fig. 3.3D). Decreasing rollout speed from 0.2% to 0.1% per day caused prioritization of adults 60+ to be favored in additional scenarios (Fig. 3.3C). Across countries, vaccination of adults 20-49 nearly always minimized infections, and vaccination of adults 60+ nearly always minimized YLL for Scenario 2, but no clear ranking of strategies emerged consistently to minimize YLL in Scenario 1 (Online Supp. Fig. S9).

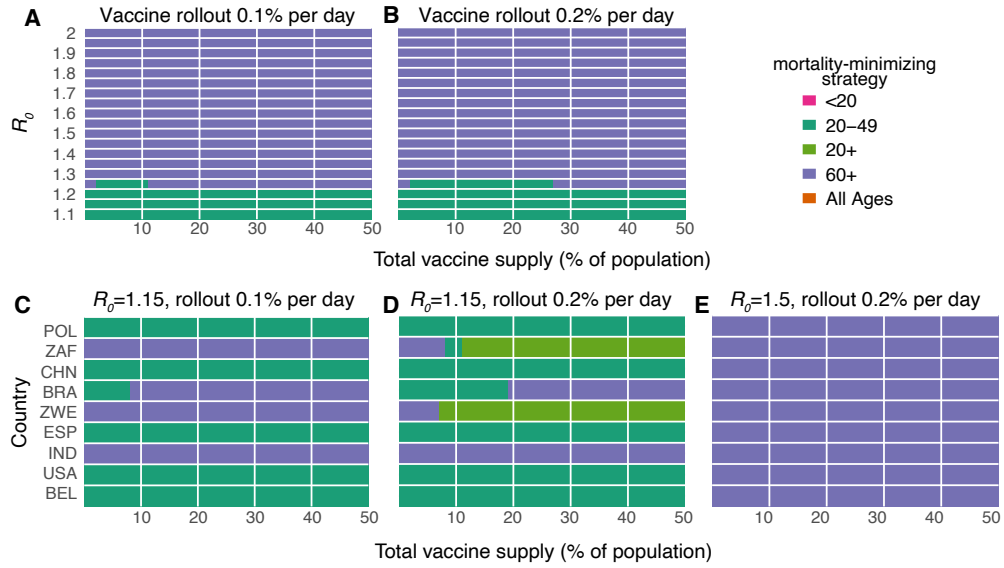

Figure 2.2: **Mortality-minimizing vaccine prioritization strategies across reproductive numbers $\mathbf{R_0}$ and countries.** Heatmaps show the prioritization strategies resulting in maximum reduction of mortality for varying values of the basic reproductive number R_0 (A, B) and across nine countries (C, D, E), for vaccine supplies between 1% and 50% of the total population, for an all-or-nothing and transmission blocking vaccine, 90% vaccine efficacy. (A, B) Shown: contact patterns and demographics of the United States [32, 33]; (C, D, E) Shown: contact patterns and demographics of POL, Poland; ZAF, South Africa; CHN, China; BRA, Brazil; ZWE, Zimbabwe; ESP, Spain; IND, India; USA, United States of America; BEL, Belgium, with R_0 and rollout speeds as indicated.

2.2.3 Vaccines with imperfect transmission blocking effects

We also considered whether the rankings of prioritization strategies to minimize mortality would change if a vaccine were to block COVID-19 symptoms and mortality with 90% efficacy but with variable impact on SARS-CoV-2 infection and transmission. We found that direct vaccination of adults 60+ minimized mortality for all vaccine supplies and transmission-blocking effects under Scenario 2, and for all vaccine supplies when up to 50% of transmission was blocked in Scenario 1 (Online Supplementary Text and Fig. S10) .

2.2.4 Variation in vaccine efficacy by age

COVID-19 vaccines may not be equally effective across age groups in preventing infection or disease, a phenomenon known to affect influenza vaccines [35–38]. To understand the impact of age-dependent

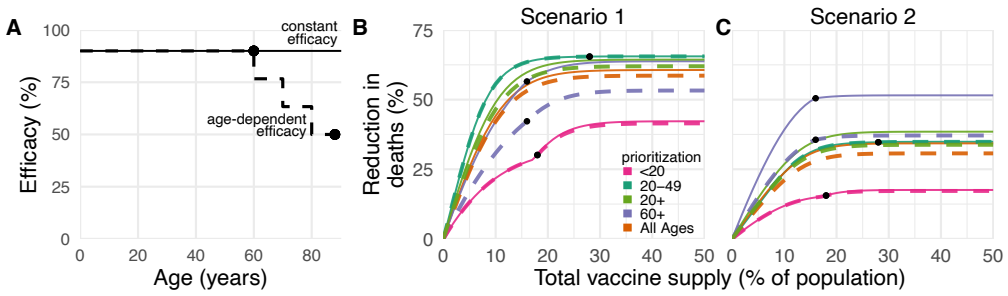

Figure 2.3: **Effects of age-dependent vaccine efficacy on the impacts of prioritization strategies.** (A) Diagram of hypothetical age-dependent vaccine efficacy shows decrease from 90% baseline efficacy to 50% efficacy among individuals 80+ beginning at age 60 (dashed line). (B, C) Percent reduction in deaths in comparison to an unmitigated outbreak for transmission-blocking all-or-nothing vaccines with either constant 90% efficacy for all age groups (solid lines) or age-dependent efficacy shown in panel A (dashed lines), covering Scenario 1 (0.2% rollout/day, $R_0 = 1.15$; B) and Scenario 2 (0.2% rollout/day, $R_0 = 1.5$; C). Black dots indicate breakpoints at which prioritized demographic groups have been 70% vaccinated, after which vaccines are distributed without prioritization. Shown: contact patterns and demographics of the United States [32, 33]; all-or nothing and transmission blocking vaccine.

COVID-19 vaccine efficacy, we incorporated a hypothetical linear decrease from a baseline efficacy of 90% for those under 60 to 50% in those 80 and older (Fig. 3.4). As expected, this diminished the benefits of any prioritization strategy that included older adults. For instance, strategies prioritizing adults 20-49 were unaffected by decreased efficacy among adults 60+, while strategies prioritizing adults 60+ were markedly diminished (Fig. 3.4). Despite these effects, prioritization of adults 60+ remained superior to the alternative strategies to minimize mortality in Scenario 2.

To test whether more substantial age-dependent vaccine effects would change which strategy minimized mortality in Scenario 2, we varied the onset age of age-dependent decreases in efficacy, the extent to which it decreased, and the baseline efficacy from which it decreased. We found that as long as the age at which efficacy began to decrease was 70 or older and vaccine efficacy among adults 80+ was at least 25%, prioritizing adults 60+ remained superior in the majority of parameter combinations. This finding was robust to whether the vaccine was modeled as leaky vs all-or-nothing, but we observed considerable variation from country to country (Online Supp. Fig. S11).

2.2.5 Incorporation of population seroprevalence and individual serological testing

Due to early indications that naturally acquired antibodies correlate with protection from reinfection [39], seroprevalence will affect vaccine prioritization in two ways. First, depending on the magnitude and age distribution of seroprevalence at the time of vaccine distribution, the ranking of strategies could change. Second, distributing vaccines to seropositive individuals would reduce the marginal benefit of vaccination per dose.

To investigate the impact of vaccinating mid-epidemic while using serology to target the vaccine to seronegative individuals, we included age-stratified seroprevalence estimates in our model by moving the data-specified proportion of seropositive individuals from susceptible to recovered status. We then simulated two approaches to vaccine distribution. In the first, vaccines were distributed according to the five prioritization strategies introduced above, regardless of any individual's serostatus. In the second, vaccines were distributed with a serological test, such that individuals with a positive serological test would not be vaccinated, allowing their dose to be given to someone else in their age group.

We included age-stratified seroprevalence estimates from New York City [August 2020; overall seroprevalence 26.9% [40]] and demographics and age-contact structure from the United States in evaluations of the previous five prioritization strategies. For this analysis, we focused on Scenario 2 (0.2% rollout per day, $R = 1.5$ inclusive of seropositives), and found that the ranking of strategies to minimize incidence, mortality, and YLL remained unchanged: prioritizing adults 60+ most reduced mortality and prioritizing adults 20-49 most reduced incidence, regardless of whether vaccination was limited to seronegative individuals (Fig. 3.5). These rankings were unchanged when we used lower or higher age-stratified seroprevalence estimates to test the consistency of results (Connecticut, July 2020, overall seroprevalence 3.4% [41] and synthetic, overall seroprevalence 39.5%; Online Supp. Figs. S12 and S13). Despite lowered sensitivity to detect past exposure due to seroreversion [42, 43], preferentially vaccinating seronegative individuals yielded large additional reductions in cumulative incidence and mortality in locations with higher seroprevalence (Figs. 3.5 and Online Supp. Fig. S13) and modest reductions in locations with low seroprevalence

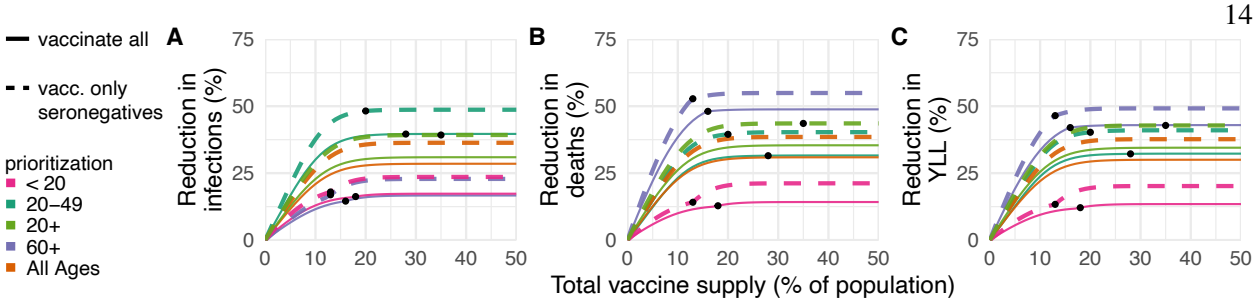

Figure 2.4: **Effects of existing seropositivity on the impacts of prioritization strategies.** Percent reductions in (A) infections, (B) deaths, and (C) years of life lost (YLL) for prioritization strategies when existing age-stratified seroprevalence is incorporated [August 2020 estimates for New York City; mean seroprevalence 26.9% [40]]. Plots show reductions for Scenario 2 (0.2% rollout/day, $R = 1.5$) when vaccines are given to all individuals (solid lines) or to only seronegatives (dashed lines), inclusive of 96% serotest sensitivity, 99% specificity [45], and approximately three months of seroreversion [42] (see Methods). Shown: U.S. contact patterns and demographics [32,33]; all-or-nothing and transmission-blocking vaccine with 90% vaccine efficacy. See Online Supp. Figs. S12 and S13 for lower and higher seroprevalence examples, respectively.

(Online Supp. Fig. S12). These results remained unchanged when statistical uncertainty, due to sample size and imperfect test sensitivity and specificity, were incorporated into the model [44].

2.3 Discussion

This study demonstrated the use of an age-stratified modeling approach to evaluate and compare vaccine prioritization strategies for SARS-CoV-2. After accounting for country-specific age structure, age-contact structure, infection fatality rates, and seroprevalence, as well as the age-varying efficacy of a hypothetical vaccine, we found that across countries those aged 60 and older should be prioritized to minimize deaths, assuming a return to high contact rates and pre-pandemic behavior during or after vaccine rollout. This recommendation is robust because of the dramatic differences in IFR by age. Our model identified three general regimes in which prioritizing adults aged 20-49 would provide greater mortality benefits than prioritizing older adults. One such regime was in the presence of substantial transmission-mitigating interventions ($R_0 = 1.15$) and a vaccine with 80% or higher transmission blocking effects. A second regime was characterized by substantial transmission-mitigating interventions ($R_0 = 1.15$) and either rollout speeds of at most 0.2% per day or vaccine supplies of at most 25% of the population. The third regime was character-

ized by vaccines with very low efficacy in older adults, very high efficacy in younger adults, and declines in efficacy starting at age 59 or 69. The advantage of prioritizing all adults or adults 20-49 vs. adults 60+ was small under these conditions. Thus, we conclude that for mortality reduction, prioritization of older adults is a robust strategy that will be optimal or close to optimal to minimize mortality for virtually all plausible vaccine characteristics.

In contrast, the ranking of infection-minimizing strategies for mid-epidemic vaccination led to consistent recommendations to prioritize adults 20-49 across efficacy values and countries. For pre-transmission vaccination, prioritization shifted toward children and teenagers for leaky vaccine efficacies 50% and below, in line with prior work [17], as well as for vaccines with weak transmission-blocking properties. Because a vaccine is likely to have properties of both leaky and all-or-nothing models, empirical data on vaccine performance could help resolve this difference in model recommendations, although data are difficult to obtain in practice [see, e.g. [46, 47]].

It is not yet clear whether the first-generation of COVID-19 vaccines will be approved everywhere for the elderly or those under 18 [48–50]. While our conclusions assumed that the vaccine would be approved for all age groups, the evaluation approaches introduced here can be tailored to evaluate a subset of approaches restricted to those within the age groups for which a vaccine is licensed, using open-source tools such as those that accompany this study [31]. Furthermore, while we considered three possible goals of vaccination—minimizing cumulative incidence, mortality, or YLL—our framework can be adapted to consider goals such as minimizing hospitalizations, ICU occupancy [17] or economic costs [20].

We demonstrated that there is value in pairing individual-level serological tests with vaccination, even when accounting for the uncertainties in seroprevalence estimates [44] and seroreversion [42]. The marginal gain in effective vaccine supply, relative to no serological testing, must be weighed against the challenges of serological testing prior to vaccination. Serostatus itself is an imperfect indicator of protection, and the relationship of prior infection, serostatus, and protection may change over time [20, 39, 42, 43]. Delays in serological tests results would impair vaccine distribution, but partial seronegative-targeting effects might

be realized if those with past PCR-confirmed infections voluntarily deprioritized their own vaccinations.

The best performing strategies depend on assumptions about the extent of a population's interactions. We used pre-pandemic contact matrices [32], reflecting the goal of a return to pre-pandemic routines once a vaccine is available, but more recent estimates of age-stratified contact rates could be valuable in modeling mid-pandemic scenarios [51, 52]. Whether pre-pandemic or mid-pandemic contact estimates are representative of contact patterns during vaccine rollout remains unknown and may vary based on numerous social, political, and other factors. The scenarios modeled here did not incorporate explicit non-pharmaceutical interventions, which might persist if vaccination coverage is incomplete, but are implicitly represented in Scenario 1 ($R_0 = 1.15$).

Our study relies on estimates of other epidemiological parameters. In local contexts, these include age-structured seroprevalence and IFR, which vary by population [29, 30, 53]. Globally, key parameters include the degree to which antibodies protect against reinfection or severity of disease and relative infectiousness by age. From vaccine trials, we also need evidence of efficacy in groups vulnerable to severe outcomes, including the elderly. Additionally, it will be critical to measure whether a vaccine that protects against symptomatic disease also blocks infection and transmission of SARS-CoV-2 [54].

The role of children during this pandemic has been unclear. Under our assumptions about susceptibility by age, children are not the major drivers of transmission in communities, consistent with emerging evidence [22]. Thus, our results differ from the optimal distribution for influenza vaccines, which prioritize school-age children and adults age 30-39 [15]. However, the relative susceptibility and infectiousness of SARS-CoV-2 by age remain uncertain. While it is unlikely that susceptibility to infection conditional on exposure is constant across age groups [22], we ran our model to test the sensitivity of this parameter. Under the scenario of constant susceptibility by age, vaccinating those under 20 has a greater impact on reducing cumulative cases than those 20-49 (Online Supp. Fig. S14 and S15).

Our study is subject to a number of limitations. First, our evaluation strategy focuses on a single country at a time, rather than on between-population allocation [55]. Second, we only consider variation

in disease severity by age. However, other factors correlate with disease outcomes, such as treatment and healthcare access and comorbidities, which may correlate with factors like rural vs urban location, socioeconomic status, sex [56, 57], and race and ethnicity [58], that are not accounted for in this study. Inclusion of these factors in a model would be possible, but only with statistically sound measurements of both their stratified infection risk, contact rates, and disease outcomes. Even in the case of age stratification, contact surveys have typically not surveyed those 80 years and older, yet it is this population that suffers dramatically more severe COVID-19 disease and higher infection fatality rates. We extrapolated contact matrices to those older than 80, but direct measurements would be superior. Last, our study focused on guiding strategy rather than providing more detailed forecasting or estimates [20]. As such, we have not made detailed parameter fits to time series of cases or deaths, but rather have used epidemiologic models to identify robust strategies across a range of transmission scenarios.

Our study also considers variation in disease risk only by age, via age-structured contact matrices and age-specific susceptibility, while many discussions around COVID-19 vaccine distribution have thus far focused on prioritizing healthcare or essential workers [59, 60]. Contact rates, and thus infection potential, vary greatly not only by occupation and age but also by living arrangement (e.g., congregate settings, dormitories), neighborhood and mobility [61–64], and whether the population has a coordinated and fundamentally effective policy to control the virus. With a better understanding of population structure during the pandemic, and risk factors of COVID-19, these limitations could be addressed. Meanwhile, the robust findings in favor of prioritizing those age groups with the highest IFR to minimize mortality could potentially be extended to prioritize those with comorbidities that predispose them to a high IFR, since the strategy of prioritizing the older age groups depends on direct rather than indirect protection.

Vaccine prioritization is not solely a question of science but a question of ethics as well. Hallmarks of the COVID-19 pandemic, as with other global diseases, are inequalities and disparities. While these modeling efforts focus on age and minimizing incidence and death within a simply structured population, other considerations are crucial, from equity in allocation between countries to disparities in access to healthcare, including vaccination, that vary by neighborhood. Thus, the model's simplistic representation of vulner-

ability (age) should be augmented by better information on the correlates of infection risk and severity. Fair vaccine prioritization should avoid further harming disadvantaged populations. We suggest that, after distribution, pairing serological testing with vaccination in the hardest hit populations is one possible equitable way to extend the benefits of vaccination in settings where vaccination might otherwise not be deemed cost-effective.

2.4 Materials and Methods

2.4.1 Susceptible Exposed Infectious Recovered (SEIR) Model Overview

We used a continuous-time ordinary differential equations (ODE) compartmental model stratified by age. Across all model variations and analyses, we simulated 365 days of dynamics, corresponding to the first-year phase of vaccine prioritization. All individuals were assumed to be initially susceptible, unless they had been effectively vaccinated or had naturally acquired immunity, which was considered to be protective in this model. Susceptible people (S) transition to the exposed state (E) after contact with an infectious individual. After a latent period, exposed individuals become infectious (I). After an infectious period, individuals move to a recovered state (R) or die. We assume that recovered individuals are no longer infectious and are immune to reinfection over the duration of simulations (up to 365 days). The duration of time spent in compartments E and I, in expectation, are specified in Table **??**. Model equations were solved using *lsoda* ODE solver from the package *deSolve*, R version 3.6.0 [65]. Fig. 2.5 shows model schematic diagrams for the variations of the SEIR model considered in this manuscript.

The force of infection, λ_i for a susceptible individual in age group i is

$$\lambda_i = u_i \sum_j c_{ij} \frac{I_j + I_{vj} + I_{xj}}{N_j - \Omega_j},$$

where u_i is the probability of a successful transmission given contact with an infectious individual and c_{ij} is the number of age-*j* individuals that an age-*i* individual contacts per day. The term $(I_j + I_{vj} + I_{xj})/(N_j - \Omega_j)$ is the probability that a random age-j individual is infectious, where I_j is the number of individuals who

are unvaccinated and infectious, I_{vj} is the number of individuals who are vaccinated yet infectious, I_{xj} is the number of individuals who are ineligible for vaccination (e.g. due to hesitancy or due to a positive serological test) and infectious, N_j is the total number of individuals in group j and Ω_j is the number of individuals from group j who have died. To calculate the basic reproductive number, R_0, we define the next-generation matrix as

$$M = D_u C D_{d_I},$$

where D_u is a diagonal matrix with diagonal entries u_i, C is the country-specific contact matrix, and D_{d_I} is a diagonal matrix with diagonal entries d_I, the infectious period. R_0 is the absolute value of the dominant eigenvalue of M. Age-stratified susceptibility values were drawn from literature estimates [23]. Table **??** details all parameters used in this manuscript and their sources.

2.4.2 Incorporation of Vaccine Hesitancy

To incorporate vaccine hesitancy, we limited vaccine uptake such that at most 70% of any age group was eligible to be vaccinated [34]. To implement this restriction, 30% of each compartment for each age group was initialized as ineligible for vaccination. These individuals were tracked using compartments S_x, E_x, I_x, and R_x (Fig. 2.5). Initial conditions, inclusive of 30% vaccine hesitancy, are listed in Table **??**.

2.4.3 Incorporation of Vaccination, Vaccine Rollout, and Vaccine Efficacy

In the simplest version of the model, the vaccine is assumed to be transmission- and infection- blocking, and to work with variable efficacy. We considered two classes of scenarios. In the first class of scenarios, vaccinations are given in advance of model dynamics, which we call pre-transmission vaccination. In the second class of scenarios, vaccinations are rolled out at the same time as the model dynamics, which we call continuous rollout vaccination.

In continuous rollout scenarios (Scenarios 1 and 2), vaccine rollout was parameterized by the percent-

age of the total population that was vaccinated in each day of simulation, with values ranging from 0.05% to 1% of total population (see Fig. **??**). Scenarios 1 and 2 of the Main Text consider rollout speeds of 0.2% per day. The prescribed number of individuals received the effects of vaccination in simulations prior to the start of each day, such that disease dynamics proceeded in continuous time while vaccine rollout was computed in discrete steps. We did not include an explicit delay between vaccination and protection, and therefore our approach may be thought of as either a model for a vaccine with immediate protective effects, or as a model in which the time of protection is explicitly modeled and injections are thus implicitly assumed to precede said protection. In continuous rollout scenarios, the model was seeded with 0.25% of individuals in each age group exposed and 0.25% of individuals in each age group infectious.

In pre-transmission vaccination scenarios (Scenario 3 and 4), all the available vaccines were distributed at the initial time step, prior to the epidemic. To incorporate vaccinations, we initialized the model by dividing the total population of each age group between the susceptible compartment (S) and vaccinated compartment (V or S_v), according to the vaccine prioritization strategy and number of vaccines available. In pre-transmission vaccination scenarios, the model was seeded with one infectious person in I and one infectious person in I_x in each age group. Scenarios 3 and 4 of the Supplementary Text use pre-transmission rollout.

We considered two ways to implement vaccine efficacy (ve): as an all-or-nothing vaccine, where the vaccine provides perfect protection to a fraction ve of individuals who receive it, or as a leaky vaccine, where all vaccinated individuals have reduced probability ve of infection after vaccination (see Supplementary Text). We ran simulations with both types of vaccine efficacy; Figures in the Main Text show results only for all-or-nothing vaccines.

To incorporate age-dependent vaccine efficacy, we parameterized the relationship between age and vaccine efficacy via an age-efficacy curve with (i) a baseline efficacy, an age at which efficacy begins to decrease (hinge age), and a minimum vaccine efficacy ve_m for adults 80+ (Fig. 3.4A). We assumed that ve is equal to the baseline value for all ages younger than the hinge age, then decreases stepwise in equal

increments for each decade to the specified minimum ve_m for the 80+ age group. To determine whether there exists a ve_m such that the mortality-minimizing strategy switches from directly vaccinating adults 60+ to an alternative strategy, we used the bisection method [66].

2.4.4 Incorporation of Existing Seroprevalence

To incorporate existing seroprevalence estimates and compare areas with differing naturally-acquired immunity, we used data and seroprevalence estimates from Connecticut [low seroprevalence; [41]] and New York City [moderate seroprevalence; [40]]. To model high seroprevalence, we simulated an unmitigated epidemic with $R_0 = 2.6$ until 40% cumulative incidence was reached. Seroprevalence was implemented by moving the proportion of seropositive individuals from each age group into the recovered compartment prior to forward simulations that incorporated vaccination.

The model's implementation of vaccination depended on whether the vaccine was rolled out during ongoing transmission or prior to transmission. For pre-transmission vaccination without consideration of serostatus, v_i doses were given to each population group i, a fraction θ_i of whom were already recovered. Thus, the total number of individuals eligible for vaccination were $S + R$, assuming currentely infected individuals do not seek vaccination. In scenarios where vaccination was targeted only at seronegative individuals, simulations were conducted with sensitivity 70% and specificity 99%, incorporating the performance of a hypothetical Euroimmun IgG test [45] and a 25% reduction in sensitivity due to seroreversion [42]. Details of continuous vaccine rollout with dose redirection using an imperfect serological test can be found in Supplementary Text.

2.4.5 Calibration to achieve target $\mathbf{R_0}$

Models were calibrated to achieve the target R_0 by multiplying the next-generation matrix by a constant to achieve the desired dominant eigenvalue, i.e. R_0. Because the constant factors out of the next-generation matrix equation, this may be mathematically interpreted as scaling up or down either the contact rates C or susceptibilities u. All model calibration was performed prior to the inclusion of vaccination,

meaning that the reproductive number R in the first days of a simulation may differ from R_0 depending on the scenario considered. Values of R_0 studied ranged from 1.1 to 2.6. When incorporating seroprevalence, calibration was performed after the inclusion of seroprevalence.

2.4.6 Measurement of outcomes: infections, deaths, and years of life lost

We ran simulations for 365 days from the date of the first vaccination to focus on the early prioritization phase of the COVID-19 vaccination programs. To compare the impact of different vaccination prioritization strategies, we calculated the cumulative number of infections and deaths. Infected individuals either move to the recovered or dead compartment, according to the age-dependent IFR [29] (see Fig. 2.5). The cumulative number of new infections since the onset of vaccine rollout is the total number of recovered and dead at the end of the simulation minus the initial number of seropositive individuals, $\sum_i R_i + R_{x,i} + R_{v,i} + \Omega_i - \theta_i N_i$. The total number of estimated deaths was the number of people in the dead compartment at the end of the simulation. To calculate years of life lost (YLL) due to a death at a particular age, we multiplied standard life expectancy (SLE) by the number of deaths per age bin. We used the country-specific SLE estimates from the WHO Global Health Observatory [67], aggregated into age bins by decade using $YLL_i = \frac{1}{10}\sum_j YLL_j$ where j are the ages corresponding to decadal age bin i.

2.4.7 Contact Matrices and Demographics

Country-specific contact matrices include four types of contact: home, work, school, and other [32]. In all simulations, we used total contact matrices, equivalent to the sums of the four contact types. Age demographics in all simulations were taken from the UN World Population Prospects 2019 for each country [33]. Age bins in each case were originally provided in 5-year increments, which were then combined into 10-year increments by addition. For instance, the number of individuals between 20 and 29 was the sum of individuals 20-24 and 25-29. The number of individuals 80 years and older was calculated as the sum of all age bins greater than 80.

We made two adaptations to existing contact matrices [32]. First, we combined their five year age

bins into ten year bins. Each entry x_{ij} in the original matrices corresponds to the number of individuals of age-group j that a person in age group i typically comes into contact with. Thus, for a country with population fraction d_i in age group i, the combined contact matrix entries are given by

$$c_{ij} = \frac{d_{2i}(x_{2i,2j} + x_{2i,2j+1}) + d_{2i+1}(x_{2i+1,2j} + x_{2i+1,2j+1})}{d_{2i} + d_{2i+1}} .$$

Second, we extrapolated matrices to include individuals aged 80+. To extrapolate, we copied the contact rates from 70-79 year-old to our new row and column for 80+, along the diagonal. Then we filled in the end of our new row and column with the 70-79 contact rates with 0-9, assuming interactions with people aged 0-9 are similar for people 70+. Lastly, to account for increased housing in long term living facilities for 80+, we decreased their contacts with people aged 0-60 by 10% and added it to the 70 and 80 contacts. Thus, 80+ year-olds have the same total number of contacts as 70-79 year-olds, but relatively fewer among 0-69-year-olds and proportionally more among 70+ year-olds.

2.5 Acknowledgements

The work in this chapter was co-authored by Kyle Reinholt, Stephen M. Kissler, Marc Lipsitch, Sarah Cobey, Yonatan H. Grad, and Daniel B. Larremore. I would also like to thank Sereina Herzog, Mark Jit, Jacco Wallinga, and Helen Johnson for their helpful feedback. **Funding:** K.M.B. was supported in part by the Interdisciplinary Quantitative Biology (IQ Biology) Ph.D. program at the BioFrontiers Institute, University of Colorado Boulder. K.M.B. and D.B.L. were supported in part through the MIDAS Coordination Center (MIDASNI2020-2) by a grant from the National Institute of General Medical Science (3U24GM132013-02S2). M.L., S.M.K., and Y.H.G. were supported in part by the Morris-Singer Fund for the Center for Communicable Disease Dynamics at the Harvard T. H. Chan School of Public Health. M.L. and D.B.L. were supported in part by the SeroNet program of the National Cancer Institute (1U01CA261277-01).

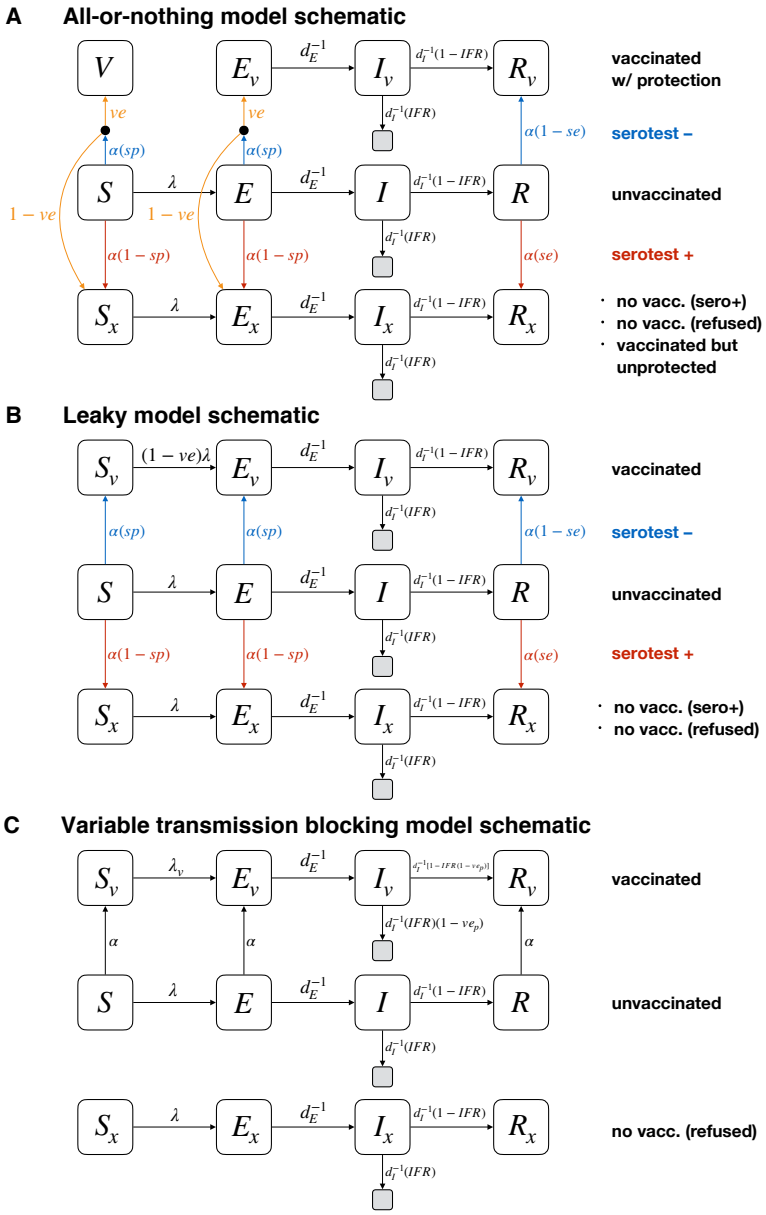

Figure 2.5: **Schematics for vaccine modeling framework.** Diagrams show compartmental models and transition rates for the (A) all-or-nothing, (B) leaky, and (C) variable transmission-blocking vaccine models used in this manuscript. S, E, I, and R represent susceptible, exposed, infectious, and recovered compartments; V represents a perfectly protected and vaccinated compartment; subscripts of v and x denote those who have been vaccinated with protection (v), and those who will either not be vaccinated (vaccine refusal or positive serotest) or have been vaccinated but without protection (x). Grey unlabeled compartments represent death. The incorporation of a point-of-care serological test can be included by using known sensitivity se and specificity sp, or can be excluded by setting $se = 0$ and $sp = 1$ (a convenient mathematical representation of the no-test scenario is simply a test that always returns a negative result). Vaccine rollout count α is given by $\alpha = n_{\text{vax}}/\left[(S+E)sp + R(1-se)\right]$ where n_{vax} is the total number of vaccines to be rolled out in a particular day. All compartments are stratified by age, in the text, with index i. See text for details and initial conditions.

Chapter 3

SARS-CoV-2 Transmission and Impacts of Unvaccinated-Only Screening in Populations of Mixed Vaccination Status

Portions of this chapter are adapted from:

K.M. Bubar*, C. E. Middleton*, K. K. Bjorkman, R. Parker, and D.B. Larremore. *SARS-CoV-2 transmission and impacts of unvaccinated-only screening in populations of mixed vaccination status.* Nature Communications. 13(2777), 2022.

* authors contributed equally

3.1 Introduction

SARS-CoV-2 has created a pandemic in which morbidity and mortality have been partially mitigated in many areas by widespread vaccination. COVID-19 vaccines have been extremely effective at preventing severe disease (vaccine efficacy, $\text{VE} > 90\%$, [68]), while also reducing susceptibility to infection (VE_S) and risk of onward transmission (VE_I). In spite of these reductions, so-called vaccine breakthrough infections and subsequent transmission have been widely documented [69], and have increased dramatically with the emergence of the omicron variant in late 2021 [70, 71]. These developments raise the question of how to best mitigate transmission in partially vaccinated populations.

Prior to the approval of COVID-19 vaccines, transmission mitigation via regular and repeated screening was shown to be an effective approach to break chains of transmission and decrease the burden of COVID-19 using both RT-PCR [72–74] and rapid antigen testing [74,75]. Specifically, screening via testing,

which we hereafter refer to simply as screening in most cases, is effective at the community level because it decreases transmission from individuals who are already infected [74, 76]. However, policy proposals in 2021 and early 2022 shifted to focus routine testing requirements on only the unvaccinated population, including an Italian requirement announced in October, 2021 [77] and a U.S. requirement for healthcare workers beginning February, 2022 [78]. By reducing rates of transmission from only the unvaccinated population, such policies may be limited by the extent to which transmission is, in fact, driven by the unvaccinated. This raises critical questions about projected policy impacts relative to other non-pharmaceutical interventions [79, 80]—particularly in areas where the unvaccinated population is small.

The role of vaccines in reducing transmission is complex and changing. First, VE_S and VE_I vary depending on which vaccine was administered [81]. Second, both VE_S and VE_I wane with time since vaccination [82–84], but can be boosted to higher levels for those receiving an additional dose [85]. Third, those who have experienced a SARS-CoV-2 infection also show decreased risks of reinfection and subsequent transmission [81], providing partial protection to those who are previously infected and remain unvaccinated, but also augmenting protection for those who are both vaccinated and previously infected [85, 86]. Finally, preliminary estimates of VE_S and VE_I, and their prior-infection equivalents, are markedly lower for the omicron variant [70, 87]. Thus, the relative estimates of risk reductions due to vaccination, prior infection, or both, as well as the sizes of the populations falling into each category of immunity, will affect transmission dynamics—with or without testing.

In this study, we model the spread of SARS-CoV-2 in populations of mixed vaccination status, focusing on three critical questions. First, how do vaccinated and unvaccinated populations each contribute to community spread and hospitalizations, and how do those contributions vary with rates of vaccination and prior infection? Second, how do testing-based screening programs focused on unvaccinated individuals alone affect community spread and hospitalizations? Third, how effective are delta-era screening strategies likely to be against variants with higher breakthrough and reinfection rates? Our study's goals are not to make perfectly calibrated predictions but instead to elucidate more general principles of transmission and unvaccinated-only testing in partially vaccinated populations. As such, our analyses consider a wide range

of parameters and scenarios.

3.2 Results

Unvaccinated-only testing-based screening programs have been discussed and implemented during transmission of both the delta and omicron variants, yet these variants differ in their transmission and disease parameters, particularly among vaccinated or previously infected individuals—the focus of the present study. As such, the analyses that follow incorporate a range of empirically estimated parameters for the delta variant and plausible parameters associated with the omicron variant.

3.2.1 High vaccination rates drive total infections and hospitalizations down, increase the proportions of vaccine breakthroughs, and shift the drivers of transmission

To examine the dynamics of transmission in a population with mixed vaccination status, we first modeled transmission within and between communities of vaccinated (V) and unvaccinated (U) individuals in the absence of a screening program. Based on a standard Susceptible Exposed Infected Recovered (SEIR) model, we tracked the four transmission modes by which an infection might spread: $U \to U$, $U \to V$, $V \to U$, and $V \to V$ (Fig. 3.1a). A constant and equivalent fraction of both populations was assumed to have experienced prior SARS-CoV-2 infection, resulting in four categories of imperfect immunity: unprotected (unvaccinated with no prior infection), infection-acquired, vaccine-acquired, and both vaccine- and infection-acquired (so-called "hybrid" immunity). To account for introductions of infection from outside the population, all susceptible individuals were subject to a small, constant rate of exposure, with infection-acquired and vaccine-acquired immunity providing partial protection against subsequent infection.

Traditionally, the basic reproductive number R_0 is defined as the number of secondary infections generated by a typical infector in an entirely susceptible population, i.e., a population without any non-pharmaceutical interventions (NPIs). At the time of writing, NPIs such as masking, ventilation and physical distancing are commonplace in many areas, so we hereafter define R_0^{NPI} to be the expected number of secondary infections generated by a typical infector in a population with possible NPIs, but prior to any

impacts of population immunity. Furthermore, because precise estimates of R_0^{NPI} vary by context, variant, and over time, we consider a range of R_0^{NPI} values from 4 to 6. In our baseline modeling scenario, vaccines were assumed to reduce susceptibility to infection by $\text{VE}_S = 65\%$, the likelihood of transmission to others by $\text{VE}_I = 35\%$, and the likelihood of disease progression to hospitalization conditioned on infection by $\text{VE}_P = 86\%$, values which land within plausible literature estimates for the effectiveness of two doses of mRNA vaccine against the delta variant in the absence of dramatic waning and without boosting [81, 85, 88, 89]. Though less often studied in the literature, we assumed that prior SARS-CoV-2 infection would lead to 63% and 13% decreases in risk of infection and transmission based on a statistical model relating immunity to neutralization [85], and that hybrid immunity would be superior to either vaccination or prior SARS-CoV-2 infection alone. We further assumed an additional 54% decrease in risk of hospitalization conditioned on infection for individuals with prior SARS-CoV-2 infection [90], and that individuals with hybrid immunity receive the greater of vaccinated or prior immunity's protection against hospitalization. See Materials and Methods and Online Supplementary Tables 1 and 2 for a complete description of the model and parameters.

In a modeled population of $N = 20,000$ with 58% vaccination rate (corresponding to U.S. estimates as of Nov. 4, 2021 [91]) and 35% past infection rate, outbreaks still occurred, despite assuming a partially mitigated delta variant ($R_0^{\text{NPI}} = 4$). During the ensuing outbreak, 59% of total infections and 89% of hospitalizations occurred in unvaccinated individuals (Fig. 3.1b,c), despite making up only 42% of the population. Furthermore, the peak burden of disease occurred first in the unvaccinated community and then one week later in the vaccinated community (Fig. 3.1b), a known consequence of disease dynamics in populations with heterogeneous susceptibility and transmissibility [92, 93]. By categorizing transmission events into four distinct modes (Fig. 3.1a), we observe that infections during a delta outbreak in both communities were driven predominantly and consistently by the unvaccinated community ($U \to U$, $U \to V$; Fig. 3.1d), but that there was nevertheless some transmission from the vaccinated community (breakthrough transmission). These differences occurred despite a "well mixed" modeling assumption—namely, that an individual with a given vaccination status is no more or less likely to associate with a member of their own group vs the other group.

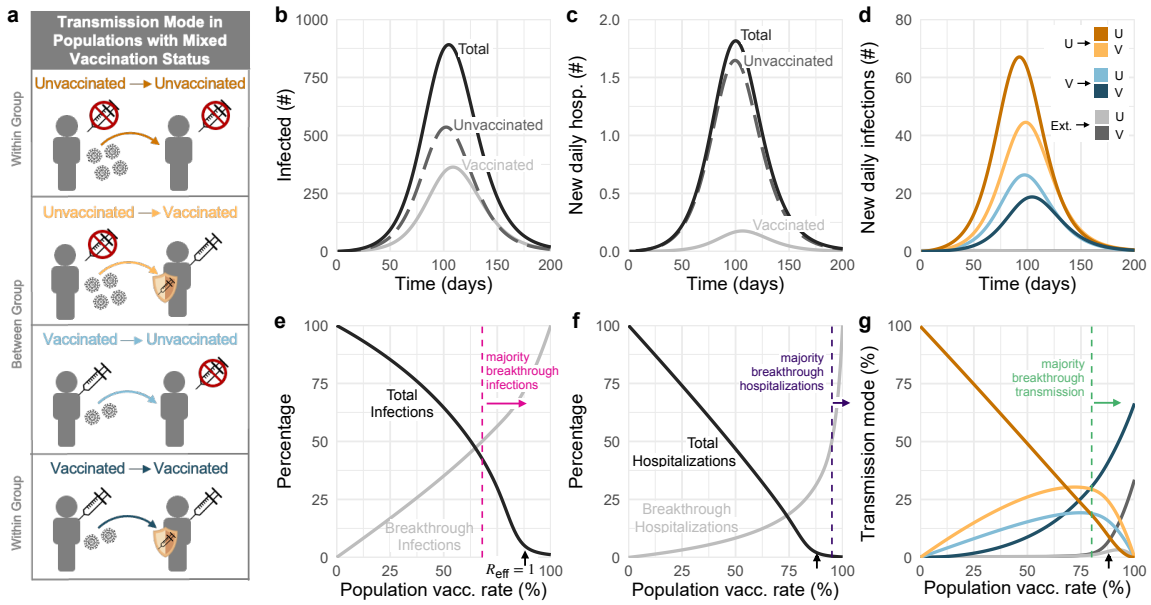

Figure 3.1: **Vaccination affects which population drives transmission and dominates infections and hospitalizations.** (a) Diagram of four transmission modes within and between vaccinated and unvaccinated communities, where vaccines and prior infection decrease risks of infection, transmission, and hospitalization. (b) Number of infected individuals and (c) new daily hospitalizations over time (solid black), stratified by unvaccinated (dashed gray) and vaccinated (solid gray) populations. (d) Daily transmission events separated and colored by transmission mode (see legend). (e) Cumulative infections and (f) hospitalizations as a percentage of total infections/hospitalizations without vaccination (black), and the percent of each accounted for by vaccine breakthroughs (gray) for varying vaccination rates. (g) Transmission mode (see legend) as a percentage of cumulative infections for varying vaccination rates. Black arrows in panels e, f, and g indicate vaccination rate at which $R_{\text{eff}} = 1$; vertical dashed lines indicate the lowest vaccination rates for which vaccinated individuals account for the majority of infections, hospitalizations, and transmission as annotated. $R_0^{\text{NPI}} = 4$ for all plots, with baseline VE and immunity parameters vs the delta variant (Materials and Methods, Online Supplementary Tables 1 and 2; no screening. Panels b, c, and d: 58% vaccination rate and 35% rate of prior infection.

Vaccination and past infection rates vary widely across the U.S. [91] and the world [94] due to impacts of both vaccine availability [94] and refusal [95], as well as the success or failure of transmission mitigation policies. We therefore asked how a population's vaccination and past infection rates would affect our observations about infections, hospitalizations, and the relative impacts of the four modes of transmission. This analysis revealed three important points.

First, our results reinforce the fact that increased vaccination rates lead to decreased total infections

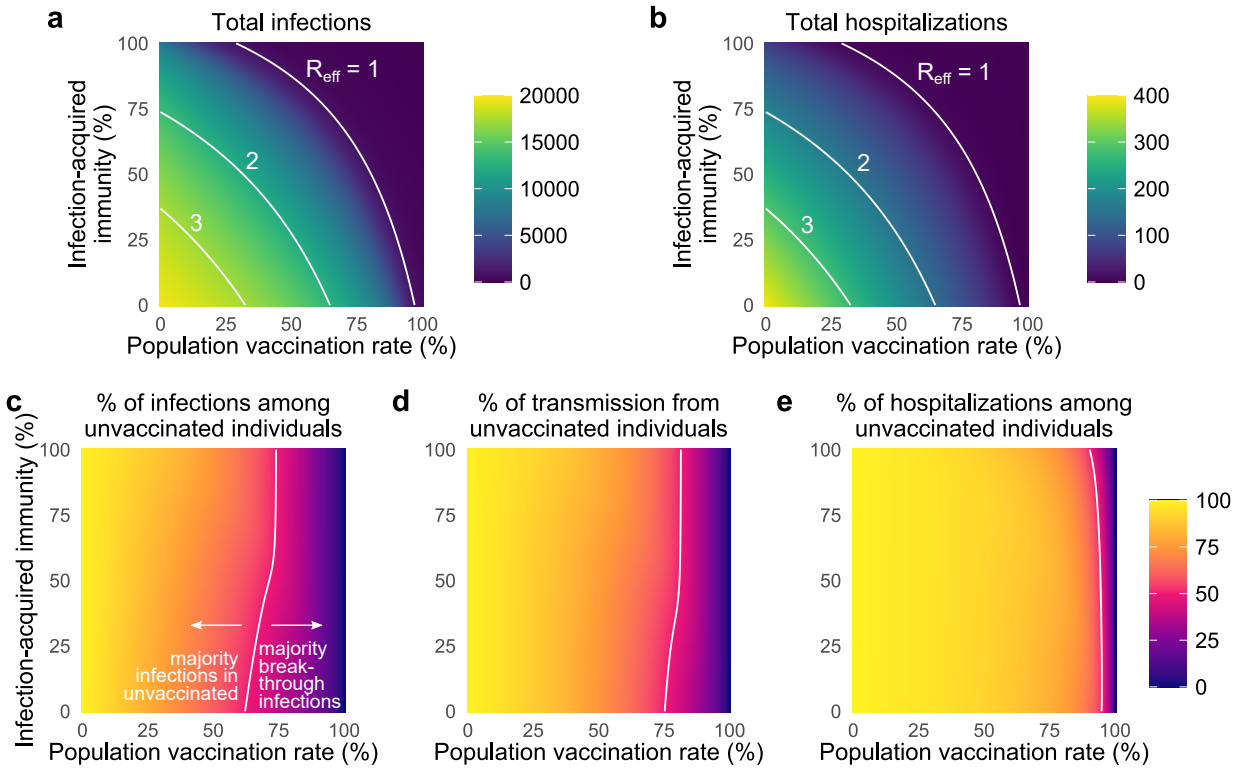

Figure 3.2: **Vaccination and prior infection rates affect epidemic potential, vaccine breakthroughs, and drivers of transmission**. Heatmaps show (a) the total number of infections, (b) the total number of hospitalizations, (c) the percentage of total infections occurring in the unvaccinated population (d) the percentage of total infections caused by the unvaccinated population, and (e) the percentage of total hospitalizations occurring in the unvaccinated population for simulated epidemics (see text). White annotation curves show (a, b) isoclines of the effective reproductive number R_{eff} calculated at $t = 0$, and the line of parameters along which (c) 50% of infections were breakthroughs, (d) 50% of transmission was due to breakthrough infections, and (e) 50% of hospitalizations were breakthroughs. $N = 20,000$ and $R_0^{\text{NPI}} = 4$ for all plots, with baseline VE and immunity parameters vs the delta variant (Materials and Methods, Online Supplementary Tables 1 and 2); no testing. See Online Supplementary Fig. 2 for $R_0^{\text{NPI}} = 6$.

and hospitalizations, both before and after the herd immunity threshold at $R_{\text{eff}} = 1$ (Fig. 3.1e,f). Moreover, when large proportions of the population are also partially protected by immunity from prior infection, the vaccination levels required to reach $R_{\text{eff}} = 1$ decrease considerably (Fig. 3.2a). For instance, increasing prior infection rates from 35% to 50% decreases the required vaccination rate for $R_{\text{eff}} = 1$ from 87% to 80% under baseline modeling parameters. Combinations of immunity from past infection and vaccination thus have the potential to create a herd immunity frontier, beyond which transmission is no longer self-sustaining even in the absence of screening. We caution that although total infections and hospitalizations may appear

equal along lines of constant R_{eff} (Fig. 3.2a,b), both actually decrease as vaccination rates increase, due to vaccines' superior protection, relative to prior infection, against infection and hospitalization.

Second, as vaccination rates increased, the fraction of infections classified as vaccine breakthroughs increased (Fig. 3.1e), creating a transition point such that when 68% of the population was vaccinated, 50% of all infections were breakthrough infections under our baseline modeling conditions for the delta variant. To determine whether this transition point of 68% was sensitive to the precise fraction of the population with immunity from past infection (35%, Fig. 3.1), we varied the fraction with infection-acquired immunity between 0% and 100%, finding that the 50/50 breakthrough infection transition occurred between 63% and 75% vaccine coverage (Fig. 3.2c). Because vaccines provide an additional level of protection against hospitalization VE_P, the 50/50 breakthrough hospitalization transition occurs at rates of vaccination of 90-96% (Figs. 3.1f and 3.2e). Thus, our results set the expectation that increasing vaccination rates will decrease total infections and hospitalizations, yet a higher proportion of both will be breakthroughs, irrespective of levels of immunity due to prior infection.

Third, as vaccination rates increased, the unvaccinated community ceased to be the primary driver of transmission. Under our baseline modeling conditions ($R_0^{\text{NPI}} = 4$, 35% with infection-acquired immunity), this transition occurred when 80% or more of the population was vaccinated (Fig. 3.1g). When we varied the fraction of the population with infection-acquired immunity between 0% and 100%, this transition point varied from 76% to 82% (Fig. 3.2d). Thus, while COVID-19 hospitalizations remain concentrated primarily in unvaccinated populations, only a minority of infections will occur in, and be driven by, the unvaccinated community when vaccine coverage is sufficiently high. Note that this implies that unvaccinated individuals living in highly vaccinated communities will still be exposed to SARS-CoV-2 and thus remain at risk of infection and severe disease.

These findings are driven by reductions in susceptibility, disease severity, and infectiousness arising from vaccination, prior SARS-CoV-2 infection, or both. However, quantitative estimates of those reductions vary depending on which vaccine was administered [84], time since vaccination or SARS-CoV-2 in-

fection [82–84], whether an additional "booster" dose was given [85], and the variant circulating at the time of the study [96, 97]. We therefore sought to determine how our findings might change under different sets of assumptions about vaccine effectiveness by comparing our baseline scenario ($VE_S = 0.65$, $VE_I = 0.35$, $VE_P = 0.86$) with a waning/low immunity scenario ($VE_S = 0.5$, $VE_I = 0.1$, $VE_P = 0.80$) and a boosted/high immunity scenario ($VE_S = 0.8$, $VE_I = 0.6$, $VE_P = 0.90$), as well as a scenario reflecting plausible VE values based on early observations for the omicron variant ($VE_S = 0.35$, $VE_I = 0.05$, $VE_P = 0.77$; [89, 98]). To explore the impact of these changes in vaccine effectiveness, we simulated outbreaks for all combinations of vaccination and infection-acquired immunity rates under the four VE scenarios. Across simulations, total infections and hospitalizations were well predicted by calculating R_{eff} at the start of each simulation (Eq. (3.3); Methods). In particular, outbreaks were small when vaccination or past infection rates crossed the herd immunity threshold ($R_{\text{eff}} < 1$). When $R_{\text{eff}} > 1$, total infections monotonically increased as R_{eff} increased (Online Supplementary Fig. 1). The herd immunity threshold was impossible to cross with vaccination alone in the waning or omicron VE scenarios with partially mitigated transmission ($R_0^{\text{NPI}} = 4$, Fig. 3.3a,d; Online Supplementary Fig. 1), and in waning, baseline, and omicron VE scenarios with unmitigated transmission ($R_0^{\text{NPI}} = 6$; Online Supplementary Fig. 1), as evidenced by the fact that the $R_{\text{eff}} = 1$ curves either fail to intersect the vaccination rate axis or appear at all.

Waning, boosting, or omicron-specific assumptions altered the proportions of infections and hospitalizations occurring in, and transmission from, the unvaccinated vs vaccinated communities. All else being equal, waning or omicron VE led to increased fractions of breakthrough infections and hospitalizations, and increased transmission from the vaccinated community, while boosted VE led to decreases of all three. In turn, the population vaccination rates at which the majority of infections or hospitalizations were breakthroughs shifted down for waning or omicron VE (Fig. 3.3a,d), while the vaccination rate at which the majority of transmission was driven by vaccinated individuals shifted up for boosted VE (Fig. 3.3c).

Among the four transition points identified in transmission dynamics, we observe that, in each VE scenario, R_{eff} is driven by both vaccination and past infection rates, as evidenced by curvature in $R_{\text{eff}} = 1$ isoclines (Fig. 3.3, black lines). In contrast, isoclines representing the transition points between majority-

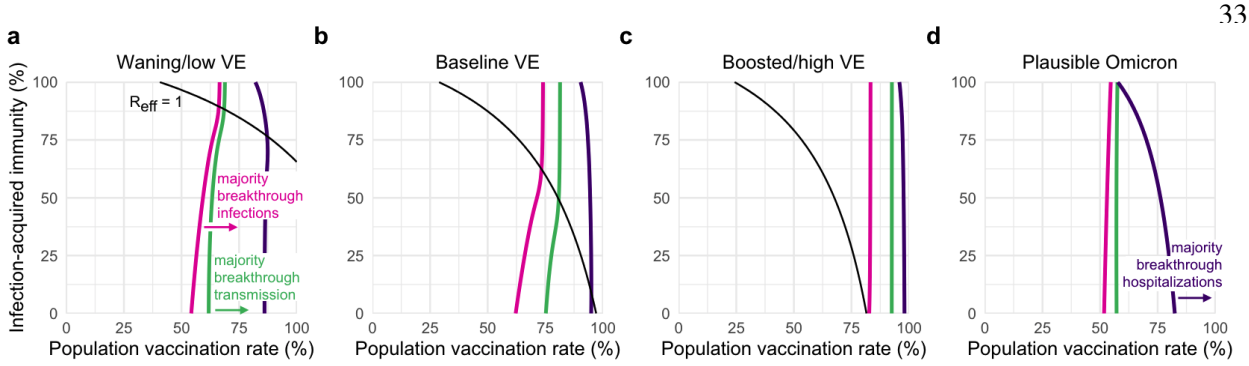

Figure 3.3: **Transition points for breakthrough infections, hospitalizations, and transmission.** All panels show curves representing the vaccination and prior infection rates infections (pink), transmission (green), and hospitalizations (purple) are composed of equal numbers of vaccinated an unvaccinated individuals, with majority-breakthrough regions to the right of each line as indicated, for (a) waning/low, (b) baseline, and (c) boosted/high VE vs the delta variant, and (d) plausible VE vs the omicron variant. Black lines indicate $R_{\text{eff}} = 1$ isoclines, which do not appear in panel (d) due to $R_{\text{eff}} > 1$. See Online Supplementary Table 2 for immunity parameter values. $R_0^{\text{NPI}} = 4$ in all panels.

unvaccinated vs majority-breakthrough infections (Fig. 3.3, pink lines), between majority-unvaccinated vs majority-breakthrough hospitalizations (Fig. 3.3, purple lines), and between majority-unvaccinated vs majority-breakthrough transmission (Fig. 3.3, green lines) are relatively insensitive to variation in rates of infection-acquired immunity, as evidenced by vertical or near-vertical isoclines. These findings suggest that the relative proportions of breakthrough infections, hospitalizations, and transmission are driven more by vaccination rates and VE, but not by rates of past infection or proximity to herd immunity; indeed, after the herd immunity threshold, all three isoclines show essentially no variation. These observations suggest that unvaccinated-only screening programs, which decrease rates of $U \to U$ and $U \to V$ transmission, may be highly effective only in regimes where transmission is driven by the unvaccinated (i.e. to the "left" of green isoclines, Fig. 3.3), an intuition we now explore in detail.

3.2.2 The impacts of unvaccinated-only screening depend on population immunity, compliance, and VE

To explore the impact of unvaccinated-only screening on population transmission, we modified our simulations so that a positive test would result in an unvaccinated individual isolating to avoid infecting others [74, 99]. We considered test sensitivity equivalent to RT-PCR with a one-day delay between sample

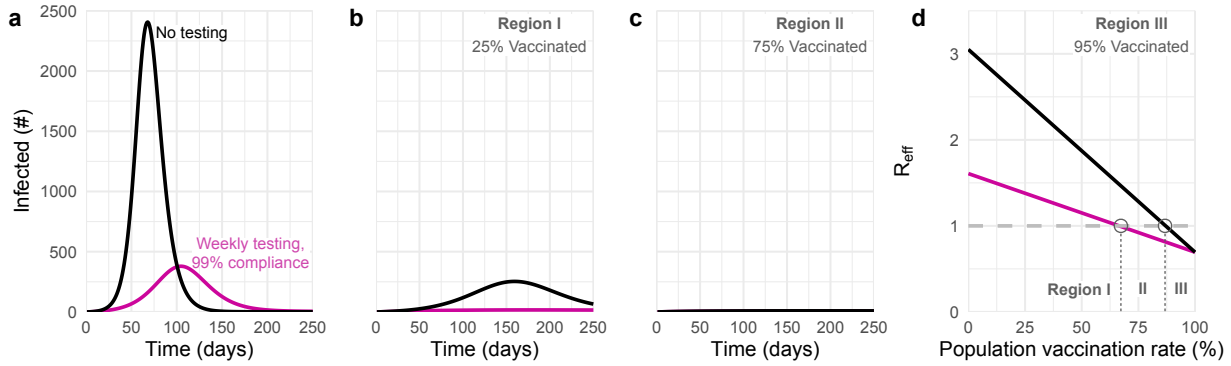

Figure 3.4: **The impact of unvaccinated-only screening corresponds to three distinct parameter regions.** Total number of infections with no screening (black) and weekly testing with 99% compliance (pink) are shown for (a) 25%, (b) 75%, and (c) 95% population vaccination rates. (d) Effective reproductive number over various population vaccination rates, where $R_{\text{eff}} = 1$ is denoted by gray dashed line. The impacts of screening fall into three categories (see text) depending on whether vaccination rate falls into region I, II, or III, as annotated. $R_0^{\text{NPI}} = 4$ and 35% rate of prior infection with baseline immunity parameters (Materials and Methods, Online Supplementary Table 2).

collection and diagnosis under three screening paradigms: weekly testing with 50% compliance—a value which reflects observed compliance with a weekly testing mandate in a university setting [72]—weekly testing with 99% compliance, and, specifically for the omicron variant, twice-weekly testing with 99% compliance.

Our analysis shows that the benefits of an unvaccinated-only screening program fall into one of three categories, depending on the population vaccination rate and transmission dynamics. These categories align with three distinct regions in parameter space, denoted in Fig. 3.4 as regions I, II and III. In region I, screening is insufficient to fully control transmission, yet nevertheless markedly reduces the peak number of total infections, colloquially "flattening the curve" (Fig. 3.4a). In region II, screening successfully brings transmission under control (Fig. 3.4b). In region III, screening has little impact on transmission due to the fact that outbreaks are already mitigated by population immunity and other control measures (Fig. 3.4c). Unvaccinated-only screening is therefore impactful in the first two regions, sufficient for transmission control in only the second region, and largely inconsequential to transmission in the third.

The three regions that correspond to different impacts of screening on transmission are separated

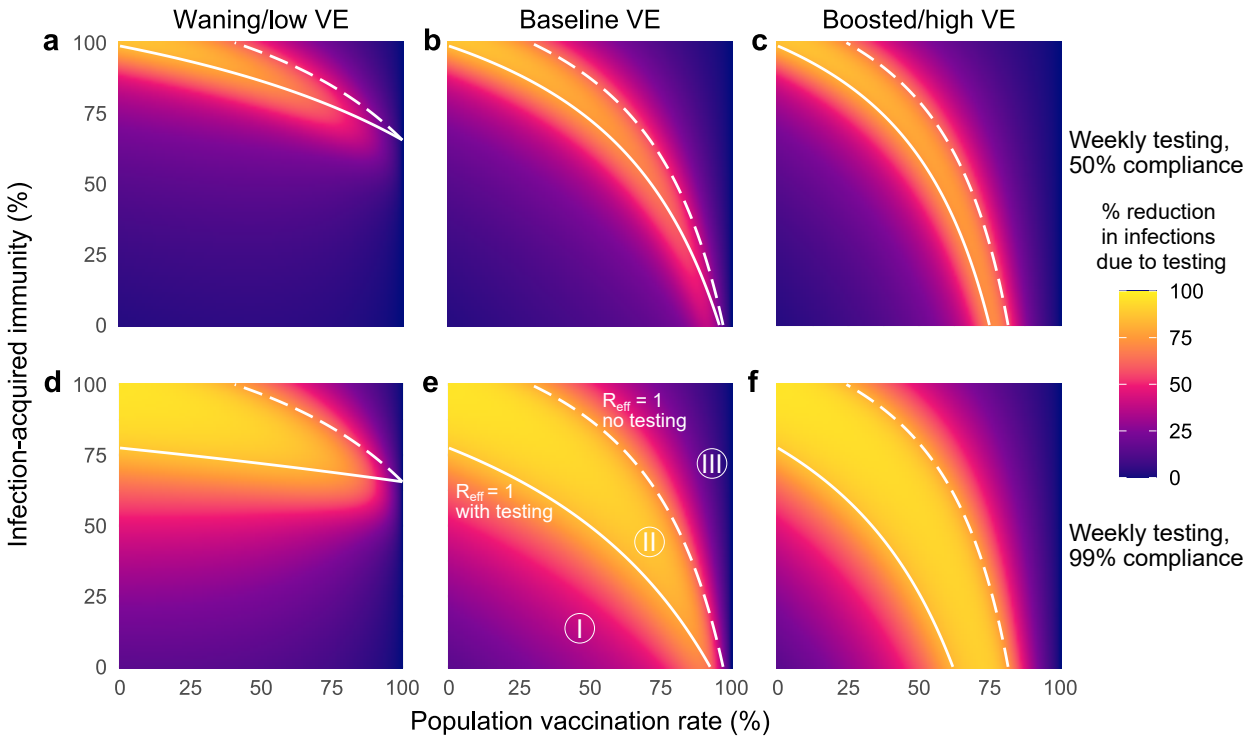

Figure 3.5: **The impacts of unvaccinated-only screening depend on population immunity, compliance, and vaccine effectiveness.** Percent reduction in cumulative infections due to screening over various population vaccination rates assuming waning/low (a, d), baseline (b, e), and boosted/high (c, f) VE with once-weekly screening at 50% (top row) and 99% (bottom row) compliance. White lines indicate the population immunity rate at which $R_{\text{eff}} = 1$ with screening (solid) and without screening (dashed), which divide the space into three regions, labeled I, II and III. See Supplementary Tables **??** and **??** for parameter values. $R_0^{\text{NPI}} = 4$ in all panels; see Online Supplementary Figure 5 for $R_0^{\text{NPI}} = 6$.

by boundaries which can be estimated from two analytical calculations of R_{eff}—one which includes the effects of screening and one which does not (Eq. 3.3, Methods). The boundary separating regions I and II is given by those parameters for which $R_{\text{eff}} = 1$ with screening, while the boundary separating regions II and III is given by those parameters for which $R_{\text{eff}} = 1$ without screening (Fig. 3.4d). Thus, the value of a screening testing program in reducing infections can be evaluated based on which of three regions the current vaccination rate, prior infection rate, and VE fall into.

To illustrate the value of this R_{eff}-based analysis, we considered vaccination rates and prior infection rates ranging from 0-100% and varied VE between waning, baseline, and boosted scenarios for the delta

variant. Across scenarios, dramatic relative reductions in cumulative infections are concentrated within the envelope between the boundaries of $R_{\text{eff}} = 1$ with and without screening, i.e., region II (Fig. 3.5). Outside of this effective screening envelope, percent reductions in cumulative infections decreased markedly, either because unvaccinated-only screening flattened the infection curve but had little impact on cumulative infections (region I), or because existing population immunity prevented large outbreaks in the first place (region III). Assuming a 35% past infection rate and $R_0^{\text{NPI}} = 4$, region III appeared only for baseline and boosted vaccine effectiveness assumptions, and only when vaccination rates were approximately 90% or greater (baseline VE) or 75% or greater (boosted VE). Sensitivity analyses show that increasing R_0^{NPI} to 6, potentially representing pre-pandemic contact rates and the SARS-CoV-2 delta variant, cause region III to shrink further (Online Supplementary Fig. 5). Thus continued screening for SARS-CoV-2 among the unvaccinated may be of limited value when vaccination rates are sufficiently high.

The role of compliance—the fraction of scheduled tests that are actually taken—can also be clarified by examining the three regions of screening testing impact. Both the simulations and equations for R_{eff} show that increasing compliance from 50% (Fig. 3.5, row 1) to 99% (Fig. 3.5, row 2) causes the lower boundary of the effective screening envelope to shift to lower vaccination and prior infection rates, decreasing the size of region I and increasing the size of region II. Moreover, increased compliance increases the magnitude of infection reductions within both regions, visible as an intensification of color in the infection reduction heatmaps (Fig. 3.5). As a result of these observations, we conclude that, in addition to test sensitivity, frequency, and turnaround time [74], high participation in screening programs is critical to expanding the impact of unvaccinated-only screening testing programs. However, we also note that compliance had little effect in region III where $R_{\text{eff}} < 1$, a result which parallels analysis of universal screening programs [76].

This R_{eff}-based analysis of transmission is not restricted to unvaccinated-only screening programs. To illustrate this, we considered an identical set of simulations as in Fig. 3.5 but with universal screening, i.e. screening via testing of the vaccinated and unvaccinated populations alike. Universal screening caused the boundary between regions I and II ($R_{\text{eff}} = 1$ with screening) to shift, expanding the size of the effective screening envelope (Online Supplementary Fig. 6). While we present these results here for com-

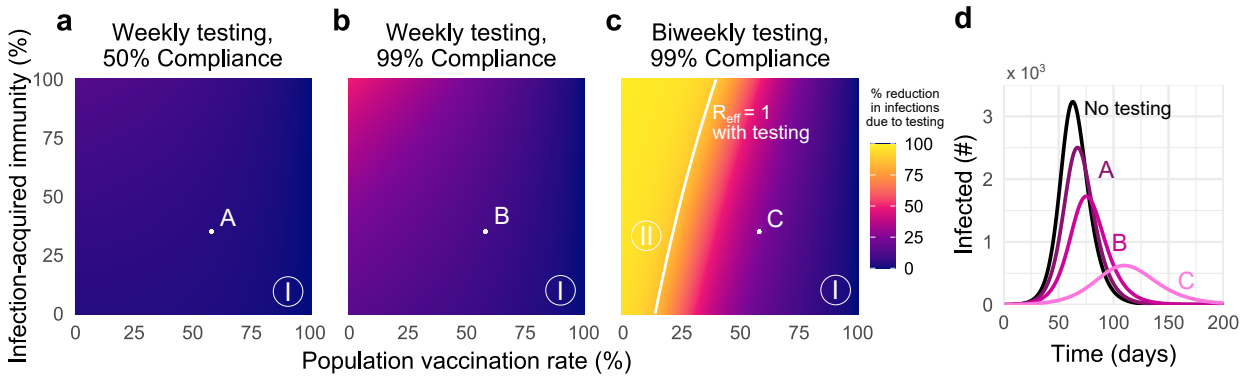

Figure 3.6: **Unvaccinated-only screening during omicron transmission cannot achieve $R_{\text{eff}} < 1$ except in low-vaccination and high-frequency regimes.** Percent reduction in cumulative infections due to screening over various population vaccination rates assuming plausible parameters for immunity versus the omicron variant, with (a) once-weekly screening at 50% compliance, (b) once-weekly screening at 99% compliance, and (c) twice-weekly screening at 99% compliance. (d) Number of individuals infected over time, under screening scenarios denoted A, B, C, compared with no screening (black) with 58% vaccination rate and 35% rate of prior infection. Solid white line indicates $R_{\text{eff}} = 1$ with screening; $R_{\text{eff}} = 1$ is not achievable without screening. See Online Supplementary Tables 1 and 2 for parameter values. $R_0^{\text{NPI}} = 4$ in all panels; see Online Supplementary Figure 4 for $R_0^{\text{NPI}} = 6$ and Supplementary Figure 5 for universal testing.

pleteness, universal testing in mixed vaccination status populations have been investigated elsewhere prior to the present work [76].

The impact of screening on hospitalizations is also predicted well by the R_{eff}-based effective screening envelope. While hospitalizations were not identical across all equal-R_{eff} combinations of vaccination and prior infection rates, dramatic relative reductions in cumulative hospitalizations were nevertheless clearly concentrated within region II, with decreasing relative reductions in regions I and III (Online Supplementary Fig. 6). We therefore find that analysis based only on the effective screening envelope, calculated via Eq. (3.3) (Methods), is useful in predicting the impact of screening regimens—both unvaccinated-only and universal—on reductions in cumulative infections and hospitalizations alike.

The omicron variant's rapid spread, and in particular its increased rates of reinfection and vaccine breakthrough, raise key questions about the role of unvaccinated-only screening programs and whether populations considering such policies may fall into region I, II, or III defined above. Because estimates of

omicron-specific immunity parameters remain either limited or nonexistent at the time of writing, we assumed plausible lower values of each based on extant data [89,98], alongside lower infection-hospitalization rates for omicron in general (Online Supplementary Tables 1 and 2). Under such assumptions, weekly unvaccinated-only screening with 50% compliance was ineffective at reducing cumulative infections even though screening reduced the peak magnitude of infections (Fig. 3.6d). Regardless of compliance, all prior infection and vaccination rate combinations with a weekly screening policy were in region I, indicating that magnitude of peak infections can be mitigated but impact on cumulative infections is low (Fig. 3.6a,b). Doubling the frequency of screening to twice weekly with 99% compliance creates a bifurcated landscape, with highly effective screening only in settings with 18-40% vaccination rates (Fig. 3.6c). For vaccination rates above 50%, even twice-weekly unvaccinated-only screening programs with near-perfect compliance are unlikely to dramatically impact the spread of the omicron variant (region I). Universal screening showed comparatively higher impact, yet, nevertheless, only twice-weekly testing regimens created broad region II regimes in which community spread was controlled (Online Supplementary Fig. 6).

3.2.3 Unvaccinated-only screening shifts the balance of unvaccinated vs breakthrough transmission but not infection or hospitalization

By reducing transmission from unvaccinated individuals, screening programs specifically mitigate $U \to U$ and $U \to V$ transmission modes, thus diminishing the role of the unvaccinated population in transmission dynamics and amplifying the relative role of vaccine breakthrough transmission. As a consequence, we observe that in the presence of screening, the vaccination rates at which the unvaccinated cease to drive a majority of transmission decrease by up to 15 percentage points (Fig. 3.7b), with the largest decreases for 99% compliance and waning VE vs delta, and the smallest decreases for 50% compliance and boosted VE vs delta, or in all screening scenarios vs the omicron variant. Under waning/low, baseline and omicron VE scenarios, unvaccinated-only screening programs shrink the regime in which the unvaccinated population drives outbreaks.

In contrast, unvaccinated-only screening programs had little effect on the percentage of infections

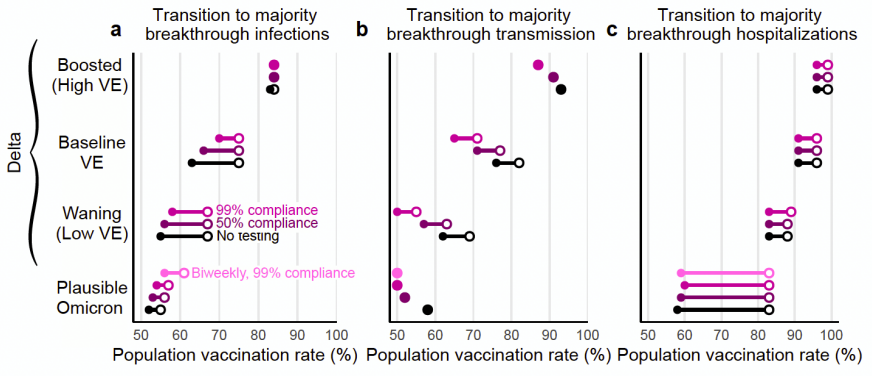

Figure 3.7: **Screening and vaccine effectiveness affect transition points to majority-breakthrough regimes.** The vaccination rates at which the vaccinated population makes up the majority of (a) infections, (b) transmission, and (c) hospitalizations for low, moderate, and high vaccine effectiveness scenarios. Minimum (filled circle) and maximum (open circle) endpoints show the variation in transition points over all combinations of vaccination and prior infection rates for no screening (black), 50% compliance (purple), 99% compliance (pink) over all possible values for past infection rates. $R_0^{\text{NPI}} = 4$ for all plots; see Online Supplementary Figure 7 for $R_0^{\text{NPI}} = 6$.

or hospitalizations that were vaccine breakthroughs. Instead, majority breakthrough regimes remained primarily dependent on vaccination rates and vaccine effectiveness (Fig. 3.7a,c), with transitions to majority-breakthrough infection regimes beginning at 55 to 67% vaccination rates (waning VE, delta), 63 to 75% vaccination rates (baseline VE, delta), 83 to 84% vaccination rates (boosted VE, delta), and 50 to 55% vaccination rates (omicron). Transitions to majority-breakthrough hospitalizations occurred at 83 to 88% (waning VE, delta), 91 to 96% (baseline VE, delta), 96 to 99% vaccination rates (boosted VE, delta), and 58 to 83% vaccination rates (omicron), regardless of screening. We therefore conclude that unvaccinated-only screening programs do not markedly alter the expectations of majority-breakthrough infections or hospitalizations at high vaccination levels, particularly if VE is low or waning.

3.3 Discussion

In this analysis, we find that in communities with mixed vaccination status, routine SARS-CoV-2 screening programs focused only on the unvaccinated may reduce infections and hospitalizations, but in a manner dependent on two conditions. First, effective screening via testing requires high participation to be most impactful, reinforcing the need for mechanisms to encourage or enforce high participation. Second,

when immunity from vaccination and past infection are high enough to curtail transmission on their own, or in concert with effective non-pharmaceutical interventions (NPIs) [79,80], testing the remaining unvaccinated population averts few infections and hospitalizations in both relative and absolute terms. On the other hand, when transmission due to reinfection and/or vaccine breakthrough is sufficiently high, unvaccinated-only screening will at best "flatten the curve" of infections, but cannot adequately control infections and hospitalizations except when testing twice weekly with near-perfect participation in low vaccination communities. Once communities reach vaccination rates of $\sim$40% or more, even twice-weekly unvaccinated-only screening, with near-perfect compliance and isolation adherence, cannot control the omicron variant. Thus, targeted unvaccinated screening programs are highly effective only in a restricted region of epidemiological parameter space, results echoed by similar work analyzing universal screening programs [76].

Key to understanding our study are three observations and findings. First, an unvaccinated-only screening program simply tests fewer and fewer individuals as vaccination rates increase. Second, the relative role of the unvaccinated population in driving transmission decreases as vaccination rates increase, regardless of vaccine effectiveness. Third, when vaccine effectiveness against infection and transmission wanes, unvaccinated-only screening programs decrease in impact. As a consequence, our work broadly suggests that unvaccinated-only screening is most beneficial when a population is undervaccinated and is close to, but has not yet achieved, herd immunity—region II in our analyses—leading to the recommendation that such testing programs be used in conjunction with other NPIs. Indeed, our work finds that unvaccinated-only screening alone is generally insufficient to markedly reduce infections and hospitalizations when (i) the population is far from the herd immunity threshold, inclusive of existing NPIs, in either direction, (ii) vaccination rates are high, or (iii) testing is weekly and/or compliance is low. Against a backdrop of waning immunity and continued emergence of antigenically distinct variants, even herd immunity may be, at best, temporary. In this context, weekly unvaccinated-only screening programs alone are an insufficient countermeasure for the omicron variant.

Indeed, while our analysis focused on a single screening-based intervention in isolation, unvaccinated-only (or universal) screening programs are typically implemented alongside other NPIs [72,73,75]. These

NPIs, including limitations on gatherings, increasing the availability of personal protective equipment, and school or restaurant closures, were estimated to have reduced the effective reproductive number R_{eff} by $0.1 - 0.2$ in 2020, particularly when implemented early [79], and by around 10% in 2021 [80]. In comparison, an unvaccinated-only weekly screening policy with a realistic (50%) compliance rate [72] and 58% vaccination rate, would reduce R_{eff} by an estimated 10.2% (Eq. (3.3)), decreasing further as vaccination rates increase, and compliance and isolation adherence decrease. Thus, while our analysis ranks vaccinate-or-test policies as potentially competitive with high-impact NPIs [79, 80], such screening will decrease in impact as vaccination rates inch higher. Because prior work has shown that pandemic countermeasures also vary in their impact depending on time, vaccination, and the presence of other NPIs or behaviors [80], an empirical assessment of vaccinate-or-test programs would be valuable. However, just as empirical estimates of NPIs' impacts on R_{eff} include wide uncertainty [79,80], similar estimates for unvaccinated-only screening programs are also likely to be highly uncertain.

Our study elucidates three critical transitions as vaccination rates increase. First, when vaccination rates are sufficiently high, a majority of the albeit reduced number of infections will be vaccine breakthrough infections. This fact should come as no surprise, as this transition must occur at some point for any vaccine below 100% effectiveness; for the delta variant, our modeling estimates it to take place between 63% and 75% vaccine coverage (baseline VE; 55-67% vaccinated with waning VE; 83-84% vaccinated with boosted VE), while for the omicron variant, we estimate it to take place between 55% and 59% vaccine coverage. Second, a transition to majority breakthrough hospitalizations will occur at some point greater than the transition to majority breakthrough infections, a natural consequence of $\text{VE}_P > 0$. Third, while community spread is driven by the unvaccinated at low vaccination rates, it is driven by the vaccinated population at high vaccination rates (Fig. 3.3). These vaccination rate transition points separating majority-unvaccinated transmission and majority-breakthrough transmission are driven lower by unvaccinated-only screening programs (Fig. 3.7). Taken together, these results suggest that while the overall number of infections during an outbreak decreases as vaccination rates increase, assuming $\text{VE}_S > 0$, vaccine breakthrough infections and transmission events from vaccinated individuals should not be surprising in highly vaccinated populations—

vaccine effectiveness is imperfect. Consequently, in anticipation of continued community transmission even in highly vaccinated communities, those at increased risk of severe COVID-19 should take additional precautions to limit their risk of infection or severe disease.

Our analyses identify two limitations of screening via testing programs in reducing community transmission which generalize beyond the specific scenarios investigated herein. First, the ability of a screening program to prevent community spread is restricted to a limited "envelope" of past infection rate and vaccination rate combinations such that R_{eff} without screening is greater than one, and R_{eff} with screening is less than one. Second, the width of that effective screening envelope, and thus the effectiveness of a screening program to control transmission more broadly, are highly sensitive to compliance and participation: weekly screening with 50% compliance—a rate which reflects observed compliance in a population with a weekly screening mandate [72]—is likely to be relatively ineffective. However, although our analyses focus on the benefits of testing in reducing transmission, testing also plays an important role in diagnosis and treatment, detection of variants, situational awareness and surveillance, and decreasing pressure on the healthcare system during outbreaks. Furthermore, testing focused on the unvaccinated population may provide additional incentives to get vaccinated and thus avoid regular testing. Our study did not explore the benefits of unvaccinated-only testing mandates for these additional purposes.

Our analysis is limited in at least three different manners. First, our modeling incorporated fixed parameters that are difficult to estimate in practice. For instance, while our analysis considered boosted, baseline, and waning scenarios for vaccines' reductions in susceptibility VE_S, infectiousness VE_I, and hospitalization given infection VE_P based on ranges of estimates in the current literature, few studies are available to guide estimates of similar risk reductions associated with prior SARS-CoV-2 infection, with or without vaccination (but see Refs. [81] and [85]). Moreover, real-time estimates for emerging variants of concern such as omicron require observational study and are thus unavailable for prospective policy analyses. Alternative parameter assumptions may be explored via the provided open-source code. Second, we assumed perfect isolation after receiving a positive test result. Were this assumption to be violated by imperfect or delayed isolation, we predict a proportional loss of screening impact across all scenarios.

Third, our model assumes values of R_0^{NPI} and immunity associated with the delta variant and plausible values for the omicron variant, but other emerging variants may dramatically shift the values of these parameters. These limitations affect the exact vaccination and past infection rates at which the three transitions identified in our study occur, and thus our analyses describe fundamental phenomena but do not make projections or predictions for specific communities.

Our analysis also uses a well-mixed SEIR model framework, inheriting two key limitations which merit direct discussion. First, we assume that vaccination and past infection statuses are uncorrelated at the population level. In reality, they may be anticorrelated due to the protective effects of vaccination, or because those with past infection may choose to forgo subsequent vaccination. We similarly assumed no homophily in contact patterns based on vaccination status, following the well-mixed assumption of the SEIR model framework, yet those who choose to be vaccinated may be more likely to be situated in a social network with others who choose to be vaccinated, and vice versa [100]. Second, compartmental SEIR models such as ours assume uniform infectiousness in the I compartment, contrasting empirical observations [101] and more sophisticated models [74, 99]. While our model's latent and infectious periods are well aligned with other SEIR models [76,102–104], they nevertheless lead to unrealistically long generation times. Decreasing these periods proportionally to achieve the same reproductive number while aligning more closely with generation time estimates [105] would change the time-scale across all simulations, but would not impact the cumulative metrics or dynamics discussed in our key results.

More broadly, our work is situated within a family of research which uses mathematical modeling to estimate the impact of targeted countermeasures or strategies in populations with heterogeneous susceptibility, transmissibility, and/or contact rates. Other areas of focus include the allocation of scarce personal protective equipment to reduce transmission [21], the prioritization of vaccines by subpopulation [15, 17, 106], proactive screening programs in specific workplace structures [107] or contact networks [76], immunity "passport" programs [99], or immune shielding strategies [108]. While our analyses are directed at SARS-CoV-2, this work illustrates contributes general principles to this literature by showing that screening programs focused on testing the unvaccinated may be less effective than hoped in the face of high vaccination

rates, waning vaccine effectiveness, or low compliance with testing.

3.4 Methods

3.4.1 SEIR model

Our analyses are based on a continuous time ordinary differential equation compartmental model with Susceptible, Exposed, Infectious, and Recovered (SEIR) compartments, stratified into vaccinated V and unvaccinated U groups. In addition to tracking infections among these two groups separately, we also tracked infections from both groups separately, enabling us to investigate four modes of transmission: from U to U, from U to V, from V to U, and from V to V. In all simulations, we used a constant total population size of $N = 20,000$ and denoted the vaccinated fraction of the population with ϕ.

To incorporate the possibility that individuals may have experienced prior infections, we further subdivided U and V into SARS-CoV-2 naive and SARS-CoV-2 experienced subpopulations, such that a fraction ψ of each was assumed to be previously infected and $1 - \psi$ remains naive. For notation, we denote the subpopulations of U to be u (unvaccinated, naive) and x (unvaccinated, experienced/prior infection), and the subpopulations of V to be v (vaccinated, naive) and h (vaccinated, experienced). We assumed that vaccination and SARS-CoV-2 experience statuses were fixed at the start of each simulation and immutable throughout, such that there was no ongoing vaccination, and individuals who were infected and recovered during each simulation were not reassigned to SARS-CoV-2 experienced status [109].

We denote the protective effects of immunity as XE, VE, HE, expressed as reductions in risk due to prior infection alone (x), vaccination alone (v), or prior infection and vaccination (i.e. so-called "hybrid" immunity; h), respectively. Immunity was modeled to (i) decrease the risk of infection upon exposure, (ii) decrease the risk of transmission upon infection, placing our vaccine and immunity model in the broader category of leaky models [110], and (iii) decrease the risk of disease progression (i.e., hospitalization) upon infection. Reductions in the risk of infection upon exposure (XE_S, VE_S, HE_S), reductions in the risk of transmission when infected (XE_I, VE_I, HE_I), and reductions in the risk of hospitalization when infected

(XE_P, VE_P, HE_P) were parameterized separately, based on ranges of estimates from the literature. Note that VE_H, the reduction in risk of hospitalization due to vaccination, is more commonly reported in the literature than VE_P, the reduction in risk of hospitalization due to vaccination conditional on infection. So, we used the formula $\text{VE}_P = 1 - \frac{1-\text{VE}_H}{1-\text{VE}_S}$ to estimate values for VE_P. We used the same relationship to estimate XE_P. See Online Supplementary Table 2. Due to broad uncertainty in these effects over time since exposure [81, 109] or vaccination [81–83], by vaccine manufacturer and schedule [84, 85, 111, 112], by context [97, 113], and by variant [85], our analyses intentionally consider a range of values. We assumed that hybrid immunity against infection, HE_S, and transmission, HE_I, would always be superior to either vaccination alone or prior infection alone, via the simple formula $\text{HE} = (1 - \text{XE})\text{VE} + \text{XE}$ and hybrid immunity against hospitalization given infection $\text{HE}_P = \max\{\text{VE}_P, \text{XE}_P\}$.

Supplementary Fig. 8 (available online) shows a model schematic diagram for the SEIR model used in the manuscript, where solid and dashed lines denote movement and transmission between classes, respectively. In lieu of including hospitalization as a model compartment, we computed total hospitalizations in each immunity class via multiplication of total infections, variant-specific infection hospitalization rates and $(1 - RR_P)$, where RR_P is the risk reduction against progression to hospitalization given infection (i.e., 0, VE_P, XE_P, or HE_P) (See Online Supplementary Tables 1 and 2).

To model a community with open boundaries, we included a uniform risk of exposure to infection from an external source at a rate of N^{-1} per person per day. For instance, in a completely naive population, S_u/N individuals would be infected per day. After including the protective effects of vaccination and past infection this resulted in importation of infections at per-capita rates of $(1 - \text{VE}_S)N^{-1}$, $(1 - \text{HE}_S)N^{-1}$, $(1 - \text{XE}_S)N^{-1}$, and N^{-1} new infections per day in the *v*, h, x, and u groups respectively.

All simulations were run for 270 days, and all individuals were initially in one of the susceptible compartments S_u, S_x, S_v, or S_h in proportions $(1 - \phi)(1 - \psi)$, $(1 - \phi)\psi$, $\phi(1 - \psi)$, and $\phi\psi$, respectively. Model equations were solved using *lsoda* solver from the package *deSolve*, R version 4.1.0.

3.4.2 Incorporation of community testing

Screening the unvaccinated population via community testing, and subsequent isolation of those testing positive, was modeled by increasing the rate at which infected individuals were removed from the unvaccinated I_u and I_x compartments. Similarly, universal screening regardless of vaccination status was modeled by increasing the rate at which infected individuals were removed from all I compartments, I_u, I_x, I_v and I_h. The effectiveness of screening tests was assumed to be equal for vaccinated and unvaccinated individuals. We estimated increased rates of removal taking into account (i) the calibrated trajectories of viral loads within individual infection [114], (ii) the relationship between viral load and infectiousness [74], (iii) the frequency of testing, (iv) the test's analytical sensitivity (i.e. limit of detection) and turnaround time [99], and (v) screening compliance and valid sample rates, i.e. the fraction of scheduled or mandated tests which actually produce a valid sample [72]. In particular, our adaptation takes a previous model [74, 99] and updates viral load dynamics for the delta variant of SARS-CoV-2 [115, 116], the dominant variant at the time of the present analysis. To incorporate the effectiveness of screening θ, we reduce the duration of infectiousness $1/\gamma$ by a factor $(1-\theta)$. Parameter values for θ are found in Supplementary Table 1 (available online), and are based on weekly PCR testing with a one-day turnaround, analytical limit of detection of 10^3 RNA copies per ml sample, and compliance rates of 50% (as in [72]) or 99% (as in [75]). These values assume that individuals immediately and successfully isolate upon receiving a positive diagnosis. We note that estimated effects of rapid antigen tests (with higher analytical limits of detection, but zero turnaround time) are highly similar to PCR testing under the assumptions above, provided that the community testing program frequencies and compliance rates are identical [74].

3.4.3 Transmission modes and forces of infection

Inclusive of all effects introduced above, the forces of infection are given by

$$\lambda_u = \alpha \left(\frac{I_u}{N_u} c_{u\to u} + [1 - \mathrm{XE}_I] \frac{I_x}{N_x} c_{x\to u} + [1 - \mathrm{VE}_I] \frac{I_v}{N_v} c_{v\to u} + [1 - \mathrm{HE}_I] \frac{I_h}{N_h} c_{h\to u} \right) + \frac{1}{N} \tag{3.1}$$

$$\lambda_i = \left[\alpha \left(\frac{I_u}{N_u} c_{u\to i} + [1 - \mathrm{XE}_I] \frac{I_x}{N_x} c_{x\to i} + [1 - \mathrm{VE}_I] \frac{I_v}{N_v} c_{v\to i} + [1 - \mathrm{HE}_I] \frac{I_h}{N_h} c_{h\to i} \right) + \frac{1}{N} \right] [1 - (RR_S)_i] \,, \tag{3.2}$$

where $i = \{x, v, h\}$, and reductions in susceptibility due to immunity are given by $(RR_S)_i = \{\mathrm{XE}_S, \mathrm{VE}_S, \mathrm{HE}_S\}$, correspondingly. The parameter α is the probability an unvaccinated, SARS-CoV-2 naive individual is infected by an infectious contact, tuned to achieve the desired R_0^{NPI}, $c_{i\to j}$ is the number of times an individual in group j is contacted by individuals from group i per day, and N_j is a convenience variable representing the number of people in subpopulation j.

To produce counts of how many infections were caused by each of the transmission modes $U \to U$, $U \to V$, $V \to U$, and $V \to V$, we integrated the appropriate terms of Eqs. (3.1) and (3.2) over the duration of each simulation. For instance, the cumulative number of vaccinated infections caused by the unvaccinated population is given by integrating over the forces of infection from u and x to *v* and h,

$$\begin{aligned} U \to V = \alpha \int_0^{270} \Bigg[& \frac{I_u(t)}{N_u} \Big(c_{u\to v} S_v(t)[1 - \mathrm{VE}_S] + c_{u\to h} S_h(t)[1 - \mathrm{HE}_S] \Big) \ \ldots \\ & + [1 - \mathrm{XE}_I] \frac{I_x(t)}{N_x} \Big(c_{x\to v} S_v(t)[1 - \mathrm{VE}_S] + c_{x\to h} S_h(t)[1 - \mathrm{HE}_S] \Big) \Bigg] dt \end{aligned}$$

3.4.4 Reproductive number

The basic reproductive number R_0 is defined as the expected number of secondary infections created by a typical infector in an entirely susceptible population, in the absence of any non-pharmaceutical interventions. Given the variety of environments in which SARS-CoV-2 spreads, and the presence of various permanent or semi-permanent non-pharmaceutical interventions, we use R_0^{NPI} in this work to denote

the reproductive number in an entirely susceptible population inclusive of varying levels of now-baseline NPIs for the delta, omicron, and future variants. We consider $R_0^{\text{NPI}} = 4$ (Main and Supplementary Figures) and $R_0^{\text{NPI}} = 6$ (Supplementary Figures). For unvaccinated-only screening programs, this model's effective reproductive number is given by

$$R_{\text{eff}} = R_0^{\text{NPI}} \left[f_u(1-\theta) + f_x r_x (1-\theta) + f_v r_v + f_h r_h \right] \ , \tag{3.3}$$

where $f_u = (1-\psi)(1-\phi)$, $f_x = \psi(1-\phi)$, $f_v = (1-\psi)\phi$, and $f_h = \phi\psi$ represent the fractions of the population in the unvaccinated, experienced, vaccinated, and hybrid immunity groups, respectively, and $r_x = (1-\text{XE}_I)(1-\text{XE}_S)$, $r_v = (1-\text{VE}_I)(1-\text{VE}_S)$, and $r_h = (1-\text{HE}_I)(1-\text{HE}_S)$ are the cumulative impacts of immunity on each group. Setting the above equation equal to a constant produces isoclines shown in plots throughout the paper. The reduction in R_{eff} due to screening is given by

$$R_{\text{no screening}} - R_{\text{screening}} = R_0^{\text{NPI}} \theta (1-\phi) \left[1 - \psi(1-r_x) \right] \ , \tag{3.4}$$

a function linear in each of its variables which goes to zero as the vaccination rate ϕ approaches 1.

For universal screening programs, similar calculations yield

$$R_{\text{eff}}^{\text{universal}} = R_0^{\text{NPI}} (1-\theta) \left[f_u + f_x r_x + f_v r_v + f_h r_h \right] \ , \tag{3.5}$$

differing from Eq. (3.3) only in the terms to which $(1-\theta)$ applies. For a complete derivation of these equations, see the Online Supplementary Materials.

3.5 Acknowledgements

The work presented in this chapter was co-authored by Casey E. Middleton, Kristen K. Bjorkman, Roy Parker and Daniel B. Larremore. I would additionally like to thank Stephen Kissler, Yonatan Grad, and Michael Mina for their helpful feedback. **Funding:** K.M.B. and C.E.M. were supported in part by the In-

terdisciplinary Quantitative Biology (IQ Biology) Ph.D. program at the BioFrontiers Institute, University of Colorado Boulder. K.M.B. was supported by the National Science Foundation Graduate Research Fellowship under Grant No. (DGE 1650115). C.E.M. and D.B.L. were supported in part by the SeroNet program of the National Cancer Institute (1U01CA261277-01). R.P. was supported by the Howard Hughes Medical Institute.

Chapter 4

Fundamental limits to the effectiveness of traveler screening with molecular test

Note: The work in this chapter is ongoing. The majority of the analyses have been completed and a draft for publication is in preparation.

4.1 Introduction

Air travel is a major driver of the geographic spread of emerging infectious diseases, directly linked to the international spread of SARS in 2003, influenza A/H1N1 in 2009, and SARS-CoV-2 in 2020 [117–119] as well as the importation of cases of influenza A/H7N9, MERS-CoV, Ebola, Lassa fever and Chikungunya [117,120–122]. Although screening travelers for symptoms of infection may therefore seem like an intuitive countermeasure, scenario modeling [117, 119, 120, 123, 124] and overwhelming empirical evidence [125–129] show that syndromic and questionnaire-based screening programs are ineffective. For example, one modeling study found that even with a theoretical symptom-based test with perfect sensitivity, fewer than 3%, 9%, 10% and 35% of infected travelers would be detected for Ebola, SARS-CoV-2, SARS-CoV-1 and influenza, respectively [130].

An infected traveler may be missed by screening for two reasons. First, their infection may be undetectable at the time they are screened. For instance, syndromic screening will fail to identify asymptomatic and pre-symptomatic travelers. Second, their infection may be detectable in principle, yet missed because of imperfect test sensitivity. For instance, a thermometer may fail to detect a fever or a person's symptoms may differ from those surveyed. Novel rapid molecular tests appear to address both of these issues, offering high

sensitivity and specificity over a long detectable window with rapid turnaround. These observations lead us to ask whether there are settings where screening travelers for an infectious disease with a state-of-the-art molecular test could be effective in preventing or delaying an outbreak at travelers' destination.

Unfortunately, empirical evidence is limited. While molecular tests were used for traveler screening during the COVID-19 pandemic [131, 132], the countries that most successfully prevented or delayed transmission of SARS-CoV-2 such as New Zealand, Australia, Hong Kong, and Taiwan also had strict border controls, post-arrival quarantine measures, widespread testing, or contact tracing. As a result, it is unclear what role molecular testing of travelers per se played in practice, and what little evidence we do have (reviewed in [133]) covers only the number of individuals screening positive, but not programs' effectiveness or impact on delaying transmission. In place of empirical data, modeling studies offer various estimates. For example, a PCR test within the 24 hours before departure is predicted to reduce the number of infectious or pre-infectious travelers by 31% [134], while a PCR test within 3 days of departure is predicted to reduce the cumulative number of infectious days over the travel period by 36%, and would identify 88% of actively infectious travellers on the day of the flight [135]. Screening at airports has been projected to reduce post-arrival transmission risk by 37-47% for rapid diagnostic tests (RDTs) [136] or 28-50% for PCR or RDTs [137].

These modeling efforts have thus offered valuable estimates, but raise two key questions which form the focus of this paper. First, why do molecular tests not perform better in traveler screening, despite their high sensitivity? Second, how do these results extend to other settings and pathogens? To answer these questions, we introduce a probabilistic model that incorporates within-host viral kinetics to evaluate the screening effectiveness of four example pathogens, influenza A, SARS-CoV-1, SARS-CoV-2, and Ebola virus. This modeling framework incorporates variation in individuals' post-travel transmission potential based on variability in individuals' viral load trajectories and differences in when individuals travel during their infection. It is generalizable and could be adapted for novel pathogens of concern or other testing settings like pre-event screening.

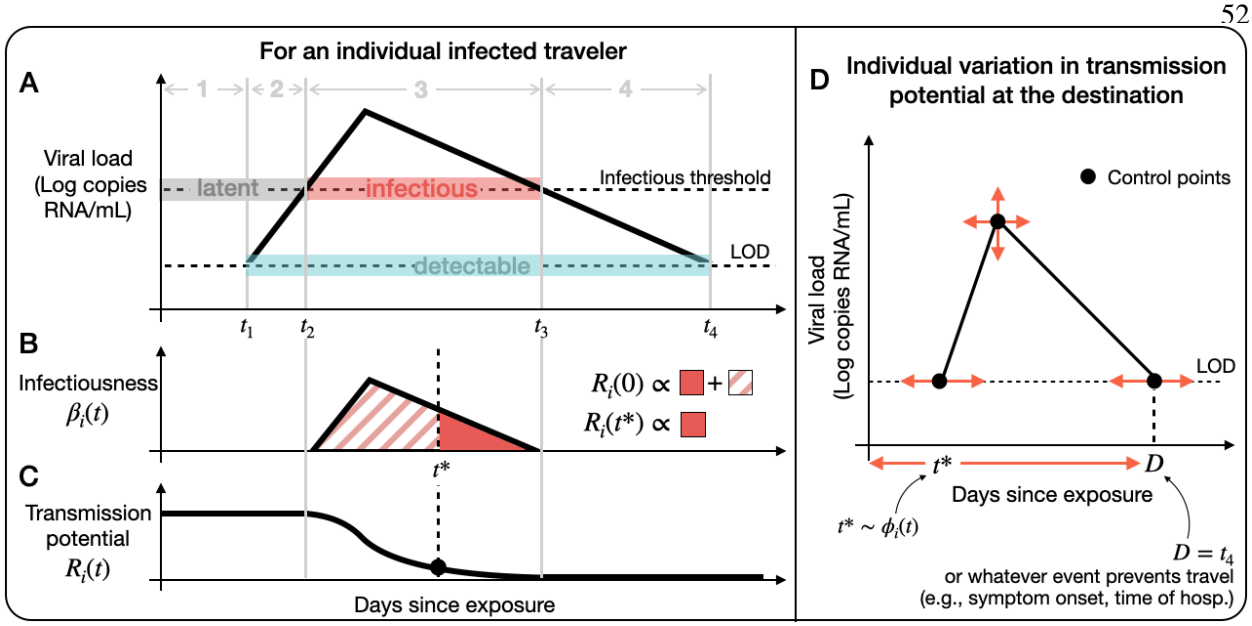

Figure 4.1: **Model diagram.** An example (**A**) viral load, (**B**) infectiousness $\beta_i(t)$, and (**C**) transmission potential $R_i(t)$ for an individual infected traveler i, with travel time t^* and post-travel transmission potential $R_i(t^*)$. There are four possible statuses for infected travelers: (1) not yet detectable or infectious, (2) detectable and not yet infectious, (3) detectable and infectious, (4) detectable and no longer infectious. (**D**) Factors that contribute to variation in $R_i(t^*)$: Stochastic realizations of viral load control points (first and last time detectable, peak viral load), when people may travel $[0, D]$, and the simulated travel time t^* drawn from $\phi_i(t)$, the infection age distribution among infected travelers.

4.2 Results

4.2.1 Model for traveler screening

From a public health perspective, the most important infections for a traveler screening program to catch are those most likely to infect others during or after travel, and the least important are those with little to no remaining infectiousness. To incorporate this concept into a mathematical model, we quantify an individual's post-travel transmission potential using a simple within-host viral kinetics model (Fig. 4.1). We define individual i's post-travel transmission potential, $R_i(t^*)$, as the expected number of secondary infections generated after traveling at time t^*. This approach accounts for variation in individual reproductive numbers and infection age at time of travel.

We considered two different approaches to quantify traveler screening effectiveness. First, we consid-

ered the number of infected travelers required to attempt travel to likely generate an outbreak with screening in comparison to no screening (ΔN). To calculate ΔN, we used theory from stochastic processes about the long-term probability of extinction to compute the number of infected travelers required to cause an outbreak with probability $p = 0.9$. Second, we considered how long it takes for an outbreak of size X to occur at the destination with screening in comparison to no screening (Δt). To calculate Δt, we assumed that the number of infected travelers arriving at the airport followed a Poisson process with mean λ infected travelers per day. We simulated transmission chains initialized by infected travelers at the destination until X infections had occurred.

Throughout this work, we make highly optimistic assumptions about test performance, assuming instantaneous tests results, perfect compliance, and a limit of detection (LOD) equal to that of RT-PCR (hereafter PCR), the gold standard LOD currently achievable for the diseases in this study. We assume 100% sensitivity above the limit of detection. For currently available technology, these assumptions are unrealistic because there is a tradeoff between sensitivity and turnaround time: PCR tests do not give instantaneous results and rapid tests are less sensitive [74]. However, making these optimistic assumptions allows us to characterize the best-case scenario, and thus the *potential* effectiveness of screening programs.

We considered two screening scenarios when an outbreak is growing exponentially at the departure location: no screening and exit screening at the airport via molecular test. We do not consider the combination of exit and entry screening because previous modeling work has found marginal gains by entry and exit screening when the screening method has high sensitivity [117, 123].

4.2.2 Screening effectiveness to delay transmission

We simulated 5,000 infected travelers for four example pathogens: SARS-CoV-1, SARS-CoV-2, influenza A, and Ebola. We chose these pathogens to explore different areas of parameter space, and because traveler screening programs have been implemented for all of them. Then, we ran 20,000 simulations of the traveling process, sampling new infected travelers arriving at the airport from the 5,000 travelers until an outbreak was likely triggered (Fig. 4.2A, B). To calculate the time until an outbreak of size X occurs at

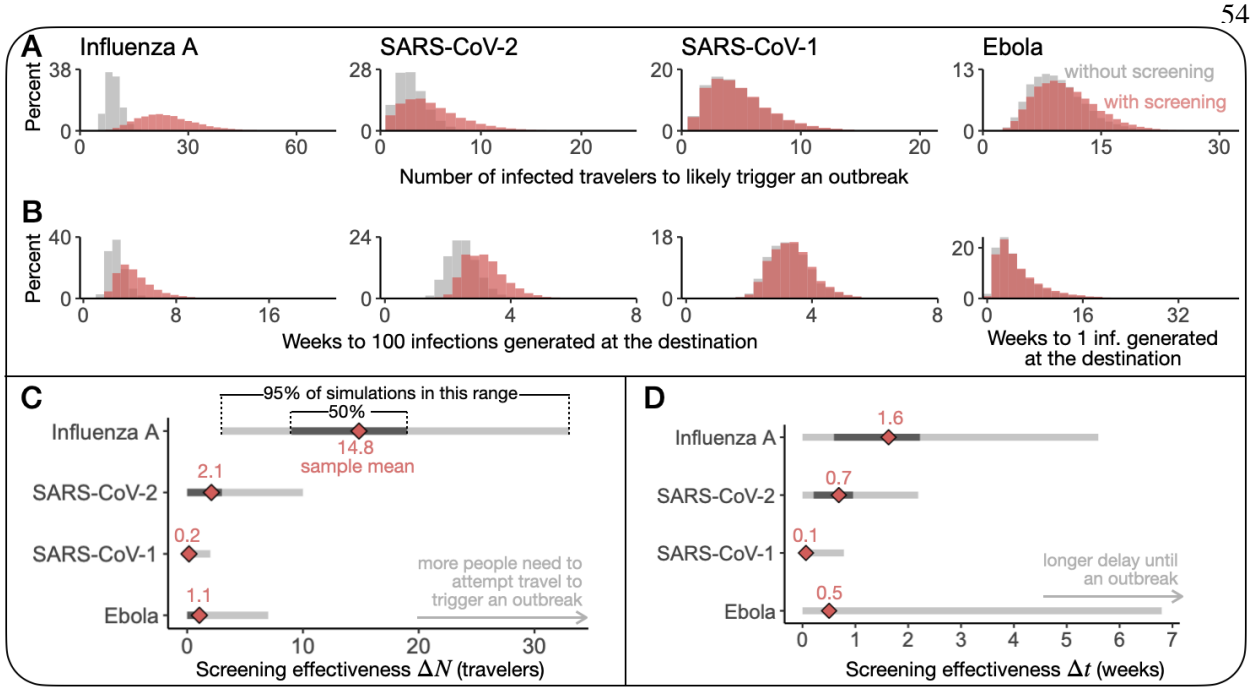

Figure 4.2: **Screening effectiveness to delay transmission is limited and highly variable.** Histograms of (**A**) the number of infected travelers to likely trigger an outbreak with (pink) and without screening (gray) and (**B**) the time to X infections generated at the destination with (pink) and without screening (gray) from 20,000 Monte Carlo simulations. $X = 100, \lambda = 1$ per day for SARS-CoV-1, SARS-CoV-2, and influenza A. $X = 1, \lambda = 2$ per month for Ebola. (**C, D**) Distributions of ΔN and Δt from 20,000 Monte Carlo simulations (sample mean (pink diamond), IQR (dark gray) and 95% percentile range (light gray)).

the destination, we considered a plausible scenario for each pathogen. For SARS-CoV-1, SARS-CoV-2, and influenza A, $X = 100$ and $\lambda = 1$ infected traveler attempting travel per day on average. For Ebola, $X = 1$ and $\lambda = 2$ per month. We considered a different scenario for Ebola because, due to the severity of symptoms, any local transmission would be of concern, and sustained local transmission is relatively rare so $X = 100$ is less appropriate. We also expect the arrival rate of infected travelers to be less frequent because Ebola's generation interval is much longer than respiratory pathogens and non-pharmaceutical interventions can usually bring Ebola transmission under control, or nearly so.

Of the four pathogens we considered, traveler screening is most effective for influenza A. With screening in place, it takes an average of 15 more infected individuals to attempt travel to trigger an outbreak in comparison to no screening program (Fig. 4.2C). In units of time, screening delayed an influenza A outbreak by 11.1 days on average (Fig. 4.2D). However, there is considerable variation in both of these outcomes,

so it is important to consider the full distribution, and not just the mean, when interpreting these results. One way to understand this variation is to consider the range of the outcomes, like the spread of the middle 50% of the data (Fig. 4.2C, D). Another way to understand this variation is to compute the probability that screening delayed an outbreak by at least x infected travelers or x days. For example, screening delayed an outbreak by at least a week in 57.6% of simulations for influenza A. See Supp. Table A.1 for more values of x.

Traveler screening was less effective for the other three pathogens. The average ΔN was 0.2, 1.1, and 2.1 infected travel attempts for SARS-CoV-1, Ebola, and SARS-CoV-2, respectively. Screening delayed outbreaks by 0.4, 3.5, and 4.8 days on average for SARS-CoV-1, Ebola, and SARS-CoV-2, respectively (Fig. 4.2D). Once again, it is important to consider the variation in these outcomes. For example, the average value of Δt for Ebola makes it seem like screening will usually delay the first secondary case by a couple of days, but in over 50% of simulations, there is no delay at all. Screening delayed an outbreak by at least a week in 1.4%, 9.3%, and 23.4% of simulations for SARS-CoV-1, Ebola, and SARS-CoV-2, respectively.

4.2.3 Fundamental limit of traveler screening

Ideally traveler screening would prevent an outbreak at the destination, or delay transmission long enough to enable some public health activation. However, even for influenza A, which had the most effective traveler screening programs on average, individual trial results varied greatly, and sometimes screening did not delay transmission at all (Fig. 4.2C, D). Why is screening not more reliably effective, especially under highly optimistic assumptions about detectability and test sensitivity?

To answer this question, we observe that, for any test or pathogen, there always exists a gap between when someone is infected and first detectable. This implies that there is a window of time when an infected individual may travel and is undetectable at the airport. Crucially, travelers who are missed by screening during this window have all of their transmission potential remaining (Fig. 4.3A). Thus, the travelers with the most transmission potential are impossible to catch.

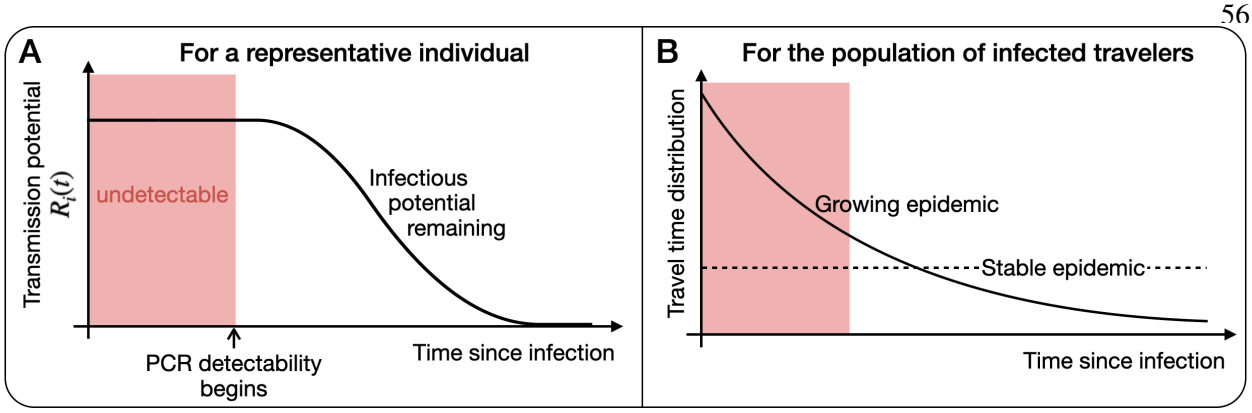

Figure 4.3: **The effectiveness of screening travelers is fundamentally limited by the gap between infection and detectability.** **(A)** Individual's are undetectable by molecular testing when their transmission potential is highest, fundamentally limiting the effectiveness of traveler screening because infected people may travel during this window. **(B)** A growing epidemic exacerbates this fundamental limit because the infection age distribution among infected travelers is positively skewed in comparison to a stable epidemic.

To quantify how this window of time limits traveler screening effectiveness, we calculated the expected proportion of transmission potential that is detectable by screening,

$$1 - \frac{E[\int_0^{t_1} R_i(t)\phi_i(t)dt]}{E[\int_0^{\omega} R_i(t)\phi_i(t)dt]}, \tag{4.1}$$

for all individuals i with transmission potential. Using the notation from Fig. 4.1, t_1 is the time i is first detectable, and ω is the time i is either no longer infectious or no longer able to travel ($\omega = \min(t_3, D)$). The infection age distribution among infected travelers, $\phi_i(t)$, is a mixture of the infection age distribution and the propensity to travel at a particular age.

We found that, during a growing epidemic, only 2.8%, 9.7%, 40.2% and 59.8% of transmission potential is expected to be detectable by traveler screening via molecular test for SARS-CoV-1, Ebola, SARS-CoV-2, and influenza A, respectively. Our estimate for SARS-CoV-2 is comparable to other modeling studies that found testing reduced post-arrival transmission risk by 29–53% [136, 137].

Expression 4.1 represents a fundamental limit to the effectiveness of traveler screening. Because of the gap between infection and detectability, the fraction in Expression 4.1 is always positive. Consequently,

traveler screening alone can never eliminate the risk of local transmission at the travel destination. Furthermore, during a growing epidemic, most of the infected traveling population would travel during this early window of undetectability coincides (Fig. 4.3B), exacerbating the consequence of this fundamental limit.

4.2.4 Ascertainment overestimates transmission reduction.

Although difficult to measure in practice, a common approach in modeling studies to evaluate the effectiveness of a screening program is to estimate ascertainment, the percentage of infections detected out of all the infections screened. Out of the 5,000 simulated travelers, we found that ascertainment is extremely low for SARS-CoV-1 and Ebola (3.1% and 10.5%, respectively), and better but still imperfect for SARS-CoV-2 and influenza A (47.8% and 70.9%, respectively). Our estimate of SARS-CoV-2 ascertainment is similar to an empirical estimate from testing at U.S. airports during 2022 (52%) [138].

The ascertainment rate of infected travelers is potentially misleading because it overestimates reductions in transmission at the destination. This occurs because one counterintuitive consequence of traveler screening is that undetected travelers typically have higher post-travel transmission potential than those who are detected. We found that the average $R_i(t^*)$ among undetected travelers is 2.6, 1.8, 2.5, and 1.2 for SARS-CoV-1, Ebola, SARS-CoV-2, and influenza A, respectively, while for detectable travelers, it is 2.8, 1.7, 1.8, and 0.8. This pattern occurs because many of the detected infected travelers are near the end of their course of infection and have little to no transmission potential (Supp. Fig. A.1). Moreover, for all four pathogens, the percent of post-travel transmission potential that is detectable by screening is always less than the corresponding ascertainment rate.

4.2.5 Sensitivity Analysis

The effectiveness of traveler screening is always limited by the amount of time people are infected before they are detectable. How variable is such imperfect screening effectiveness across different epidemic scenarios, test characteristics, infectiousness profiles and traveling behaviors?

Across various epidemic scenarios ($\lambda = \{1 \text{ per day}, 1 \text{ per week}, 2 \text{ per month}\}$, $X = \{1, 10, 100\}$),

we intuitively found that it takes longer for an outbreak to occur with screening in place when infected people travel less frequently or when the outbreak threshold is larger (Supp. Figs. A.2, A.3, A.4, and A.5). However, even in the best case scenario ($\lambda = 2$ per month, $X = 100$), Δt remains highly variable. For example, in this scenario, the average delay to 100 influenza A infections is 95.8 days, yet Δt is less than a week in 38.9% of simulations (Supp. Fig. A.2). We found negligible differences in ΔN and Δt when modeling the rate at which infected people attempt travel as either a homogeneous or non-homogeneous Poisson process as in [123].

Infectious thresholds are reported in the literature for SARS-CoV-2 and influenza A (Table A.2) but not for SARS-CoV-1 or Ebola. For these pathogens, we chose infectious thresholds so the distribution of $R_i(0)$ are similar to the gamma distribution with mean R_0 and dispersion parameter k [139] and ran sensitivity analyses with thresholds 10x larger and 10x smaller. A lower infectious threshold decreases the amount of time it takes to generate X infections at the destination because more infected travelers have post-travel transmission potential (Supp. Fig. A.6). However, the change in the average ΔN and Δt due to different infectious thresholds was at most 1 person or 2.4 days (Supp. Figs. A.7, A.8, A.9, and A.10).

Finally, we assume the probability an individual travels is uniform from infection to viral clearance for SARS-CoV-2 and influenza A. For SARS-CoV-1 and Ebola, we assume symptoms prevent travel, limiting travel from infection to the time of hospitalization. If symptom severity did not impede travel for these pathogens, screening would be more effective because travelers are more likely to be detectable. The mean Δt increased from 3.5 to 7.9 days for Ebola, (Supp. Fig. A.11) and from 0.5 to 3.8 days for SARS-CoV-1 (Supp. Fig. A.12).

4.3 Discussion

This study modeled the potential effectiveness of traveler screening programs with highly sensitive molecular diagnostics to delay transmission at the destination. Overall, we found that screening effectiveness is generally quite limited, or at best, highly variable. Of the four pathogens we considered, traveler screening was most effective for influenza A, but even in this case with extremely optimistic assumptions about test

performance, over 40% of post-travel transmission potential is *not* preventable by screening. This limitation is exemplified by what we refer to as the fundamental limit of traveler screening. The idea is simple: the effectiveness of traveler screening programs will always be limited because, for every diagnostic test and pathogen, the newest infections with the most remaining transmission potential are impossible to catch. Even with state-of-the-art tests where people are detectable before they are infectious, there is a window of time after the infection event when individuals are not yet detectable and may travel, and their infectious period will not begin until they are at the destination.

The consequences of this fundamental limit are exacerbated during a growing epidemic, precisely when traveler screening programs would likely be implemented, because infections are more likely to be recent. This fact reinforces the idea that any post-screening countermeasures such as arrival quarantines should be sized and scoped for the full duration of when infections are likely undetectable [137], or in the case of syndromic screening, the full incubation period [130].

The fundamental limit can help us understand when traveler screening programs are more likely to be effective. The best case scenario for screening would involve a pathogen such that people are detectable very quickly after infected (ideally within hours [130]) or, if individuals are undetectable for a long period of time, they have low post-travel transmission potential (i.e., t_1 and $R_i(t)$ are negatively correlated). Additionally, screening is more likely to be effective if transmission is highly dispersed simply because most individuals who are missed by screening are unlikely to infect others [139]. Importantly, this notion of controllability differs from that of Fraser et. al. [140] and Middleton and Larremore [141], who focus on the existence of detectability before infectiousness. While necessary for traveler screening effectiveness, this condition is insufficient. One also needs no undetectable window.

While molecular tests are typically more sensitive than syndromic screening, they are not always superior for traveler screening. For example, we found traveler screening via molecular tests is extremely ineffective for SARS-CoV-1, even though it is considered a controllable pathogen [140]. This discrepancy is due to symptom onset occuring before infectiousness and typically before detectability by PCR. In the initial

days post symptom-onset, 50-80% of infections test PCR negative with nasopharyngeal aspirate samples [142–147], possibly because viral replication starts in the lower respiratory tract [142]. Thus, effective screening depends on the natural history of the disease.

This work assumes the goal of traveler screening is to delay or prevent local transmission at the destination, yet screening may also be used for general surveillance, sequencing, and public awareness of an ongoing outbreak. For example, in Venezuela in 2021, the introduction of the SARS-CoV-2 Omicron variant was rapidly detected in samples from airport screening [148]. Our work cautions that measurements of prevalence among travelers are likely to be poor, even with a state-of-the-art test, yet could be corrected using our model's ascertainment estimates.

Our findings are subject to a number of limitations. First, the exact effectiveness of screening programs will depend on whether our model truly captures viral kinetics and infectiousness profiles. The data available to parameterize viral load trajectories varies widely in quality and quantity. For example, the control points for the log viral load hinge function are well-established for SARS-CoV-2, but often meager or nonexistent for other pathogens. In these cases, we used the best estimates available or extrapolated plausible ranges from other available information like the percent of PCR positivity upon hospitalization (Table A.2). Additionally, while the use of log viral load as a proxy for infectiousness is supported in the literature (SARS-CoV-1 [140, 149], SARS-CoV-2 [150, 151], Ebola [152], influenza A [153]), other relationships between viral load and infectiousness [74, 154], or other proxies for infectiousness [155, 156], are possible.

Another limitation of this model is that the simplistic model of $\beta_i(t)$ assumes that all variation in individuals' transmission potential is due to their viral load, and not differences in social contacts or behavior. This model also excludes other modes of transmission like post-mortem transmission that is known to be an important driver in the spread of Ebola. Improved characterization of individual viral load trajectories, and how they relate to infectiousness, symptoms and behavior, would greatly improve the impact and value of this, and other [74, 141, 157], modeling studies. Moreover, while the simple triangular model of $\beta_i(t)$ is used

in other modeling studies [141, 158], the modeling framework is flexible and more sophisticated functional forms of $\beta_i(t)$ could capture time-varying contact patterns or behavior.

We assumed tests have a highly sensitive PCR limit of detection, around $10^{2.6}$ copies of RNA/mL (Table A.2). One way to improve screening effectiveness would be to design tests with a lower limit of detection so individuals are detectable earlier. Lower PCR limits of detection are physically possible, for example by using more sensitive PCR enzymes or optimizing the PCR conditions, but reliability at lower thresholds is very challenging. We did not consider lower LODs because rapid tests that could be realistically used at the airport are typically designed for quick and easy detection of higher levels of viral load, so a lower LOD than the already optimistic PCR LOD is highly unlikely in this setting, and detecting lower viral loads would be unreliable. Any operational delays in testing would substantially lower screening effectiveness, so our results represent an upper bound on the potential effectiveness of traveler screening.

More broadly, our work is situated within a family of research which uses mathematical modeling to evaluate different testing scenarios. Other areas that our modeling framework could easily extend to include pre-event testing [136, 157], screening in combination with other interventions such as quarantine or contact tracing [119, 134, 135, 137], and combining multiple screening methods such as fever screening and health questionnaires with molecular testing [117, 120].

Traveler screening programs are typically expensive and resource intensive to implement. Our results suggest that, while traveler screening may delay an outbreak at the destination, combining traveler screening with other interventions is necessary to more consistently delay, or ideally prevent, an outbreak post-travel. Unfortunately, screening travelers with more sophisticated rapid molecular diagnostics will not be as effective as hoped at delaying transmission because the travelers with the highest transmission potential are likely impossible to detect.

4.4 Methods

4.4.1 Approximation of $R_i(t)$

Let $\beta_i(t)$ be the infectiousness of a single individual i at time t during their course of infection. We assume that $\beta_i(t)$ reflects infectiousness and an average over typical behavior in the absence of interventions. Mathematically,

$$R_i(t) = \int_t^\infty \beta_i(\tilde{t}) d\tilde{t}, \tag{4.2}$$

where $R_i(t)$ is the expected number of secondary infections i will generate after time t. Here, $R_i(0)$ is i's individual reproductive number and the population-level basic reproductive number $R_0 = E[R_i(0)]$. The individual reproductive number is also commonly referred to as ν [139] or simply R_i. $R_i(t)$ is a monotonically decreasing function, which is biologically realistic: the number of expected secondary transmission events ahead in time decreases as an individual's infection progresses (Fig. 4.1C).

To compute $R_i(t)$, we approximate $\beta_i(t)$ using a simple within-host viral kinetics model with an infectious threshold as a proxy for infectiousness over time (Fig. 4.1A, 4.1B). The within-host model assumes there is a period after infection where the virus is undetectable, and then a proliferation phase of exponential growth followed by a clearance phase of exponential decay. This type of log-linear proliferation and clearance model, sometimes referred to as a hinge or tent function, is commonly used to describe the proliferation and clearance phase of viral infection [74, 116, 157, 159]. We assume there is an infectious threshold such that infectiousness is proportional to log viral loads above this threshold.

For SARS-CoV-2 and influenza A, we found estimates for the infectious threshold in the literature (Table A.2). For SARS-CoV-1 and Ebola, we estimated infectious thresholds to result in distributions of $R_i(0)$ similar to the gamma distribution with mean R_0 and dispersion parameter k, a typical choice for the distribution of individual reproductive numbers [139]. Fitting the infectious threshold directly to the gamma distribution would assume that all the variation in individual reproductive numbers is due to differences in viral loads. However, we know that other factors contribute to differences in individual reproductive

numbers so we would not expect the distribution of $R_i(0)$ from the viral load model to identically match the distribution of $R_i(0)$ fit to contact tracing data. We checked how sensitive our results were to the infectious threshold value in the sensitivity analyses (Supp. Fig. A.6, A.7, A.8, A.9, A.10).

4.4.2 Simulations

Each simulated infected traveller is assigned a time they are first and last detectable by a molecular test with a PCR limit of detection, a time and magnitude of peak viral load, and a time of hospitalization (for SARS-CoV-1 and Ebola) sampled from the distributions in Table A.2. Some of these distributions are hard to estimate in practice so the distributions used were optimistic estimates informed by existing literature when well-characterized distributions were not available (Described further in the Supp. Materials). Individuals' travel times t^* are sampled from the infected travelers infection age distribution $\phi(t)$ using the inverse CDF method (see Section 4.4.5). With these parameters, we compute individuals' $R_i(t^*)$ and screening result at the time of travel.

For each individual, we simulate their contribution to infection at the destination using a branching process in which the offspring distribution of the first generation is a Poisson distribution with $\lambda = R_i(t^*)$, and for subsequent generations, a Negative binomial distribution with mean R_0 and a disease-specific dispersion parameter k [139]. If i is not detected, the simulated branching processes are identical with and without screening. This approach of comparing counterfactual scenarios ensures our results reflect the impact of screening alone and not the stochasticity of transmission.

4.4.3 Number required to likely trigger an outbreak

Following Clifford et. al. [123], we can calculate the long-term probability of disease extinction with offspring distribution NegBinom(R_0, k), s_0, from the implicit equation

$$s_0 = (1 + \frac{R_0}{k}(1 - s_0))^{-k}.$$

Let s_i be the long-term probability of disease extinction in a population where the first generation of infections is caused by infected traveler i with transmission potential $R_i(t^*)$, and each subsequent generation follows NegBinom(R_0, k). Then,

$$\begin{aligned} s_i =& \mathbb{P}(Z=0) + \mathbb{P}(Z=1)\cdot s_0 + \mathbb{P}(Z=2)\cdot s_0^2 + \mathbb{P}(Z=3)\cdot s_0^3 + ... \\ =& e^{-R_i(t^*)} + R_i(t^*)e^{-R_i(t^*)}s_0 + \frac{R_i(t^*)^2}{2!}e^{-R_i(t^*)}s_0^2 + \frac{R_i(t^*)^3}{3!}e^{-R_i(t^*)}s_0^3 + ... \\ =& e^{-R_i(t^*)(1-s_0)}. \end{aligned}$$

As in [123], the probability that infected traveler i causes an outbreak at the destination is $q_i = 1 - s_i$.

To calculate N, the number of infected travelers required to trigger an outbreak, we know that the first $N-1$ travelers did not cause an outbreak. If $q_i = q$ for all infected travelers, $X \sim$ geometric(q) so

$$P(X \leq k) = 1 - (1-q)^k.$$

However, since q_i is dependent on an individual's $R_i(t^*)$, q_i is a random variable so

$$P(X \leq n) = 1 - (1-q_1)(1-q_2)...(1-q_n)$$

for n infected travelers. For each run of our model simulation, we can use this equation to compute the number of infected travelers N required to cause an outbreak with probability p. For our analyses, we set $p = 0.9$.

4.4.4 Time to X infections generated at the destination

To compute this outcome via simulation, we first generate an arrival time for an infected traveler and simulate any transmission chains they generated using the distributions described above. We store the first X subsequent cases and the timing of infection using the pathogen-specific generation interval. Then, we generate the arrival time of the next infected traveler. If this infected traveler arrived before the last stored case, or the number of cases at the destination is less than X, we repeat these steps until the requirements have been met. The output, time to X infections generated at the destination is the time of the X^{th} infection.

4.4.5 Infection age distribution

We assume traveler screening programs would be implemented at the beginning of an emerging infectious disease outbreak when infections are growing exponentially. So, as previously described in [117], the probability that an infected traveler has infection age t at the time of travel is

$$\phi(t) = \begin{cases} \frac{\frac{R_0}{D} e^{\frac{-R_0}{D} t}}{1-e^{-R_0}}, & t \in [0, D] \\ 0, & t > D \end{cases}$$

where D is the duration of infection in which an infected individual is assumed to travel. If the disease does not prevent someone from traveling, D is the time from infection to viral clearance. If symptoms prevent an individual from traveling, we assume D is the average time from infection to hospitalization.

The corresponding CDF is the probability that an infected traveler was infected less than or equal to t days before travel,

$$F(t) = \begin{cases} \frac{1-e^{\frac{-R_0}{D} t}}{1-e^{-R_0}}, & t \in [0, D] \\ 0, & t > D. \end{cases}$$

4.5 Acknowledgements

The work presented in this chapter was developed in collaboration with Casey Middleton, Dan Larremore and Katie Gostic. I additionally want to thank Stephen Kissler and Ellen DeGennaro for their feedback. **Funding:** K.M.B. was supported in part by the Interdisciplinary Quantitative Biology (IQ Biology) Ph.D. program at the BioFrontiers Institute, University of Colorado Boulder, and by the National Science Foundation Graduate Research Fellowship under Grant No. (DGE 1650115). D.B.L. was supported in part by an NSF Alan T. Waterman Award (SMA-2226343).

Chapter 5

Conclusion

The chapters of this thesis highlight how a variety of mathematical modeling approaches and analyses can directly inform decision-making regarding infectious disease interventions. In Chapter 2, we developed an age-structured SEIR-type model to explore who should be prioritized for the first doses of a COVID-19 vaccine when initial supplies were limited. We identified that prioritizing the oldest adults first is a robust choice to minimize deaths in comparison to other age-based prioritization strategies. Next, in Chapter 3, we modeled SARS-CoV-2 transmission dynamics in populations with mixed immunity in light of evaluating the impact of unvaccinated-only testing programs. We found that in communities with mixed vaccination status, vaccinate-or-test policies can be highly effective but only within a restricted region of epidemiological parameter space. In areas with high vaccination rates, testing the remaining unvaccinated population averts few infections, hospitalizations and deaths in both relative and absolute terms. Finally, in Chapter 4, we modeled the potential effectiveness of traveler screening programs with highly sensitive molecular diagnostics to delay transmission at the destination for various pathogens. We found that screening effectiveness is generally quite limited, or at best, highly variable, because of an concept we term the fundamental limit to traveler screening: the effectiveness of traveler screening programs is always limited because, for every diagnostic test and pathogen, the newest infections with the most remaining transmission potential are impossible to catch.

5.1 Significance

Altogether, these studies achieve the two broad goals described in Chapter 1. The first goal was to deepen scientific knowledge of the role of individual variation in infectious disease transmission and to target interventions in light of such variation. Chapter 2 accomplished this goal by highlighting the importance of age in the dynamics and outcomes of SARS-CoV-2 transmission. The result of prioritizing those 60+ to minimize deaths was such a robust choice across a wide range of scenarios because of the exponential increase in the infection fatality rate by age. In Chapter 3, stratifying by immune status was necessary to explore how the effectiveness of vaccinate-or-test policies depends on population-level immunity. The results challenged our intuition that routinely testing the unvaccinated would be most effective when the unvaccinated are driving the majority of transmission. In Chapter 4, explicitly including variation in individuals' infection ages at the time of travel was crucial for understanding and quantifying how the gap between infection and detectability fundamentally limits the effectiveness of traveler screening.

The second goal was to use the results from the first goal to identify specific and realistic recommendations for public health policy. The work described in Chapter 2 accomplished this goal by defining clear and straightforward recommendations for vaccine prioritization. Furthermore, this work was presented to the WHO SAGE working group on COVID-19 vaccines during the summer of 2020. The work in Chapter 3 also accomplished this goal, by demonstrating the small impact unvaccinated-only testing programs would likely have in settings with high vaccination rates, like many university campuses. The University of Colorado Boulder considered this result when designing their requirements for in-person schooling in fall 2021. Since the work in Chapter 4 is not yet published at the time of writing, this work has not influenced relevant policy. However, the results still accomplish the goal of providing clear and actionable recommendations regarding the expected effectiveness of traveler screening programs.

5.2 Limitations

Each study here has limitations, as already discussed in detail in each chapter. Two consistent limitations that apply to all three studies are (1) the difficulty to model and predict changes in human behavior

as it relates to disease transmission and (2) the difficulty to retrospectively evaluate the effectiveness of interventions because counterfactual scenarios are hard to measure in practice. Ideally, we would be able to compare how outbreaks progress over time in socially and geographically similar locations with similar immunity profiles and disease states that implement distinctly different policies, but these conditions rarely exists in practice. However, one way to validate the robustness of our results in light of these two limitations is to compare our results to other modeling studies. For example, since the work in Chapter 2 was published, other modeling groups have found similar results and conclusions [17, 160–162]. This addresses the first limitation since different modeling groups often make different assumptions about contacts and behavior, but the general results remain true regardless of these details. Similarly, it helps build trust in the policy recommendations in place of analyzing counterfactual situations.

It is also worth stating that these models are not intended to forecast the exact number of infections, deaths, etc. that will occur. Rather, the types of analyses described in Chapters 2-4 are meant to help us understand possible contagion scenarios, and general principles about the effectiveness of different interventions.

5.3 Future Research

The work presented in this thesis provides clarity on who to prioritize first for COVID-19 vaccines, when unvaccinated-only testing policies are likely to be effective in populations with mixed immunity, and the effectiveness of traveller screening programs. In the following sections, I will describe a few possible directions for future work inspired by Chapters 2-4.

5.3.1 Updating contact matrices for changing demographics

In Chapter 2, we used age-structured contact matrices from Prem et. al. to model how different age groups interact with each other [32]. Contact matrices, which describe how often different age groups typically interact with each other on a daily basis, are typically generated from diary-based contact surveys. Prem et. al. developed synthetic contact matrices for 177 geographical regions in the COVID-19 era, extrap-

olating empirical contact matrices to other countries lacking such survey data.

While contact matrices are not symmetric because they are defined per capita, there is a symmetry condition that should hold in theory:

$$C_{ij}N_j = C_{ji}N_i \tag{5.1}$$

where N_i is the number of individuals in class i, C is the contact matrix and C_{ij} is the average number of individuals in age class i that an individual from class j contacts per unit time. In practice, I have found that this symmetry condition does not hold exactly with the synthetic contact matrices. One initial area of future work is to develop a simple and reasonable method to ensure the symmetry condition holds with a synthetic contact matrix and corresponding age distribution N. I would then compare how different this updated contact matrix is from the previous, and if it affects any key epidemiological outcomes when simulating an outbreak. If it is not necessary for modelling outcomes for the symmetry condition to be met, another area of future work would be to determine when new contact matrices are needed to adapt to changing age distributions. Large contact surveys are time consuming and labor intensive to implement so contact matrices are infrequently updated, but updated data on the age structure of a population is more readily available. Over time, or for very quickly changing populations, the use of potentially outdated contact matrices that do not correspond to the current age distribution will likely have a greater affect on modelling results. Is there a simple and reasonable method to update synthetic contact matrices without more surveys? At what point should we use such a method?

5.3.1.1 Stratifying contacts by vaccination status

The model developed in Chapter 3 assumed homogeneous mixing throughout the population because we are unaware of any currently available data describing contact patterns stratified by vaccination status. However, I would expect some degree of homophily, the idea that "birds of a feather flock together", in realistic social settings. While working on Chapter 3, we did explore a simple approach to adding homophily to the SEIR-type model, and found that the main takeaways of the paper did not change. However, detailed contact matrices stratified by both age and vaccination status are currently under development by Jonathan

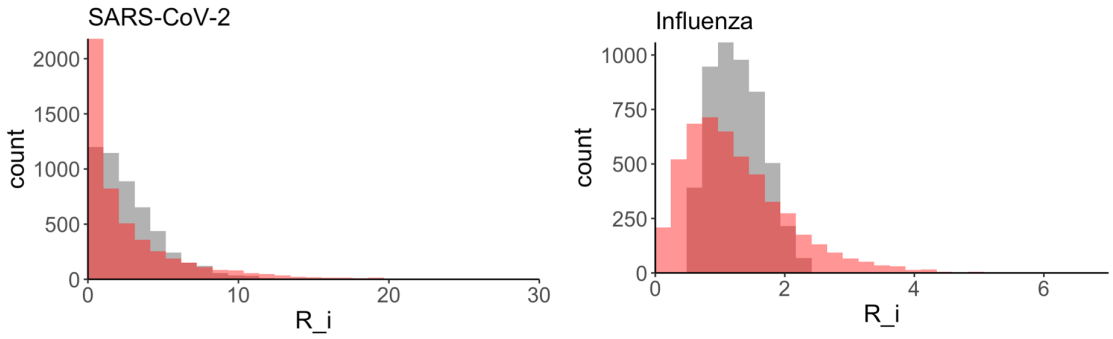

Figure 5.1: Distribution of individual reproductive numbers from 5,000 viral load trajectories using the within-host method (gray) and drawing from a $\Gamma(R_0, k)$ distribution (red) for SARS-CoV-2 (left) and influenza (right). Parameter values for viral load trajectories, infectiousness thresholds, R_0 and k are found in Table A.2.

Read's lab at Lancaster University. I believe an interesting area of future research would be to extend our model to include these contact matrices when they become available. I think the addition of age to our SARS-CoV-2 transmission model would be beneficial, as highlighted by Chapter 2, and a more realistic model of social interaction would strengthen our understanding of targeted routine screening programs.

5.3.2 Estimating individual reproductive numbers using within-host models

In Chapter 4, we used a within-host modeling approach to calculate individual's reproductive number, which we will denote here as R_i. The approach considers an individual's infectiousness $\beta_i(t)$, as a function of time and asserts that R_i is proportional to the area under $\beta_i(t)$. A common approach to approximate $\beta_i(t)$ is to set $\beta_i(t)$ equal to the logarithm of viral load above an infectiousness threshold [74, 141, 157]. Another way to estimate the distribution of R_i is to do so empirically, by fitting different candidate models to contact tracing data and using model selection to determine which model is best of the candidates. Lloyd-Smith et. al. used this approach for various pathogens and found that $R_i \sim \Gamma(R_0, k)$ was typically the best candidate model to describe outbreak data [139].

The distribution of R_i estimated from the within-host approach does not align with the distribution estimated from contact tracing data (Figure 5.1). While this result is perhaps unsurprising, since contact tracing data accounts for social behavior and the within-host method does not, it highlights a flaw in this

methodology. Future work to develop theory that more closely aligns these approaches would improve our understanding of individuals' reproductive numbers and enable more complex multiscale modeling that could explore the role of variation in viral dynamics on population-level transmission dynamics.

Bibliography

[1] Mark Jit and Marc Brisson. Modelling the epidemiology of infectious diseases for decision analysis: a primer. *Pharmacoeconomics*, 29:371–386, 2011.

[2] Nathan C Lo, Kristin Andrejko, Poojan Shukla, Tess Baker, Veronica Ivey Sawin, Susan L Norris, and Joseph A Lewnard. Contribution and quality of mathematical modeling evidence in world health organization guidelines: A systematic review. *Epidemics*, 39:100570, 2022.

[3] World Health Organization. "WHO COVID-19 dashboard". Online, 2024 (accessed June 26, 2024). https://data.who.int/dashboards/covid19/deaths?n=o.

[4] United Nations News. "WHO chief declares end to COVID-19 as a global health emergency". Online, 2023 (accessed June 26, 2024). https://news.un.org/en/story/2023/05/1136367.

[5] Jessica Colarossi. "Is COVID-19 still a pandemic? *Boston University's The Brink*, 2024 (accessed June 26, 2024). https://www.bu.edu/articles/2024/is-covid-19-still-a-pandemic/#:~:text=Right%20now%2C%20COVID%20cases%20are,the%20disease%20we%20normally%20expect.

[6] T Thanh Le, Zacharias Andreadakis, Arun Kumar, R Gómez Román, Stig Tollefsen, Melanie Saville, Stephen Mayhew, et al. The COVID-19 vaccine development landscape. *Nat Rev Drug Discov*, 19(5):305–306, 2020.

[7] Karin Bok, Sandra Sitar, Barney S Graham, and John R Mascola. Accelerated COVID-19 vaccine development: milestones, lessons, and prospects. *Immunity*, 54(8):1636–1651, 2021.

[8] Jill Diesel. COVID-19 vaccination coverage among adults—United States, December 14, 2020–May 22, 2021. *Morbidity and Mortality Weekly Report*, 70, 2021.

[9] Paula G. Sanders Theresa A. Mongiovi, Angela H. Sanders. U.S. Supreme Court Blocks OSHA "Vaccinate or Test" Mandate But Upholds CMS' Vaccine Requirement for Healthcare Workers. Online, 2022 (accessed June 27, 2024). https://www.postschell.com/insights/us-supreme-court-blocks-osha-ldquovaccinate-or-testrdquo-mandate-but-upholds-
~:text=On%20January%2013%2C%202022%2C%20the,vaccine%20requirement%20for%20healthcare%20workers.

[10] Gerard T Flaherty, Davidson H Hamer, and Lin H Chen. Travel in the time of COVID: a review of international travel health in a global pandemic. *Current Infectious Disease Reports*, 24(10):129–145, 2022.

[11] COVID-19 Dashboard by the Center for Systems Science and Engineering at Johns Hopkins University. Online, 2020 (accessed January 4, 2021). https://coronavirus.jhu.edu/map.html.

[12] Roxanne Khamsi. If a coronavirus vaccines arrives, can the world make enough? *Nature*, 580(7805):578–580, 2020.

[13] Framework for equitable allocation of COVID-19 vaccine. Online, 2020 (accessed December 6, 2020). https://www.nap.edu/catalog/25917/framework-for-equitable-allocation-of-covid-19-vaccine.

[14] Derek Weycker, John Edelsberg, M. Elizabeth Halloran, Ira M. Longini, Azhar Nizam, Vincent Ciuryla, and Gerry Oster. Population-wide benefits of routine vaccination of children against influenza. *Vaccine*, 23(10):1284 – 1293, 2005.

[15] Jan Medlock and Alison P. Galvani. Optimizing influenza vaccine distribution. *Science*, 325(5948):1705–1708, 2009.

[16] Shweta Bansal, Babak Pourbohloul, and Lauren Ancel Meyers. A comparative analysis of influenza vaccination programs. *PLoS Medicine*, 3(10):e387, 2006.

[17] Laura Matrajt, Julia Eaton, Tiffany Leung, and Elizabeth R. Brown. Vaccine optimization for COVID-19: Who to vaccinate first? *Science Advances*, 7(6):eabf1374, 2021. Publisher: American Association for the Advancement of Science.

[18] Molly E Gallagher, Andrew J Sieben, Kristin N Nelson, Alicia NM Kraay, Walter A Orenstein, Ben Lopman, Andreas Handel, and Katia Koelle. Indirect benefits are a crucial consideration when evaluating sars-cov-2 vaccine candidates. *Nature medicine*, 27(1):4–5, 2021.

[19] Jack H Buckner, Gerardo Chowell, and Michael R Springborn. Dynamic prioritization of COVID-19 vaccines when social distancing is limited for essential workers. *Proceedings of the National Academy of Sciences*, 118(16):e2025786118, 2021.

[20] Frank G Sandmann, Nicholas G Davies, Anna Vassall, W John Edmunds, Mark Jit, Fiona Yueqian Sun, C Julian Villabona-Arenas, Emily S Nightingale, Alicia Showering, Gwenan M Knight, et al. The potential health and economic value of SARS-CoV-2 vaccination alongside physical distancing in the UK: a transmission model-based future scenario analysis and economic evaluation. *The Lancet infectious diseases*, 21(7):962–974, 2021.

[21] Colin J. Worby and Hsiao-Han Chang. Face mask use in the general population and optimal resource allocation during the COVID-19 pandemic. *Nature Communications*, 11(4049), 2020.

[22] Edward Goldstein, Marc Lipsitch, and Muge Cevik. On the effect of age on the transmission of SARS-CoV-2 in households, schools and the community. *The Journal of Infectious Diseases*, 2020.

[23] Nicholas Davies, Petra Klepac, Yang Liu, Kiesha Prem, Mark Jit, and Rosalind M Eggo. Age-dependent effects in the transmission and control of COVID-19 epidemics. *Nature Medicine*, 26(1205-1211), 2020.

[24] Juanjuan Zhang, Maria Litvinova, Yuxia Liang, Yan Wang, Wei Wang, Shanlu Zhao, Qianhui Wu, Stefano Merler, Cécile Viboud, Alessandro Vespignani, Marco Ajelli, and Hongjie Yu. Changes in contact patterns shape the dynamics of the COVID-19 outbreak in China. *Science*, 368(6498):1481–1486, 2020.

[25] Sereina Annik Herzog, Jessie De Bie, Steven Abrams, Ine Wouters, Esra Ekinci, Lisbeth Patteet, Astrid Coppens, Sandy De Spiegeleer, Philippe Beutels, Pierre Van Damme, et al. Seroprevalence of IgG antibodies against SARS-CoV-2–a serial prospective cross-sectional nationwide study of residual samples, Belgium, March to October 2020. *Eurosurveillance*, 27(9):2100419, 2022.

[26] Amber L. Mueller, Maeve S. McNamara, and David A. Sinclair. Why does COVID-19 disproportionately affect older people? *Aging*, 12(10):9959–9981, 2020.

[27] Yang Liu, Bei Mao, Shuo Liang, Jia-Wei Yang, Hai-Wen Lu, Yan-Hua Chai, Lan Wang, Li Zhang, Qiu-Hong Li, Lan Zhao, Yan He, Xiao-Long Gu, Xiao-Bin Ji, Li Li, Zhi-Jun Jie, Qiang Li, Xiang-Yang Li, Hong-Zhou Lu, Wen-Hong Zhang, Yuan-Lin Song, Jie-Ming Qu, and Jin-Fu Xu. Association between age and clinical characteristics and outcomes of COVID-19. *European Respiratory Journal*, 55(5):2001112, 2020.

[28] Jaana Westmeier, Krystallenia Paniskaki, Zehra Karaköse, Tanja Werner, Kathrin Sutter, Sebastian Dolff, Marvin Overbeck, Andreas Limmer, Jia Liu, Xin Zheng, et al. Impaired cytotoxic CD8+ T cell response in elderly COVID-19 patients. *MBio*, 11(5), 2020.

[29] Andrew T Levin, William P. Hanage, Nana Owusu-Boaitey, Kensington B. Cochran, Seamus P. Walsh, and Gideon Meyerowitz-Katz. Assessing the age specificity of infection fatality rates for COVID-19: systematic review, meta-analysis, and public policy implications. *Eur J Epidemiol*, 35(12):1123–1138, 2020.

[30] Henrik Salje, Cécile Tran Kiem, Noémie Lefrancq, Noémie Courtejoie, Paolo Bosetti, Juliette Paireau, Alessio Andronico, Nathanaël Hozé, Jehanne Richet, Claire-Lise Dubost, Yann Le Strat, Justin Lessler, Daniel Levy-Bruhl, Arnaud Fontanet, Lulla Opatowski, Pierre-Yves Boelle, and Simon Cauchemez. Estimating the burden of SARS-CoV-2 in France. *Science*, 369(6500):208–211, 2020.

[31] Kate M. Bubar, Kyle Reinholt, Stephen M. Kissler, Marc Lipsitch, Sarah Cobey, Yonatan H. Grad, and Daniel B. Larremore. COVID-19 vaccine prioritization code. Online, 2020. https://doi.org/10.5281/zenodo.4308794.

[32] Kiesha Prem, Kevin van Zandvoort, Petra Klepac, Rosalind M Eggo, Nicholas G Davies, Centre for the Mathematical Modelling of Infectious Diseases COVID-19 Working Group, Alex R Cook, and Mark Jit. Projecting contact matrices in 177 geographical regions: an update and comparison with empirical data for the COVID-19 era. *PLoS computational biology*, 17(7):e1009098, 2021.

[33] United Nations Department of Economic and Social Affairs Population Division. World population prospects. Online, 2019 (accessed August 30, 2020). https://population.un.org/wpp/.

[34] Megan Brenan. Willingness to Get COVID-19 Vaccine Ticks Up to 63% in U.S. Online, December 8, 2020. https://news.gallup.com/poll/327425/willingness-covid-vaccine-ticks.aspx.

[35] Peter A. Gross, Alicia W. Hermogenes, Henry S. Sacks, and Joseph Lau. The efficacy of influenza vaccine in elderly persons. *Annals of Internal Medicine*, 123(7):518–527, 1995. PMID: 7661497.

[36] Jason K. H. Lee, Gary K. L. Lam, Thomas Shin, Jiyeon Kim, Anish Krishnan, David P. Greenberg, and Ayman Chit. Efficacy and effectiveness of high-dose versus standard-dose influenza vaccination for older adults: a systematic review and meta-analysis. *Expert Review of Vaccines*, 17(5):435–443, 2018. PMID: 29715054.

[37] Th. M. E. Govaert, C. T. M. C. N. Thijs, N. Masurel, M. J. W. Sprenger, G. J. Dinant, and J. A. Knottnerus. The Efficacy of Influenza Vaccination in Elderly Individuals: A Randomized Double-blind Placebo-Controlled Trial. *JAMA*, 272(21):1661–1665, 1994.

[38] Joseph A Lewnard and Sarah Cobey. Immune history and influenza vaccine effectiveness. *Vaccines*, 6(2):28, 2018.

[39] Sheila F Lumley, Denise O'Donnell, Nicole E Stoesser, Philippa C Matthews, Alison Howarth, Stephanie B Hatch, Brian D Marsden, Stuart Cox, Tim James, Fiona Warren, et al. Antibody status and incidence of sars-cov-2 infection in health care workers. *New England Journal of Medicine*, 384(6):533–540, 2021.

[40] City of New York. COVID-19 data. Online, 2020 (accessed August 31, 2020). https://www1.nyc.gov/site/doh/covid/covid-19-data-testing.page.

[41] Kristina L Bajema, Ryan E Wiegand, Kendra Cuffe, Sadhna V Patel, Ronaldo Iachan, Travis Lim, Adam Lee, Davia Moyse, Fiona P Havers, Lee Harding, et al. Estimated SARS-CoV-2 Seroprevalence in the US as of September 2020. *JAMA Internal Medicine*, 2020.

[42] Helen Ward, Graham S Cooke, Christina Atchison, Matthew Whitaker, Joshua Elliott, Maya Moshe, Jonathan C Brown, Barnaby Flower, Anna Daunt, Kylie Ainslie, et al. Prevalence of antibody positivity to sars-cov-2 following the first peak of infection in england: Serial cross-sectional studies of 365,000 adults. *The Lancet Regional Health–Europe*, 4, 2021.

[43] Jennifer M Dan, Jose Mateus, Yu Kato, Kathryn M Hastie, Caterina Faliti, Sydney I Ramirez, April Frazier, D Yu Esther, Alba Grifoni, Stephen A Rawlings, et al. Immunological memory to SARS-CoV-2 assessed for greater than six months after infection. *bioRxiv*, 2020. https://www.biorxiv.org/content/10.1101/2020.11.15.383323v2.

[44] Daniel B Larremore, Bailey K Fosdick, Kate M Bubar, Sam Zhang, Stephen M Kissler, C Jessica E Metcalf, Caroline O Buckee, and Yonatan H Grad. Estimating SARS-CoV-2 seroprevalence and epidemiological parameters with uncertainty from serological surveys. *Elife*, 10:e64206, 2021.

[45] Corine H GeurtsvanKessel, Nisreen MA Okba, Zsofia Igloi, Susanne Bogers, Carmen WE Embregts, Brigitta M Laksono, Lonneke Leijten, Casper Rokx, Bart Rijnders, Janette Rahamat-Langendoen, et al. An evaluation of COVID-19 serological assays informs future diagnostics and exposure assessment. *Nature Communications*, 11(1):1–5, 2020.

[46] Dennis Ellenberger, Ronald A Otten, Bin Li, Michael Aidoo, I Vanessa Rodriguez, Carlos A Sariol, Melween Martinez, Michael Monsour, Linda Wyatt, Michael G Hudgens, et al. HIV-1 DNA/MVA vaccination reduces the per exposure probability of infection during repeated mucosal SHIV challenges. *Virology*, 352(1):216–225, 2006.

[47] Kate E Langwig, Andrew R Wargo, Darbi R Jones, Jessie R Viss, Barbara J Rutan, Nicholas A Egan, Pedro Sá-Guimarães, Min Sun Kim, Gael Kurath, M Gabriela M Gomes, et al. Vaccine effects on heterogeneity in susceptibility and implications for population health management. *mBio*, 8(6), 2017.

[48] Paula Span. Older adults may be left out of some COVID-19 trials. *New York Times*, June 19, 2020. https://www.nytimes.com/2020/06/19/health/vaccine-trials-elderly.html.

[49] Hannah R Sharpe, Ciaran Gilbride, Elizabeth Allen, Sandra Belij-Rammerstorfer, Cameron Bissett, Katie Ewer, and Teresa Lambe. The early landscape of coronavirus disease 2019 vaccine development in the UK and rest of the world. *Immunology*, 160:223 – 232, 2020.

[50] Meryl Kornfield. When will children get a coronavirus vaccine? Not in time for the new school year, experts fear. *Washington Post*, December 2, 2020. https://www.washingtonpost.com/health/2020/12/02/kids-vaccine-delay/.

[51] Christopher I Jarvis, Kevin Van Zandvoort, Amy Gimma, Kiesha Prem, CMMID COVID-19 working group, Petra Klepac, G James Rubin, and W John Edmunds. Quantifying the impact of physical distance measures on the transmission of COVID-19 in the UK. *BMC Med*, 18(124), 2020.

[52] Jantien A Backer, Liesbeth Mollema, Eric RA Vos, Don Klinkenberg, Fiona Rm Van Der Klis, Hester E De Melker, Susan van den Hof, and Jacco Wallinga. Impact of physical distancing measures against covid-19 on contacts and mixing patterns: repeated cross-sectional surveys, the netherlands, 2016–17, april 2020 and june 2020. *Eurosurveillance*, 26(8):2000994, 2021.

[53] Selene Ghisolfi, Ingvild Almas, Justin Sandefur, Tillmann von Carnap, Jesse Heitner, and Tessa Bold. Predicted COVID-19 fatality rates based on age, sex, comorbidities, and health system capacity. *Center for Global Development*, 2020.

[54] Marc Lipsitch and Natalie E Dean. Understanding COVID-19 vaccine efficacy. *Science*, 370(6518):763–765, 2020.

[55] Lotty E Duijzer, Willem L van Jaarsveld, Jacco Wallinga, and Rommert Dekker. Dose-optimal vaccine allocation over multiple populations. *Production and Operations Management*, 27(1):143–159, 2018.

[56] Takehiro Takahashi, Mallory K. Ellingson, Patrick Wong, Benjamin Israelow, Carolina Lucas, Jon Klein, Julio Silva, Tianyang Mao, Ji Eun Oh, Maria Tokuyama, Peiwen Lu, et al. Sex differences in immune responses that underlie COVID-19 disease outcomes. *Nature*, 588:1–6, 2020.

[57] Dimple Chakravarty, Sujit S. Nair, Nada Hammouda, Parita Ratnani, Yasmine Gharib, Vinayak Wagaskar, Nihal Mohamed, Dara Lundon, Zachary Dovey, Natasha Kyprianou, and Ashutosh K. Tewari. Sex differences in SARS-CoV-2 infection rates and the potential link to prostate cancer. *Communications Biology*, 3(374), 2020.

[58] Monica Webb Hooper, Anna María Nápoles, and Eliseo J. Pérez-Stable. COVID-19 and Racial/Ethnic Disparities. *JAMA*, 323(24):2466–2467, 2020.

[59] Melissa Jenco. CDC vaccine committee may prioritize health care workers for COVID-19 vaccines. *AAP News*, August 2020. https://www.aappublications.org/news/2020/08/27/covid19vaccinepriorities082620.

[60] Jon Cohen. The line is forming for a COVID-19 vaccine. Who should be at the front? *Science*, 369(6499):15–16, 2020.

[61] Sharmistha Mishra, Jeffrey C. Kwong, Adrienne K. Chan, and Stefan D. Baral. Understanding heterogeneity to inform the public health response to COVID-19 in Canada. *CMAJ*, 192(25):E684–E685, 2020.

[62] Laura Hawks, Steffie Woolhandler, and Danny McCormick. COVID-19 in Prisons and Jails in the United States. *JAMA Internal Medicine*, 180(8):1041–1042, 2020.

[63] Hamada S Badr, Hongru Du, Maximilian Marshall, Ensheng Dong, Marietta M Squire, and Lauren M Gardner. Association between mobility patterns and COVID-19 transmission in the USA: a mathematical modelling study. *The Lancet Infectious Diseases*, 2020.

[64] Jamie Ducharme. These maps show how drastically COVID-19 risk varies by neighborhood. *Time*, 2020. https://time.com/5870041/COVID-19-neighborhood-risk/.

[65] R Core Team. *R: A Language and Environment for Statistical Computing*. R Foundation for Statistical Computing, Vienna, Austria, 2019.

[66] Kendall E. Atkinson. *An Introduction to Numerical Analysis*, chapter 2, pages 56–58. Wiley, New York, second edition, 1989.

[67] WHO Global Health Observatory. Life tables by country. Online, 2016 (accessed December 3, 2020). https://apps.who.int/gho/data/view.main.LT62160?lang=en.

[68] Hana M. El Sahly, Lindsey R. Baden, Brandon Essink, Susanne Doblecki-Lewis, Judith M. Martin, Evan J. Anderson, Thomas B. Campbell, Jesse Clark, Lisa A. Jackson, Carl J. Fichtenbaum, Marcus Zervos, Bruce Rankin, Frank Eder, Gregory Feldman, Christina Kennelly, Laurie Han-Conrad, Michael Levin, Kathleen M. Neuzil, Lawrence Corey, Peter Gilbert, Holly Janes, Dean Follmann, Mary Marovich, Laura Polakowski, John R. Mascola, Julie E. Ledgerwood, Barney S. Graham,

Allison August, Heather Clouting, Weiping Deng, Shu Han, Brett Leav, Deb Manzo, Rolando Pajon, Florian Schödel, Joanne E. Tomassini, Honghong Zhou, and Jacqueline Miller. Efficacy of the mRNA-1273 SARS-CoV-2 vaccine at completion of blinded phase. *New England Journal of Medicine*, 2021.

[69] Anoop S.V. Shah, Ciara Gribben, Jennifer Bishop, Peter Hanlon, David Caldwell, Rachael Wood, Martin Reid, Jim McMenamin, David Goldberg, Diane Stockton, Sharon Hutchinson, Chris Robertson, Paul M. McKeigue, Helen M. Colhoun, and David A. McAllister. Effect of vaccination on transmission of SARS-CoV-2. *New England Journal of Medicine*, 2021.

[70] Nick Andrews, Julia Stowe, Freja Kirsebom, Samuel Toffa, Tim Rickeard, Eileen Gallagher, Charlotte Gower, Meaghan Kall, Natalie Groves, Anne-Marie O'Connell, et al. Covid-19 vaccine effectiveness against the Omicron (B. 1.1. 529) variant. *New England Journal of Medicine*, 386(16):1532–1546, 2022.

[71] Jamie Ducharme. We need to start thinking differently about breakthrough infections, Dec. 21, 2021. https://time.com/6130704/breakthrough-infections-omicron/.

[72] Kristen K Bjorkman, Tassa K Saldi, Erika Lasda, Leisha Conners Bauer, Jennifer Kovarik, Patrick K Gonzales, Morgan R Fink, Kimngan L Tat, Cole R Hager, Jack C Davis, and et al. Higher viral load drives infrequent severe acute respiratory syndrome coronavirus 2 transmission between asymptomatic residence hall roommates. *The Journal of Infectious Diseases*, 2021.

[73] Diana Rose E Ranoa, Robin L Holland, Fadi G Alnaji, Kelsie J Green, Leyi Wang, Richard L Fredrickson, Tong Wang, George N Wong, Johnny Uelmen, Sergei Maslov, et al. Mitigation of SARS-CoV-2 transmission at a large public university. *Nature communications*, 13(1):3207, 2022.

[74] Daniel B. Larremore, Bryan Wilder, Evan Lester, Soraya Shehata, James M. Burke, James A. Hay, Milind Tambe, Michael J. Mina, and Roy Parker. Test sensitivity is secondary to frequency and turnaround time for COVID-19 screening. *Science Advances*, 7(1), 2021.

[75] Martin Pavelka, Kevin Van-Zandvoort, Sam Abbott, Katharine Sherratt, Marek Majdan, CMMID COVID-19 Working Group, Inštitút Zdravotnỳch Analỳz, Pavol Jarčuška, Marek Krajčí, Stefan Flasche, et al. The impact of population-wide rapid antigen testing on SARS-CoV-2 prevalence in Slovakia. *Science*, 372(6542):635–641, 2021.

[76] Ryan S. McGee, Julian R. Homburger, Hannah E. Williams, Carl T. Bergstrom, and Alicia Y. Zhou. Proactive COVID-19 testing in a partially vaccinated population. *medRxiv*, 2021.

[77] Jason Horowitz. Italy puts in force tough new law requiring workers to test or vaccinate. *The New York Times*, Oct. 15, 2021. https://www.nytimes.com/2021/10/15/world/europe/italy-vaccination-law-covid.html.

[78] Katie Rogers and Sheryl Gay Stolberg. Biden mandates vaccines for workers, saying, 'Our patience is wearing thin'. *The New York Times*, Sept. 9, 2021. https://www.nytimes.com/2021/09/09/us/politics/biden-mandates-vaccines.html.

[79] Nils Haug, Lukas Geyrhofer, Alessandro Londei, Elma Dervic, Amélie Desvars-Larrive, Vittorio Loreto, Beate Pinior, Stefan Thurner, and Peter Klimek. Ranking the effectiveness of worldwide covid-19 government interventions. *Nature human behaviour*, 4(12):1303–1312, 2020.

[80] Mrinank Sharma, Sören Mindermann, Charlie Rogers-Smith, Gavin Leech, Benedict Snodin, Janvi Ahuja, Jonas B Sandbrink, Joshua Teperowski Monrad, George Altman, Gurpreet Dhaliwal, et al. Understanding the effectiveness of government interventions against the resurgence of covid-19 in europe. *Nature communications*, 12(1):1–13, 2021.

[81] Toon Braeye, Laura Cornelissen, Lucy Catteau, Freek Haarhuis, Kristiaan Proesmans, Karin De Ridder, Achille Djiena, Romain Mahieu, Frances De Leeuw, Alex Dreuw, Naima Hammami, Sophie Quoilin, Herman Van Oyen, Chloé Wyndham-Thomas, and Dieter Van Cauteren. Vaccine effectiveness against infection and onwards transmission of COVID-19: Analysis of Belgian contact tracing data, January-June 2021. *Vaccine*, 39(39):5456–5460, 2021.

[82] Hiam Chemaitelly, Patrick Tang, Mohammad R Hasan, Sawsan AlMukdad, Hadi M Yassine, Fatiha M Benslimane, Hebah A Al Khatib, Peter Coyle, Houssein H Ayoub, Zaina Al Kanaani, et al. Waning of BNT162b2 vaccine protection against SARS-CoV-2 infection in Qatar. *New England Journal of Medicine*, 2021.

[83] Yair Goldberg, Micha Mandel, Yinon M Bar-On, Omri Bodenheimer, Laurence S Freedman, Eric Haas, Ron Milo, Sharon Alroy-Preis, Nachman Ash, and Amit Huppert. Waning immunity of the BNT162b2 vaccine: A nationwide study from Israel. *NEJM*, 2021.

[84] Nick Andrews, Elise Tessier, Julia Stowe, Charlotte Gower, Freja Kirsebom, Ruth Simmons, Eileen Gallagher, Simon Thelwall, Natalie Groves, Gavin Dabrera, et al. Duration of protection against mild and severe disease by Covid-19 vaccines. *New England Journal of Medicine*, 386(4):340–350, 2022.

[85] Billy J Gardner and A Marm Kilpatrick. Third doses of COVID-19 vaccines reduce infection and transmission of SARS-CoV-2 and could prevent future surges in some populations. *medRxiv*, 2021.

[86] Sho Miyamoto, Takeshi Arashiro, Yu Adachi, Saya Moriyama, Hitomi Kinoshita, Takayuki Kanno, Shinji Saito, Harutaka Katano, Shun Iida, Akira Ainai, et al. Vaccination-infection interval determines cross-neutralization potency to SARS-CoV-2 Omicron after breakthrough infection by other variants. *Med*, 3(4):249–261, 2022.

[87] Christian Holm Hansen, Astrid Blicher Schelde, Ida Rask Moustsen-Helm, Hanne-Dorthe Emborg, Tyra Grove Krause, Kare Molbak, and Palle Valentiner-Branth. Vaccine effectiveness against SARS-CoV-2 infection with the Omicron or Delta variants following a two-dose or booster BNT162b2 or mRNA-1273 vaccination series: A Danish cohort study. *medRxiv*, 2021.

[88] David W Eyre, Donald Taylor, Mark Purver, David Chapman, Tom Fowler, Koen B Pouwels, A Sarah Walker, and Tim EA Peto. The impact of SARS-CoV-2 vaccination on alpha & delta variant transmission. *medRxiv*, 2021.

[89] Billy J. Gardner and A. Marm Kilpatrick. Estimates of reduced vaccine effectiveness against hospitalization, infection, transmission and symptomatic disease of a new SARS-CoV-2 variant, omicron (B.1.1.529), using neutralizing antibody titers. *medRxiv*, 2021.

[90] Heba N Altarawneh, Hiam Chemaitelly, Mohammad R Hasan, Houssein H Ayoub, Suelen Qassim, Sawsan AlMukdad, Peter Coyle, Hadi M Yassine, Hebah A Al-Khatib, Fatiha M Benslimane, et al. Protection against the Omicron variant from previous SARS-CoV-2 infection. *New England Journal of Medicine*, 386(13):1288–1290, 2022.

[91] Centers for Disease Control and Prevention (CDC). COVID-19 Vaccinations in the United States. https://covid.cdc.gov/covid-data-tracker/#vaccinations_vacc-total-admin-rate-total, accessed Sept. 22, 2021.

[92] Mark EJ Woolhouse, C Dye, J-F Etard, T Smith, JD Charlwood, GP Garnett, P Hagan, JLK Hii, PD Ndhlovu, RJ Quinnell, et al. Heterogeneities in the transmission of infectious agents: implications for the design of control programs. *Proceedings of the National Academy of Sciences*, 94(1):338–342, 1997.

[93] Christopher Rose, Andrew J Medford, C Franklin Goldsmith, Tejs Vegge, Joshua S Weitz, and Andrew A Peterson. Heterogeneity in susceptibility dictates the order of epidemic models. *Journal of Theoretical Biology*, 528:110839, 2021.

[94] Hannah Ritchie, Edouard Mathieu, Lucas Rodés-Guirao, Cameron Appel, Charlie Giattino, Esteban Ortiz-Ospina, Joe Hasell, Bobbie Macdonald, Diana Beltekian, and Max Roser. Coronavirus pandemic (COVID-19). *Our World in Data*, 2021. https://ourworldindata.org/coronavirus.

[95] Amiel A. Dror, Netanel Eisenbach, Shahar Taiber, Nicole G. Morozov, Matti Mizrachi, Asaf Zigron, Samer Srouji, and Eyal Sela. Vaccine hesitancy: the next challenge in the fight against COVID-19. *European Journal of Epidemiology*, 35(8):775–779, 2020.

[96] Chris Davis, Nicola Logan, Grace Tyson, Richard Orton, William Harvey, John Haughney, Jon Perkins, Thomas Peacock, Wendy S Barclay, Peter Cherepanov, et al. Reduced neutralisation of the delta (B. 1.617. 2) SARS-CoV-2 variant of concern following vaccination. *PLOS Pathogens*, 17(12):e1010022, 2021.

[97] Srinivas Nanduri, Tamara Pilishvili, Gordana Derado, Minn Minn Soe, Philip Dollard, Hsiu Wu, Qunna Li, Suparna Bagchi, Heather Dubendris, Ruth Link-Gelles, et al. Effectiveness of Pfizer-BioNTech and Moderna vaccines in preventing SARS-CoV-2 infection among nursing home residents before and during widespread circulation of the SARS-CoV-2 B. 1.617. 2 (delta) variant—national healthcare safety network, March 1–August 1, 2021. *Morbidity and Mortality Weekly Report*, 70(34):1163, 2021.

[98] Mark G. Thompson, Karthik Natarajan, Stephanie A. Irving, Elizabeth A. Rowley, Eric P. Griggs, Manjusha Gaglani, Nicola P. Klein, Shaun J. Grannis, Malini B. DeSilva, Edward Stenehjem, Sarah E. Reese, et al. Effectiveness of a third dose of mRNA vaccines against COVID-19–associated emergency department and urgent care encounters and hospitalizations among adults during periods of delta and omicron variant predominance — VISION network, 10 states, August 2021–January 2022. *Morbidity and Mortality Weekly Report*, 71, 2021.

[99] Daniel B. Larremore, Derek Toomre, and Roy Parker. Modeling the effectiveness of olfactory testing to limit SARS-CoV-2 transmission. *Nature Communications 2021 12:1*, 12(1):1–9, 2021.

[100] Pinelopi Konstantinou, Katerina Georgiou, Navin Kumar, Maria Kyprianidou, Christos Nicolaides, Maria Karekla, and Angelos P Kassianos. Transmission of vaccination attitudes and uptake based on social contagion theory: A scoping review. *Vaccines*, 9(6):607, 2021.

[101] Xi He, Eric H. Y. Lau, Peng Wu, Xilong Deng, Jian Wang, Xinxin Hao, Yiu Chung Lau, Jessica Y. Wong, Yujuan Guan, Xinghua Tan, Xiaoneng Mo, Yanqing Chen, Baolin Liao, Weilie Chen, Fengyu Hu, Qing Zhang, Mingqiu Zhong, Yanrong Wu, Lingzhai Zhao, Fuchun Zhang, Benjamin J. Cowling, Fang Li, and Gabriel M. Leung. Temporal dynamics in viral shedding and transmissibility of COVID-19. *Nature*, 26(5):672–675, 2020.

[102] Gavin M. Abernethy and David H Glass. Optimal COVID-19 lockdown strategies in an age-structured SEIR model of Northern Ireland. *Journal of The Royal Society Interface*, 19(188):20210896, 2022.

[103] Lauren Childs, David W Dick, Zhilan Feng, Jane M Heffernan, Jing Li, and Gergely Röst. Modeling waning and boosting of COVID-19 in Canada with vaccination. *Epidemics*, 39:100583, 2022.

[104] Peter I. Frazier, J. Massey Cashore, Ning Duan, Shane G. Henderson, Alyf Janmohamed, Brian Liu, David B. Shmoys, Jiayue Wan, and Yujia Zhang. Modeling for COVID-19 college reopening decisions: Cornell, a case study. *Proceedings of the National Academy of Sciences*, 119(2):e2112532119, 2022.

[105] William S Hart, Elizabeth Miller, Nick J Andrew, Pauline Waight, Phillip K Maini, Sebastian Funk, et al. Generation time of the alpha and delta SARS-CoV-2 variants: an epidemiological analysis. *The Lancet Infectious Diseases*, 22(5):603–610, 2022.

[106] Kate M Bubar, Kyle Reinholt, Stephen M Kissler, Marc Lipsitch, Sarah Cobey, Yonatan H Grad, and Daniel B Larremore. Model-informed COVID-19 vaccine prioritization strategies by age and serostatus. *Science*, 371(6532):916–921, 2021.

[107] Rowland W Pettit, Bo Peng, Patrick Yu, Peter Matos, Alexander L Greninger, Julie McCashin, and Christopher Ian Amos. Optimized post-vaccination strategies and preventative measures for SARS-CoV-2. *medRxiv*, 2021.

[108] Joshua S Weitz, Stephen J Beckett, Ashley R Coenen, David Demory, Marian Dominguez-Mirazo, Jonathan Dushoff, Chung-Yin Leung, Guanlin Li, Andreea Măgălie, Sang Woo Park, et al. Modeling shield immunity to reduce COVID-19 epidemic spread. *Nature medicine*, 26(6):849–854, 2020.

[109] Laith J Abu-Raddad, Hiam Chemaitelly, Peter Coyle, Joel A Malek, Ayeda A Ahmed, Yasmin A Mohamoud, Shameem Younuskunju, Houssein H Ayoub, Zaina Al Kanaani, Einas Al Kuwari, et al. SARS-CoV-2 antibody-positivity protects against reinfection for at least seven months with 95% efficacy. *EClinicalMedicine*, 35:100861, 2021.

[110] M. Elizabeth Halloran, Michael Haber, and Jr. Longini, Ira M. Interpretation and estimation of vaccine efficacy under heterogeneity. *American Journal of Epidemiology*, 136(3):328–343, 1992.

[111] Madhumita Shrotri, Maria Krutikov, Tom Palmer, Rebecca Giddings, Borscha Azmi, Sathyavani Subbarao, Christopher Fuller, Aidan Irwin-Singer, Daniel Davies, Gokhan Tut, et al. Vaccine effectiveness of the first dose of ChAdOx1 nCoV-19 and BNT162b2 against SARS-CoV-2 infection in

residents of long-term care facilities in England (vivaldi): a prospective cohort study. *The Lancet Infectious Diseases*, 21(11):1529–1538, 2021.

[112] Brian Grunau, David M Goldfarb, Michael Asamoah-Boaheng, Liam Golding, Tracy L Kirkham, Paul A Demers, and Pascal M Lavoie. Immunogenicity of extended mRNA SARS-CoV-2 vaccine dosing intervals. *JAMA*, 327(3):279–281, 2022.

[113] Victoria Jane Hall, Sarah Foulkes, Ayoub Saei, Nick Andrews, Blanche Oguti, Andre Charlett, Edgar Wellington, Julia Stowe, Natalie Gillson, Ana Atti, et al. COVID-19 vaccine coverage in health-care workers in England and effectiveness of BNT162b2 mRNA vaccine against infection (SIREN): a prospective, multicentre, cohort study. *The Lancet*, 397(10286):1725–1735, 2021.

[114] Muge Cevik, Matthew Tate, Ollie Lloyd, Alberto Enrico Maraolo, Jenna Schafers, and Antonia Ho. SARS-CoV-2, SARS-CoV, and MERS-CoV viral load dynamics, duration of viral shedding, and infectiousness: a systematic review and meta-analysis. *The Lancet Microbe*, 2(1):e13–e22, 2021.

[115] François Blanquart, Clémence Abad, Joevin Ambroise, Mathieu Bernard, Gina Cosentino, Jean-Marc Giannoli, and Florence Débarre. Spread of the delta variant, vaccine effectiveness against PCR-detected infections and within-host viral load dynamics in the community in France. *HAL archives-ouvertes*, 2021.

[116] Stephen M Kissler, Joseph R Fauver, Christina Mack, Caroline G Tai, Mallery I Breban, Anne E Watkins, Radhika M Samant, Deverick J Anderson, Jessica Metti, Gaurav Khullar, , Rachel Baits, Matthew MacKay, Daisy Salgado, Tim Baker, Joel T. Dudley, Christopher E. Mason, David D. Ho, Nathan D. Grubaugh, and Yonatan H. Grad. Viral dynamics of sars-cov-2 variants in vaccinated and unvaccinated persons. *New England Journal of Medicine*, 385(26):2489–2491, 2021.

[117] Katelyn M Gostic, Adam J Kucharski, and James O Lloyd-Smith. Effectiveness of traveller screening for emerging pathogens is shaped by epidemiology and natural history of infection. *eLife*, 4, 2015.

[118] Sarah A Nadeau, Timothy G Vaughan, Jérémie Scire, Jana S Huisman, and Tanja Stadler. The origin and early spread of sars-cov-2 in europe. *Proceedings of the National Academy of Sciences*, 118(9):e2012008118, 2021.

[119] Chad R Wells, Pratha Sah, Seyed M Moghadas, Abhishek Pandey, Affan Shoukat, Yaning Wang, Zheng Wang, Lauren A Meyers, Burton H Singer, and Alison P Galvani. Impact of international travel and border control measures on the global spread of the novel 2019 coronavirus outbreak. *Proceedings of the National Academy of Sciences*, 117(13):7504–7509, 2020.

[120] Katelyn M Gostic, Ana CR Gomez, Riley O Mummah, Adam J Kucharski, and James O Lloyd-Smith. Estimated effectiveness of symptom and risk screening to prevent the spread of covid-19. *eLife*, 9, 2020.

[121] Mary Van Beusekom. Studies trace COVID-19 spread to international flights. https://www.cidrap.umn.edu/covid-19/studies-trace-covid-19-spread-international-flights, September 2020. CIDRAP News.

[122] Aidan Findlater and Isaac I Bogoch. Human mobility and the global spread of infectious diseases: a focus on air travel. *Trends in parasitology*, 34(9):772–783, 2018.

[123] Samuel Clifford, Carl AB Pearson, Petra Klepac, Kevin Van Zandvoort, Billy J Quilty, CMMID COVID-19 working group, Rosalind M Eggo, and Stefan Flasche. Effectiveness of interventions targeting air travellers for delaying local outbreaks of sars-cov-2. *Journal of travel medicine*, 27(5):taaa068, 2020.

[124] Billy J. Quilty, Sam Clifford, CMMID nCoV working Group2, Stefan Flasche, and Rosalind M. Eggo. Effectiveness of airport screening at detecting travellers infected with novel coronavirus (2019-nCoV). *Eurosurveillance*, 25(5):2000080, 2020. Publisher: European Centre for Disease Prevention and Control.

[125] Annelies Wilder-Smith, Kee Tai Goh, and Nicholas I Paton. Experience of severe acute respiratory syndrome in singapore: importation of cases, and defense strategies at the airport. *Journal of Travel Medicine*, 10(5):259–262, 2003.

[126] Gina Samaan, Jenean Spencer, Leslee Roberts, and Mahomed Patel. Border screening for sars in australia: what has been learnt? *Medical journal of Australia*, 180(5):220–223, 2004.

[127] David Mabey, Stefan Flasche, and W. John Edmunds. Airport screening for Ebola. *BMJ (Clinical research ed.)*, 349:g6202, 2014.

[128] Linda A. Selvey, Catarina Antão, and Robert Hall. Evaluation of Border Entry Screening for Infectious Diseases in Humans. *Emerging Infectious Diseases*, 21(2):197–201, 2015.

[129] Nicole J Cohen, Clive M. Brown, Francisco Alvarado-Ramy, Heather Bair-Brake, Gabrielle A. Benenson, Tai-Ho Chen, Andrew J. Demma, N. Kelly Holton, Katrin S. Kohl, Amanda W. Lee, David McAdam, Nicki Pesik, Shahrokh Roohi, C. Lee Smith, Stephen H. Waterman, and Martin S. Cetron. Travel and border health measures to prevent the international spread of Ebola. *Morbidity and Mortality Weekly Report Supplements*, 65(3):57–67, 2016.

[130] Declan Bays, Emma Bennett, and Thomas Finnie. What effect might border screening have on preventing the importation of COVID-19 compared with other infections? A modelling study. *Epidemiology & Infection*, 149:e238, 2021.

[131] CDC Staff. International Travel to and from the United States. https://www.cdc.gov/coronavirus/2019-ncov/travelers/international-travel-during-covid19.html#:~:text=Testing%20%E2%80%93%20ALL%20Travelers&text=result%20before%20travel%3A-,Consider%20getting%20tested%20with%20a%20viral%20test%20as%20close%20to,days%2C%20see%20specific%20testing%20recommendations., 2023.

[132] Aaron J Tande, Matthew J Binnicker, Henry H Ting, Carlos Del Rio, Lindsey Jalil, Matthew Brawner, Peter W Carter, Kathleen Toomey, Nilay D Shah, and Elie F Berbari. Sars-cov-2 testing before international airline travel, december 2020 to may 2021. In *Mayo Clinic Proceedings*, volume 96, pages 2856–2860. Elsevier, 2021.

[133] Remidius Kamuhabwa Kakulu, Esther Gwae Kimaro, and Emmanuel Abraham Mpolya. Effectiveness of point of entry health screening measures among travelers in the detection and containment of the international spread of covid-19: A review of the evidence. *International Journal of Environmental Research and Public Health*, 21(4):410, 2024.

[134] Samuel Clifford, Billy J Quilty, Timothy W Russell, Yang Liu, Yung-Wai D Chan, Carl AB Pearson, Rosalind M Eggo, Akira Endo, Stefan Flasche, W John Edmunds, et al. Strategies to reduce the risk of SARS-CoV-2 importation from international travellers: modelling estimations for the United Kingdom, July 2020. *Eurosurveillance*, 26(39):2001440, 2021.

[135] Mathew V Kiang, Elizabeth T Chin, Benjamin Q Huynh, Lloyd AC Chapman, Isabel Rodríguez-Barraquer, Bryan Greenhouse, George W Rutherford, Kirsten Bibbins-Domingo, Diane Havlir, Sanjay Basu, et al. Routine asymptomatic testing strategies for airline travel during the COVID-19 pandemic: a simulation study. *The Lancet Infectious Diseases*, 21(7):929–938, 2021.

[136] Chad R Wells, Senay Gokcebel, Abhishek Pandey, Alison P Galvani, and Jeffrey P Townsend. Testing for COVID-19 is much more effective when performed immediately prior to social mixing. *International journal of public health*, 67:1604659, 2022.

[137] Michael A Johansson, Hannah Wolford, Prabasaj Paul, Pamela S Diaz, Tai-Ho Chen, Clive M Brown, Martin S Cetron, and Francisco Alvarado-Ramy. Reducing travel-related SARS-CoV-2 transmission with layered mitigation measures: symptom monitoring, quarantine, and testing. *BMC medicine*, 19:1–13, 2021.

[138] Stephen M Bart. Effect of predeparture testing on postarrival SARS-CoV-2–positive test results among international travelers—CDC traveler-based genomic surveillance program, four US airports, March–September 2022. *Morbidity and Mortality Weekly Report*, 72, 2023.

[139] James O Lloyd-Smith, Sebastian J Schreiber, P Ekkehard Kopp, and Wayne M Getz. Superspreading and the effect of individual variation on disease emergence. *Nature*, 438(7066):355–359, 2005.

[140] Christophe Fraser, Steven Riley, Roy M Anderson, and Neil M Ferguson. Factors that make an infectious disease outbreak controllable. *Proceedings of the National Academy of Sciences*, 101(16):6146–6151, 2004.

[141] Casey Middleton and Daniel B Larremore. Modeling the transmission mitigation impact of testing for infectious diseases. *Science Advances*, 10(24):eadk5108, 2024.

[142] Leo LM Poon, Kwok Hung Chan, On Kei Wong, Timothy KW Cheung, Iris Ng, Bojian Zheng, Wing Hong Seto, Kwok Yung Yuen, Yi Guan, and Joseph SM Peiris. Detection of sars coronavirus in patients with severe acute respiratory syndrome by conventional and real-time quantitative reverse transcription-pcr assays. *Clinical chemistry*, 50(1):67–72, 2004.

[143] Peter KC Cheng, Derek A Wong, Louis KL Tong, Sin-Ming Ip, Angus CT Lo, Chi-Shan Lau, Eugene YH Yeung, and Wilina WL Lim. Viral shedding patterns of coronavirus in patients with probable severe acute respiratory syndrome. *The Lancet*, 363(9422):1699–1700, 2004.

[144] Kwok H Chan, Leo LLM Poon, VCC Cheng, Yi Guan, IFN Hung, James Kong, Loretta YC Yam, Wing H Seto, Kwok Y Yuen, and Joseph S Malik Peiris. Detection of sars coronavirus in patients with suspected sars. *Emerging infectious diseases*, 10(2):294, 2004.

[145] Paul KS Chan, Wing-Kin To, King-Cheung Ng, Rebecca KY Lam, Tak-Keung Ng, Rickjason CW Chan, Alan Wu, Wai-Cho Yu, Nelson Lee, David SC Hui, et al. Laboratory diagnosis of sars. *Emerging infectious diseases*, 10(5):825, 2004.

[146] CM Chu, WS Leung, VCC Cheng, KH Chan, AWN Lin, VL Chan, JYM Lam, KS Chan, and KY Yuen. Duration of rt-pcr positivity in severe acute respiratory syndrome. *European Respiratory Journal*, 25(1):12–14, 2005.

[147] Joseph Sriyal Malik Peiris, Chung-Ming Chu, Vincent Chi-Chung Cheng, KS Chan, IFN Hung, Leo LM Poon, Kin-Ip Law, BSF Tang, TYW Hon, CS Chan, et al. Clinical progression and viral load in a community outbreak of coronavirus-associated sars pneumonia: a prospective study. *The Lancet*, 361(9371):1767–1772, 2003.

[148] Rossana C Jaspe, Yoneira Sulbaran, Carmen L Loureiro, Zoila C Moros, Ernestina Marulanda, Francis Bracho, Nieves A Ramírez, Yeilis Canonico, Pierina D'Angelo, Lieska Rodríguez, et al. Detection of the Omicron variant of SARS-CoV-2 in international travelers returning to Venezuela. *Travel Medicine and Infectious Disease*, 48:102326, 2022.

[149] Roy M Anderson, Christophe Fraser, Azra C Ghani, Christl A Donnelly, Steven Riley, Neil M Ferguson, Gabriel M Leung, Tai H Lam, and Anthony J Hedley. Epidemiology, transmission dynamics and control of sars: the 2002–2003 epidemic. *Philosophical Transactions of the Royal Society of London. Series B: Biological Sciences*, 359(1447):1091–1105, 2004.

[150] Aurélien Marc, Marion Kerioui, François Blanquart, Julie Bertrand, Oriol Mitja, Marc Corbacho-Monné, Michael Marks, and Jeremie Guedj. Quantifying the relationship between SARS-CoV-2 viral load and infectiousness. *eLife*, 10:e69302, 2021.

[151] Ruian Ke, Carolin Zitzmann, David D Ho, Ruy M Ribeiro, and Alan S Perelson. In vivo kinetics of SARS-CoV-2 infection and its relationship with a person's infectiousness. *Proceedings of the National Academy of Sciences*, 118(49):e2111477118, 2021.

[152] Mary R Reichler, Dana Bruden, Harold Thomas, Bobbie Rae Erickson, Barbara Knust, Nadia Duffy, John Klena, and Thomas Hennessy. Ebola patient virus cycle threshold and risk of household transmission of Ebola virus. *The Journal of infectious diseases*, 221(5):707–714, 2020.

[153] Lincoln LH Lau, Benjamin J Cowling, Vicky J Fang, Kwok-Hung Chan, Eric HY Lau, Marc Lipsitch, Calvin KY Cheng, Peter M Houck, Timothy M Uyeki, JS Malik Peiris, et al. Viral shedding and clinical illness in naturally acquired influenza virus infections. *The Journal of infectious diseases*, 201(10):1509–1516, 2010.

[154] Andreas Handel and Pejman Rohani. Crossing the scale from within-host infection dynamics to between-host transmission fitness: a discussion of current assumptions and knowledge. *Philosophical Transactions of the Royal Society B: Biological Sciences*, 370(1675):20140302, 2015.

[155] Tim K Tsang, Vicky J Fang, Kwok-Hung Chan, Dennis KM Ip, Gabriel M Leung, JS Malik Peiris, Benjamin J Cowling, and Simon Cauchemez. Individual correlates of infectivity of influenza A virus infections in households. *PloS one*, 11(5):e0154418, 2016.

[156] Bryan Charleston, Bartlomies M Bankowski, Simon Gubbins, Margo E Chase-Topping, David Schley, Richard Howey, Paul V Barnett, Debi Gibson, Nicholas D Juleff, and Mark EJ Woolhouse. Relationship between clinical signs and transmission of an infectious disease and the implications for control. *Science*, 332(6030):726–729, 2011.

[157] Stephen M Kissler, Joseph R Fauver, Christina Mack, Scott W Olesen, Caroline Tai, Kristin Y Shiue, Chaney C Kalinich, Sarah Jednak, Isabel M Ott, Chantal BF Vogels, et al. Viral dynamics of acute sars-cov-2 infection and applications to diagnostic and public health strategies. *PLoS biology*, 19(7):e3001333, 2021.

[158] Corey M Peak, Lauren M Childs, Yonatan H Grad, and Caroline O Buckee. Comparing nonpharmaceutical interventions for containing emerging epidemics. *Proceedings of the National Academy of Sciences*, 114(15):4023–4028, 2017.

[159] James A Hay, Stephen M Kissler, Joseph R Fauver, Christina Mack, Caroline G Tai, Radhika M Samant, Sarah Connolly, Deverick J Anderson, Gaurav Khullar, Matthew MacKay, et al. Quantifying the impact of immune history and variant on sars-cov-2 viral kinetics and infection rebound: A retrospective cohort study. *eLife*, 11:e81849, 2022.

[160] Alexandra B. Hogan, Peter Winskill, Oliver J. Watson, Patrick G. T. Walker, Charles Whittaker, Marc Baguelin, Nicholas F. Brazeau, Giovanni D. Charles, Katy A. M. Gaythorpe, Arran Hamlet, Edward Knock, Daniel J. Laydon, John A. Lees, Alessandra Løchen, Robert Verity, Lilith K. Whittles, Farzana Muhib, Katharina Hauck, Neil M. Ferguson, and Azra C. Ghani. Within-country age-based prioritisation, global allocation, and public health impact of a vaccine against SARS-CoV-2: A mathematical modelling analysis. *Vaccine*, 39(22):2995–3006, 2021.

[161] Lloyd AC Chapman, Poojan Shukla, Isabel Rodríguez-Barraquer, Priya B Shete, Tomás M León, Kirsten Bibbins-Domingo, George W Rutherford, Robert Schechter, and Nathan C Lo. Risk factor targeting for vaccine prioritization during the covid-19 pandemic. *Scientific Reports*, 12(1):3055, 2022.

[162] Sam Moore, Edward M. Hill, Louise Dyson, Michael J. Tildesley, and Matt J. Keeling. Modelling optimal vaccination strategy for SARS-CoV-2 in the UK. *PLOS Computational Biology*, 17(5):e1008849, May 2021. Publisher: Public Library of Science.

[163] David SC Hui and Alimuddin Zumla. Severe acute respiratory syndrome: historical, epidemiologic, and clinical features. *Infectious Disease Clinics*, 33(4):869–889, 2019.

[164] Annelies Wilder-Smith, Monica D Teleman, Bee H Heng, Arul Earnest, Ai E Ling, and Yee S Leo. Asymptomatic SARS coronavirus infection among healthcare workers, Singapore. *Emerging infectious diseases*, 11(7):1142, 2005.

[165] Mary-Anne Hartley, Alyssa Young, Anh-Minh Tran, Harry Henry Okoni-Williams, Mohamed Suma, Brooke Mancuso, Ahmed Al-Dikhari, and Mohamed Faouzi. Predicting Ebola severity: a clinical prioritization score for Ebola virus disease. *PLoS neglected tropical diseases*, 11(2):e0005265, 2017.

[166] Tanja Stadler, Denise Kühnert, David A Rasmussen, and Louis du Plessis. Insights into the early epidemic spread of ebola in sierra leone provided by viral sequence data. *PLoS currents*, 6, 2014.

[167] Gustavo E Velásquez, Omowunmi Aibana, Emilia J Ling, Ibrahim Diakite, Eric Q Mooring, and Megan B Murray. Time from infection to disease and infectiousness for Ebola virus disease, a systematic review. *Clinical Infectious Diseases*, 61(7):1135–1140, 2015.

[168] Jens H Kuhn and Sina Bavari. Asymptomatic Ebola virus infections—myth or reality? *The Lancet Infectious Diseases*, 17(6):570–571, 2017.

[169] Mark G Kortepeter, Daniel G Bausch, and Mike Bray. Basic clinical and laboratory features of filoviral hemorrhagic fever. *The Journal of Infectious Diseases*, 204(suppl_3):S810–S816, 2011.

[170] Luke Hunt, Ankur Gupta-Wright, Victoria Simms, Fayia Tamba, Victoria Knott, Kongoneh Tamba, Saidu Heisenberg-Mansaray, Emmanuel Tamba, Sulaiman Conteh, Tom Smith, et al. Clinical presentation, biochemical, and haematological parameters and their association with outcome in patients with Ebola virus disease: an observational cohort study. *The Lancet Infectious Diseases*, 15(11):1292–1299, 2015.

[171] Pierre Nouvellet, Tini Garske, Harriet L Mills, Gemma Nedjati-Gilani, Wes Hinsley, Isobel M Blake, Maria D Van Kerkhove, Anne Cori, Ilaria Dorigatti, Thibaut Jombart, et al. The role of rapid diagnostics in managing Ebola epidemics. *Nature*, 528(7580):S109–S116, 2015.

[172] Muge Cevik, Matthew Tate, Ollie Lloyd, Alberto Enrico Maraolo, Jenna Schafers, and Antonia Ho. Sars-cov-2, sars-cov, and mers-cov viral load dynamics, duration of viral shedding, and infectiousness: a systematic review and meta-analysis. *The Lancet Microbe*, 2(1):e13–e22, 2021.

[173] Michael K Hourfar, W Kurt Roth, Erhard Seifried, and Michael Schmidt. Comparison of two real-time quantitative assays for detection of severe acute respiratory syndrome coronavirus. *Journal of clinical microbiology*, 42(5):2094–2100, 2004.

[174] IFN Hung, VCC Cheng, AKL Wu, BSF Tang, KH Chan, CM Chu, MML Wong, WT Hui, LLM Poon, DMW Tse, et al. Viral loads in clinical specimens and sars manifestations. *Emerging infectious diseases*, 10(9):1550, 2004.

[175] Wei-Ju Chen, Jyh-Yuan Yang, Jih-Hui Lin, Cathy SJ Fann, Valeriy Osyetrov, Chwan-Chuen King, Yi-Ming Arthur Chen, Hsiao-Ling Chang, Hung-Wei Kuo, Fong Liao, et al. Nasopharyngeal shedding of severe acute respiratory syndrome—associated coronavirus is associated with genetic polymorphisms. *Clinical infectious diseases*, 42(11):1561–1569, 2006.

[176] Christian Drosten, Stephan Günther, Wolfgang Preiser, Sylvie Van Der Werf, Hans-Reinhard Brodt, Stephan Becker, Holger Rabenau, Marcus Panning, Larissa Kolesnikova, Ron AM Fouchier, et al. Identification of a novel coronavirus in patients with severe acute respiratory syndrome. *New England journal of medicine*, 348(20):1967–1976, 2003.

[177] Gabriel M Leung, Anthony J Hedley, Lai-Ming Ho, Patsy Chau, Irene OL Wong, Thuan Q Thach, Azra C Ghani, Christl A Donnelly, Christophe Fraser, Steven Riley, et al. The epidemiology of severe acute respiratory syndrome in the 2003 hong kong epidemic: an analysis of all 1755 patients. *Annals of internal medicine*, 141(9):662–673, 2004.

[178] Christl A Donnelly, Azra C Ghani, Gabriel M Leung, Anthony J Hedley, Christophe Fraser, Steven Riley, Laith J Abu-Raddad, Lai-Ming Ho, Thuan-Quoc Thach, Patsy Chau, et al. Epidemiological determinants of spread of causal agent of severe acute respiratory syndrome in hong kong. *The lancet*, 361(9371):1761–1766, 2003.

[179] Marc Lipsitch, Ted Cohen, Ben Cooper, James M Robins, Stefan Ma, Lyn James, Gowri Gopalakrishna, Suok Kai Chew, Chorh Chuan Tan, Matthew H Samore, et al. Transmission dynamics and control of severe acute respiratory syndrome. *Science*, 300(5627):1966–1970, 2003.

[180] Olha Puhach, Benjamin Meyer, and Isabella Eckerle. SARS-CoV-2 viral load and shedding kinetics. *Nature Reviews Microbiology*, 21(3):147–161, 2023.

[181] Ying Liu, Albert A Gayle, Annelies Wilder-Smith, and Joacim Rocklöv. The reproductive number of covid-19 is higher compared to sars coronavirus. *Journal of travel medicine*, 2020.

[182] Zhanwei Du, Chunyu Wang, Caifen Liu, Yuan Bai, Sen Pei, Dillon C Adam, Lin Wang, Peng Wu, Eric HY Lau, and Benjamin J Cowling. Systematic review and meta-analyses of superspreading of sars-cov-2 infections. *Transboundary and Emerging Diseases*, 69(5):e3007–e3014, 2022.

[183] William S Hart, Sam Abbott, Akira Endo, Joel Hellewell, Elizabeth Miller, Nick Andrews, Philip K Maini, Sebastian Funk, and Robin N Thompson. Inference of the sars-cov-2 generation time using uk household data. *eLife*, 11:e70767, 2022.

[184] Fabrice Carrat, Elisabeta Vergu, Neil M. Ferguson, Magali Lemaitre, Simon Cauchemez, Steve Leach, and Alain-Jacques Valleron. Time lines of infection and disease in human influenza: A review of volunteer challenge studies. *American Journal of Epidemiology*, 167(7):775–785, 2008.

[185] Susan E Sloan, Kristy J Szretter, Bharathi Sundaresh, Kristin M Narayan, Patrick F Smith, David Skurnik, Sylvain Bedard, José M Trevejo, David Oldach, and Zachary Shriver. Clinical and virological responses to a broad-spectrum human monoclonal antibody in an influenza virus challenge study. *Antiviral research*, 184:104763, 2020.

[186] Dennis KM Ip, Lincoln LH Lau, Kwok-Hung Chan, Vicky J Fang, Gabriel M Leung, Malik JS Peiris, and Benjamin J Cowling. The dynamic relationship between clinical symptomatology and viral shedding in naturally acquired seasonal and pandemic influenza virus infections. *Clinical Infectious Diseases*, 62(4):431–437, 2016.

[187] Ashish Goyal, Daniel B Reeves, E Fabian Cardozo-Ojeda, Joshua T Schiffer, and Bryan T Mayer. Viral load and contact heterogeneity predict SARS-CoV-2 transmission and super-spreading events. *eLife*, 10:e63537, 2021.

[188] Dennis E te Beest, Jacco Wallinga, Tjibbe Donker, and Michiel van Boven. Estimating the generation interval of influenza A (H1N1) in a range of social settings. *Epidemiology*, pages 244–250, 2013.

[189] M Jana Broadhurst, Tim JG Brooks, and Nira R Pollock. Diagnosis of Ebola virus disease: past, present, and future. *Clinical microbiology reviews*, 29(4):773–793, 2016.

[190] Daniel S Chertow, Christian Kleine, Jeffrey K Edwards, Roberto Scaini, Ruggero Giuliani, and Armand Sprecher. Ebola virus disease in West Africa—clinical manifestations and management. *New England Journal of Medicine*, 371(22):2054–2057, 2014.

[191] Shevin T Jacob, Ian Crozier, William A Fischer, Angela Hewlett, Colleen S Kraft, Marc-Antoine de La Vega, Moses J Soka, Victoria Wahl, Anthony Griffiths, Laura Bollinger, et al. Ebola virus disease. *Nature reviews Disease primers*, 6(1):13, 2020.

[192] Simone Lanini, Gina Portella, Francesco Vairo, Gary P Kobinger, Antonio Pesenti, Martin Langer, Soccoh Kabia, Giorgio Brogiato, Jackson Amone, Concetta Castilletti, et al. Blood kinetics of Ebola virus in survivors and nonsurvivors. *The Journal of clinical investigation*, 125(12):4692–4698, 2015.

[193] Jonathan S Towner, Pierre E Rollin, Daniel G Bausch, Anthony Sanchez, Sharon M Crary, Martin Vincent, William F Lee, Christina F Spiropoulou, Thomas G Ksiazek, Mathew Lukwiya, et al. Rapid diagnosis of Ebola hemorrhagic fever by reverse transcription-PCR in an outbreak setting and assessment of patient viral load as a predictor of outcome. *Journal of virology*, 78(8):4330–4341, 2004.

[194] M Jeremiah Matson, Emily Ricotta, Friederike Feldmann, Moses Massaquoi, Armand Sprecher, Ruggero Giuliani, Jeffrey K Edwards, Kyle Rosenke, Emmie de Wit, Heinz Feldmann, et al. Evaluation of viral load in patients with Ebola virus disease in Liberia: a retrospective observational study. *The Lancet Microbe*, 3(7):e533–e542, 2022.

[195] Manuel Schibler, Pauline Vetter, Pascal Cherpillod, Tom J Petty, Samuel Cordey, Gaël Vieille, Sabine Yerly, Claire-Anne Siegrist, Kaveh Samii, Julie-Anne Dayer, et al. Clinical features and viral kinetics in a rapidly cured patient with Ebola virus disease: a case report. *The Lancet Infectious Diseases*, 15(9):1034–1040, 2015.

[196] Maria D Van Kerkhove, Ana I Bento, Harriet L Mills, Neil M Ferguson, and Christl A Donnelly. A review of epidemiological parameters from Ebola outbreaks to inform early public health decision-making. *Scientific data*, 2(1):1–10, 2015.

[197] WHO Ebola Response Team. West African Ebola epidemic after one year—slowing but not yet under control. *New England Journal of Medicine*, 372(6):584–587, 2015.

[198] David Fisman, Edwin Khoo, and Ashleigh Tuite. Early epidemic dynamics of the West African 2014 Ebola outbreak: estimates derived with a simple two-parameter model. *PLoS currents*, 6, 2014.

[199] Marcelo FC Gomes, Ana Pastore y Piontti, Luca Rossi, Dennis Chao, Ira Longini, M Elizabeth Halloran, and Alessandro Vespignani. Assessing the international spreading risk associated with the 2014 West African Ebola outbreak. *PLoS currents*, 6, 2014.

[200] Christian L Althaus. Estimating the reproduction number of Ebola virus (EBOV) during the 2014 outbreak in West Africa. *PLoS currents*, 6, 2014.

Appendix A

Supplementary Materials to Chapter 4

A.0.1 Viral load parameterization

Table A.2 contains all of the parameter values and distributions used to simulate infected travelers for each pathogen. For each parameter that is treated as a random variable, we used the reported distribution when reported in the literature. If we could not find a reported distribution, we used a truncated normal when a mean and standard deviation were reported, truncated either at the lowest and highest reported values or within a reasonable range that captured the vast majority of measurements. If mean and SD were not reported, then we used a uniform distribution within a reasonable range that captured the vast majority of measurements. We used the serial interval as an approximation for the generation interval when generation interval estimates were not available. Examples of 100 simulated viral load trajectories for these four pathogens are shown in Supp. Fig. A.13. We chose the lowest reported PCR limit of detection, since this corresponds to a best case scenario for testing. Below we elaborate on specific assumptions and rationale for each pathogen.

A.0.1.1 SARS-CoV-1

We assumed that all the cases are hospitalized. This is appropriate because hospitalization rates for symptomatic SARS-CoV-1 were high and, while estimates of asymptomatic infections vary from 0.1% [163] to 13% [164], there is no known transmission from asymptomatic patients so we do not consider them in our analyses [164]. We chose the distribution uniform(0,9) days post symptom onset as an optimistic guess

for the time first detectable by PCR. This range was chosen based off data that reported 50-80% did not test positive via PCR in initial days post symptom onset [142–147], >50% were positive by day 6-7 [143, 144], and >95% are PCR positive by day 10 [147]. Although not necessary for the model, we also parameterized individuals' time of symptom onset since other parameters were measured in units of the time since symptom onset.

A.0.1.2 SARS-CoV-2

We parameterized the model for the ancestral strain of SARS-CoV-2. Many of the parameters needed for our model are well characterized by Kissler et. al. [157]. We did not distinguish between symptomatic and asymptomatic cases, nor did we include hospitalization.

A.0.1.3 Influenza A

We parameterized the model for influenza A. The majority of references reported data from influenza H1N1 subtype, a few from influenza H3N2, and some simply referenced influenza A without specifying the subtype. We did not distinguish between symptomatic and asymptomatic cases, nor did we include hospitalization.

A.0.1.4 Ebola

For Ebola, higher viral load is correlated with mortality [165]. We parameterized the model for non-fatal cases assuming they would be more likely to travel and assumed all such cases are hospitalized. Although not necessary for the model, we parameterized individuals' time of dry and wet symptom onset since other parameters were measured in units of the time since symptom onset. Note that the model parameters are not as well characterized for Ebola as other pathogens, possibly because the incubation and infectious periods are highly variable [166].

Our model of infectiousness implicitly assumes that we are only considering direct transmission via fomites, droplets, or aerosols [167], and not post-mortem transmission. Thus, we did not consider asymp-

tomatic cases because they would not have transmission potential, and asymptomatic cases are rare [168].

We chose the distribution uniform(0, 3) days post onset of dry symptoms as an optimistic guess for the time first detectable by PCR. This range implies that individuals are sometimes detectable when they have dry symptoms, and everyone is detectable by the time their symptoms progress to wet symptoms. This was informed by the notion that there is no evidence that infected people are viremic before symptom onset, but some are PCR positive on the day of illness onset [169]. Additionally, most are detectable by the time they are hospitalized (87% [170]).

Note that viral load measurements are measured in mL of serum. This is appropriate for our model, since RDTs that could potentially be used for airport screening can collect a blood sample through a finger prick [171].

	$\mathbb{P}(\Delta N \geq x)$			$\mathbb{P}(\Delta t \geq x)$		
x	7 days	14 days	21 days	1 person	10 people	20 people
SARS-CoV-1	0.014	0.001	0	0.055	0.001	0
SARS-CoV-2	0.234	0.037	0.004	0.567	0.026	0
Influenza A	0.576	0.289	0.149	0.998	0.728	0.248
Ebola	0.093	0.078	0.061	0.350	0.006	0

Table A.1: **Examples of the CCDF $\mathbb{P}(X \geq x)$ for screening effectiveness ΔN and Δt.** For Δt, we used the same scenarios as the main text where $X = 100, \lambda = 1$ for SARS-Cov-1, SARS-CoV-2 and influenza A, and $X = 1, \lambda = 1/14$ for Ebola.

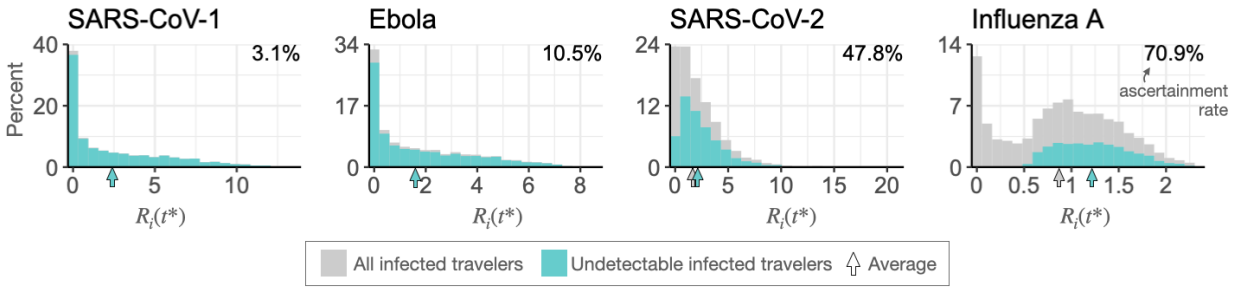

Figure A.1: **Traveler screening programs decrease the number of infected travelers reaching the destination, but the average imported case has more transmission potential than without screening.** Histograms of simulated infected travelers' transmission potential at the destination, $R_i(t^*)$, with all 5,000 travelers shown in gray and undetectable travelers in teal. Vertical arrows indicate the mean of each distribution. The means overlap for SARS-CoV-1 and Ebola. Ascertainment rates are reported in each upper right corner.

Pathogen	Parameter	Value/Distribution	Units	Source
SARS-CoV-1	time first detectable	Unif(0,9)	days from SO	[142–147]
	time of peak VL	Unif(7, 14)	days from SO	[143, 147, 149, 172]
	time last detectable	Unif(18, 28)	days from SO	[143, 144, 147]
	PCR LOD	2.6	log10 copies/mL	[173]
	infectious threshold	6.5	log10 copies/mL	See Methods
	peak VL	Unif(5.8, 8.5)	log10 copies/mL	[147, 174–176]
	time to symptoms	Unif(2,10)	days from infection	[177, 178]
	time to hospitalization	Trunc. normal ($\mu = 2.9$, $\sigma = 2.6, a = -1, b = 9$)	days from SO	[177]
	R_0	2.55	/	[139]
	k	0.21	/	[139]
	generation interval	8.4	days	[179]
SARS-CoV-2 (ancestral)	time first detectable	Unif(2.6, 3.8)	days since infection	[180]
	time of peak VL	Γ(shape=2.3, rate=0.7)	days from first detect.	[157]
	time last detectable	Γ(shape=2.4, rate=0.3)	days from peak	[157]
	PCR LOD	40	CT	[157]
	infectious threshold	5	log10 copies/mL	[**?**, 157]
	peak VL	Normal($\mu = 22.3, \sigma = 4.2$)	CT	[157]
	R_0	2.8	/	[181]
	k	0.55	/	[182]
	generation interval	5.9	days	[183]
Influenza A	time first detectable	Unif(0.5, 1.5)	days from infection	[184, 185]
	time of peak VL	Unif(1, 3)	days from first detect.	[184–186]
	time last detectable	Unif(2, 3)	days from peak	[184–186]
	PCR LOD	2.95	log10 copies/mL	[186]
	infectious threshold	4	log10 copies/mL	[153]
	peak VL	Unif(6, 8.5)	log10 copies/mL	[186]
	R_0	1.26	/	[187]
	k	2.36	/	[187]
	generation interval	2.6	days	[188]
Ebola	time first detectable	Unif(0, 3)	days from SO	[189–191]
	time of peak VL	Unif(3, 6)	days from SO	[192–195]
	time last detectable	Trunc. normal(μ = 12.7, $\sigma = 3.8, a = 9, b = 16.5$)	days from SO	[192]
	PCR LOD	2.7	log10 copies/mL	[194]
	infectious threshold	7	log10 copies/mL	See Methods
	peak VL	Unif(6.5, 9.2)	log10 copies/mL	[192, 193, 195]
	time to dry symptoms	Unif(5, 13)	days from infection	[196, 197]
	time to wet symptoms	Unif(3, 5)	days from SO	[190]
	time to hospitalization	Trunc. normal(μ = 4.5, $\sigma = 2.5, a = 2, b = 7$)	days from SO	[192]
	R_0	1.8	/	[198–200]
	k	0.18	/	[200]
	generation interval	13	days	[197]

Table A.2: **Model parameters.** Values or distributions used for each pathogen-specific parameter. SO stands for symptom onset.

Influenza A							
	Arrival rate (λ)	Outbreak threshold (X)	N_0 or t_0	N' or t'	ΔN or Δt		% of simulations where Δt > 1 week
			Mean (sd)	Mean (sd)	Average	IQR	
Number required to attempt travel to							
Likely trigger an outbreak (theory)	/	/	9.9 (2)	24.7 (8.2)	14.8	[9,19]	/
Generate a secondary case at the destination (simulation)	/	/	1.9 (1.3)	4.9 (4.4)	3	[0, 5]	/
Time to X infections generated at the destination (simulation)	1 per day	1	3.2 (2.1)	7 (5)	3.9	[0, 5.9]	19.8%
		10	8.1 (3.2)	15.1 (7.8)	6.9	[2.2, 9.6]	36.1%
		100	20.2 (5.3)	31.6 (11.7)	11.4	[4.2, 15.6]	57.6%
	1 per week	1	14.7 (13.4)	36.7 (34.7)	22	[0, 32.4]	51.4%
		10	30.8 (22.3)	68.2 (56.1)	37.4	[0.1, 56.0]	58.8%
		100	28.3 (27.2)	71.3 (69.1)	43	[2.6, 71.6]	56.4%
	2 per month	1	28.3 (27.2)	71.3 (69.1)	43	[0, 61.7]	56.4%
		10	54.9 (45.1)	128.4 (113)	73.5	[0, 109.2]	61.2%
		100	89.3 (64)	185 (158.3)	95.8	[0, 136.3]	61.1%

Figure A.2: **Screening effectiveness for influenza A.** Screening effectiveness ΔN and Δt for a range of scenarios. The gray row is the plausible example reported in the Main Text.

SARS-CoV-2							
	Arrival rate (λ)	Outbreak threshold (X)	N_0 or t_0	N' or t'	ΔN or Δt		% of simulations where Δt > 1 week
			Mean (sd)	Mean (sd)	Average	IQR	
Number required to attempt travel to							
Likely trigger an outbreak (theory)	/	/	3.1 (1.5)	5.2 (3.1)	2.1	[0, 3]	/
Generate a secondary case at the destination (simulation)	/	/	1.5 (0.9)	2.5 (2)	1	[0, 1]	/
Time to X infections generated at the destination (simulation)	1 per day	1	4.6 (2.5)	7 (2.7)	2.4	[0, 5.0]	11.6%
		10	8 (3)	12 (4)	4	[0.6, 5.9]	18.1%
		100	17.4 (3.5)	22.2 (4.7)	4.8	[1.5, 6.7]	23.4%
	1 per week	1	13.6 (10.7)	22.3 (18)	8.6	[0, 11.8]	33.1%
		10	23.4 (13.9)	34.3 (22.6)	10.9	[0, 14.5]	35.6%
		100	35.7 (14.9)	47.3 (23.7)	11.6	[0, 15.4]	36.6%
	2 per month	1	24.1 (21)	39.8 (35.4)	15.7	[0, 20.5]	36.3%
		10	37.3 (26.6)	57.2 (44.8)	19.9	[0, 25.3]	37.8%
		100	51.2 (28.6)	71.6 (46.3)	20.4	[0, 26.1]	38.7%

Figure A.3: **Screening effectiveness for SARS-CoV-2.** Screening effectiveness ΔN and Δt for a range of scenarios. The gray row is the plausible example reported in the Main Text.

Ebola with infectious threshold = 7 (value used in the main text)							
	Arrival rate (λ)	Outbreak threshold (X)	N_0 or t_0	N' or t'	ΔN or Δt		% of simulations where Δt > 1 week
			Mean (sd)	Mean (sd)	Average	IQR	
Number required to attempt travel to							
Likely trigger an outbreak (theory)	/	/	9.5 (3.4)	10.6 (3.9)	1.1	[0, 1]	/
Generate a secondary case at the destination (simulation)	/	/	1.9 (1.3)	2.1 (1.5)	0.2	[0, 0]	/
Time to X infections generated at the destination (simulation)	1 per day	1	10.1 (4.1)	11 (3.8)	0.9	[0, 0]	6.8%
		10	14.6 (4.5)	16.1 (4.7)	1.5	[0, 1.8]	6.7%
		100	36.5 (6.7)	38.8 (7.2)	2.3	[0, 3.3]	10.2%
	1 per week	1	21.6 (13.8)	23.8 (15.1)	2.1	[0, 0]	9.1%
		10	41.7 (21.6)	45.4 (23.8)	3.7	[0, 0]	14.1%
		100	84.8 (34.8)	90 (38)	5.2	[0, 0]	15.7%
	2 per month	1	34.7 (26.6)	38.3 (29.6)	3.5	[0, 0]	9.2%
		10	68.1 (43.3)	74.3 (48.2)	6.2	[0, 0]	13.7%
		100	122.5 (66.3)	130.8 (73.3)	8.3	[0, 0]	14.4%

Figure A.4: **Screening effectiveness for Ebola.** Screening effectiveness ΔN and Δt for a range of scenarios. The gray row is the plausible example reported in the Main Text.

SARS-CoV-1 with infectious threshold = 6.5 (value used in main text)							
	Arrival rate (λ)	Outbreak threshold (X)	N_0 or t_0	N' or t'	ΔN or Δt		% of simulations where Δt > 1 week
			Mean (sd)	Mean (sd)	Average	IQR	
Number required to attempt travel to							
Likely trigger an outbreak (theory)	/	/	4.7 (2.6)	4.9 (2.7)	0.2	[0, 0]	/
Generate a secondary case at the destination (simulation)	/	/	1.9 (1.3)	1.9 (1.3)	0.1	[0, 0]	/
Time to X infections generated at the destination (simulation)	1 per day	1	7.5 (3)	7.7 (3)	0.2	[0, 0]	1.4%
		10	10.4 (3.8)	10.8 (3.8)	0.3	[0, 0]	1.4%
		100	23.1 (4.8)	23.6 (4.9)	0.5	[0, 0]	1.4%
	1 per week	1	18.7 (13.2)	19.2 (13.6)	0.5	[0, 0]	2.5%
		10	30.2 (18)	31 (18.5)	0.8	[0, 0]	3.4%
		100	50 (21.8)	50.9 (22.3)	0.9	[0, 0]	3.6%
	2 per month	1	31.7 (25.9)	32.5 (26.6)	0.8	[0, 0]	2.6%
		10	50 (36)	51.4 (37.2)	1.4	[0, 0]	3.5%
		100	72.1 (41.2)	73.6 (42.4)	1.5	[0, 0]	3.6%

Figure A.5: **Screening effectiveness for SARS-CoV-1.** Screening effectiveness ΔN and Δt for a range of scenarios. The gray row is the plausible example reported in the Main Text.

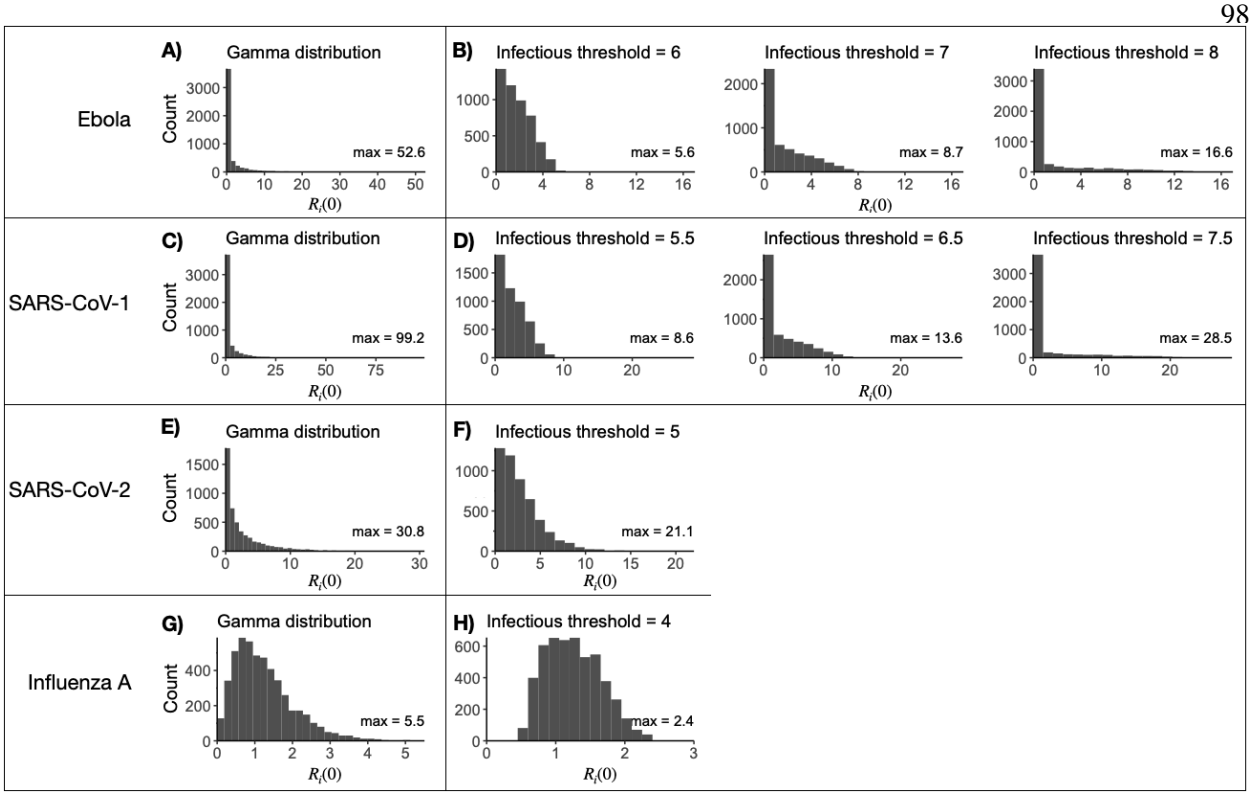

Figure A.6: **Different approaches to calculate the individual reproductive number $R_i(0)$ result in important differences in the population-level distributions of $R_i(0)$.** (A, C, E, G) Distribution of the individual reproductive number $R_i(0)$ sampled from a gamma distribution with mean R_0 and dispersion parameter k. (B, D, F, H) Distribution of $R_i(0)$ from the within-host viral kinetics model with various infectious thresholds.

Ebola with infectious threshold = 6							
	Arrival rate (λ)	Outbreak threshold (X)	N_0 or t_0	N' or t'	ΔN or Δt		% of simulations where Δt > 1 week
			Mean (sd)	Mean (sd)	Average	IQR	
Number required to attempt travel to							
Likely trigger an outbreak (theory)	/	/	9.1 (2)	10 (2.5)	0.9	[0, 1]	/
Generate a secondary case at the destination (simulation)	/	/	1.4 (0.8)	1.6 (1)	0.2	[0, 0]	/
Time to X infections generated at the destination (simulation)	1 per day	1	9.7 (3.9)	10.5 (3.5)	0.8	[0, 0]	6.4%
		10	14.3 (3.7)	15.8 (3.8)	1.5	[0, 2.1]	4.9%
		100	36.1 (5.9)	38.5 (6.4)	2.3	[0, 3.4]	9.5%
	1 per week	1	18.2 (10.6)	19.9 (11.4)	1.7	[0, 0]	8.4%
		10	39.5 (17.8)	42.8 (19.6)	3.3	[0, 0]	14.5%
		100	82.4 (31.2)	87.6 (34.6)	5.1	[0, 0.4]	16.7%
	2 per month	1	27.9 (20.1)	30.7 (22.1)	2.8	[0, 0]	9.2%
		10	61.9 (35.4)	67.2 (39)	5.3	[0, 0]	15.1%
		100	117.7 (59.8)	125.6 (66)	7.9	[0, 0]	14.9%

Figure A.7: **Screening effectiveness for Ebola with a lower infectious threshold.** Screening effectiveness ΔN and Δt for a range of scenarios. The infectious threshold is 6 log10 copies RNA/mL. An infectious threshold of 7 log10 copies RNA/mL was used in the Main Text.

Ebola with infectious threshold = 8							
	Arrival rate (λ)	Outbreak threshold (X)	N_0 or t_0	N' or t'	ΔN or Δt		% of simulations where Δt > 1 week
			Mean (sd)	Mean (sd)	Average	IQR	
Number required to attempt travel to							
Likely trigger an outbreak (theory)	/	/	10.6 (5.8)	11.8 (6.5)	1.1	[0, 0]	/
Generate a secondary case at the destination (simulation)	/	/	3.1 (2.6)	3.4 (2.9)	0.3	[0, 0]	/
Time to X infections generated at the destination (simulation)	1 per day	1	11.5 (4.8)	12.4 (4.7)	0.9	[0, 0]	6.8%
		10	15.5 (6.1)	16.9 (6.4)	1.5	[0, 0]	8.2%
		100	37.2 (8.3)	39.4 (8.9)	2.2	[0, 2.9]	11.5%
	1 per week	1	30.2 (22)	33.1 (24)	2.9	[0, 0]	9.1%
		10	48.3 (31.3)	52.6 (34.8)	4.2	[0, 0]	11.6%
		100	90.7 (42.6)	96.4 (46.9)	5.7	[0, 0]	14.3%
	2 per month	1	52.3 (44.1)	57.5 (48.8)	5.2	[0, 0]	9.2%
		10	82.2 (62.1)	89.6 (68.7)	7.3	[0, 0]	11.4%
		100	135.9 (82.1)	145.6 (90.7)	9.7	[0, 0]	13.1%

Figure A.8: **Screening effectiveness for Ebola with a higher infectious threshold.** Screening effectiveness ΔN and Δt for a range of scenarios. The infectious threshold is 8 log10 copies RNA/mL. An infectious threshold of 7 log10 copies RNA/mL was used in the Main Text.

SARS-CoV-1 with infectious threshold = 5.5							
	Arrival rate (λ)	Outbreak threshold (X)	N_0 or t_0	N' or t'	ΔN or Δt		% of simulations where Δt > 1 week
			Mean (sd)	Mean (sd)	Average	IQR	
Number required to attempt travel to							
Likely trigger an outbreak (theory)	/	/	4.3 (1.5)	4.4 (1.6)	0.1	[0, 0]	/
Generate a secondary case at the destination (simulation)	/	/	1.3 (0.6)	1.4 (0.7)	0	[0, 0]	/
Time to X infections generated at the destination (simulation)	1 per day	1	6.9 (2.7)	7.1 (2.6)	0.2	[0, 0]	1.1%
		10	10.2 (3)	10.4 (3)	0.3	[0, 0]	0.5%
		100	22.9 (4.1)	23.2 (4.2)	0.4	[0, 0]	0.7%
	1 per week	1	14.9 (9.6)	15.3 (9.8)	0.4	[0, 0]	1.9%
		10	27.8 (14.2)	28.4 (14.5)	0.6	[0, 0]	2.7%
		100	27.8 (14.2)	28.4 (14.5)	0.7	[0, 0]	3%
	2 per month	1	24.2 (18.6)	24.8 (19.1)	0.6	[0, 0]	2.2%
		10	43.5 (28.1)	44.5 (28.9)	1	[0, 0]	3.3%
		100	66.9 (35)	67.9 (35.7)	1	[0, 0]	3%

Figure A.9: **Screening effectiveness for SARS-CoV-1 with a lower infectious threshold.** Screening effectiveness ΔN and Δt for a range of scenarios. The infectious threshold is 5.5 log10 copies RNA/mL. An infectious threshold of 6.5 log10 copies RNA/mL was used in the Main Text.

SARS-CoV-1 with infectious threshold = 7.5							
	Arrival rate (λ)	Outbreak threshold (X)	N_0 or t_0	N' or t'	ΔN or Δt		% of simulations where Δt > 1 week
			Mean (sd)	Mean (sd)	Average	IQR	
Number required to attempt travel to							
Likely trigger an outbreak (theory)	/	/	6.2 (4.9)	6.4 (5.1)	0.2	[0,0]	/
Generate a secondary case at the destination (simulation)	/	/	3.4 (2.9)	3.5 (3)	0.1	[0,0]	/
Time to X infections generated at the destination (simulation)	1 per day	1	9.1 (4.2)	9.3 (4.2)	0.2	[0,0]	1.55%
		10	11.5 (5.5)	11.8 (5.6)	0.3	[0,0]	1.54%
		100	23.9 (6.5)	24.3 (6.7)	0.3	[0,0]	1.52%
	1 per week	1	30 (24.4)	30.8 (25)	0.7	[0,0]	2.26%
		10	39.7 (30.2)	40.5 (30.9)	0.8	[0,0]	2.39%
		100	58.5 (32.1)	59.5 (33)	1	[0,0]	2.94%
	2 per month	1	54 (48.4)	55.4 (49.4)	1.3	[0,0]	2.36%
		10	70.7 (58.9)	72.5 (60.5)	1.8	[0,0]	2.83%
		100	91.7 (63.8)	93.2 (65)	1.5	[0,0]	2.5%

Figure A.10: **Screening effectiveness for SARS-CoV-1 with a higher infectious threshold.** Screening effectiveness ΔN and Δt for a range of scenarios. The infectious threshold is 7.5 log10 copies RNA/mL. An infectious threshold of 6.5 log10 copies RNA/mL was used in the Main Text.

Ebola with infectious threshold = 7 (value used in the main text), D = t_clearance							
	Arrival rate (λ)	Outbreak threshold (X)	N_0 or t_0	N' or t'	ΔN or Δt		% of simulations where Δt > 1 week
			Mean (sd)	Mean (sd)	Average	IQR	
Number required to attempt travel to							
Likely trigger an outbreak (theory)	/	/	11.6 (4.3)	13.9 (5.5)	2.3	[0, 4]	/
Generate a secondary case at the destination (simulation)	/	/	2.2 (1.7)	2.7 (2.1)	0.5	[0, 0]	/
Time to X infections generated at the destination (simulation)	1 per day	1	9.5 (4.5)	11.1 (4.2)	1.6	[0, 0]	12.1%
		10	15 (5.2)	17.6 (5.7)	2.6	[0, 4.2]	13.9%
		100	38.5 (7.7)	42.6 (8.9)	4.1	[0, 6.4]	22.2%
	1 per week	1	23.2 (16.3)	27.5 (19.1)	4.3	[0, 0]	15.7%
		10	46.5 (26)	53.8 (31.3)	7.3	[0, 4.8]	22.9%
		100	92.5 (41.5)	103.1 (49.9)	10.5	[0, 7.6]	25.4%
	2 per month	1	38.7 (31.7)	46.6 (38.7)	7.9	[0, 0]	16.5%
		10	76.8 (52.1)	89.2 (62.4)	12.4	[0, 1.5]	22.4%
		100	137.1 (79.3)	154.2 (93.8)	17.1	[0, 2.9]	23.2%

Figure A.11: **Screening effectiveness ΔN and Δt for Ebola, assuming people travel until viral clearance.** Screening effectiveness ΔN and Δt for a range of scenarios. In the Main Text, we assumed people traveled up until the time they hospitalized.

SARS-CoV-1 with infectious threshold = 6.5 (value used in main text), D = t_clearance							
	Arrival rate (λ)	Outbreak threshold (X)	N_0 or t_0	N' or t'	ΔN or Δt		% of simulations where Δt > 1 week
			Mean (sd)	Mean (sd)	Average	IQR	
Number required to attempt travel to							
Likely trigger an outbreak (theory)	/	/	5.7 (3.2)	7.6 (4.6)	1.9	[0,3]	/
Generate a secondary case at the destination (simulation)	/	/	2.1 (1.5)	2.9 (2.3)	0.8	[0,1]	/
Time to X infections generated at the destination (simulation)	1 per day	1	5.2 (3.6)	7 (4)	1.8	[0, 0.5]	12.5
		10	8.6 (4.1)	11.3 (5)	2.7	[0, 4.5]	14.5
		100	22 (5.3)	25.8 (6.5)	3.8	[0, 6.0]	20.5
	1 per week	1	18.1 (15.3)	24.3 (20.6)	6.2	[0, 1.2]	21.9
		10	31.1 (21.2)	39.6 (28)	8.5	[0, 8.4]	27.5
		100	51.7 (25)	61.4 (32.6)	9.7	[0, 8.4]	28.2
	2 per month	1	32.8 (29.9)	44.3 (40.5)	11.5	[0, 4.1]	23.6
		10	52.9 (41)	68.9 (55.4)	16	[0, 8.4]	28.7
		100	76.7 (48.1)	94.3 (63.5)	17.6	[0, 8.4]	28.4

Figure A.12: **Screening effectiveness ΔN and Δt for SARS-CoV-1 assuming people travel until viral clearance.** In the Main Text, we assumed people traveled up until the time they hospitalized.

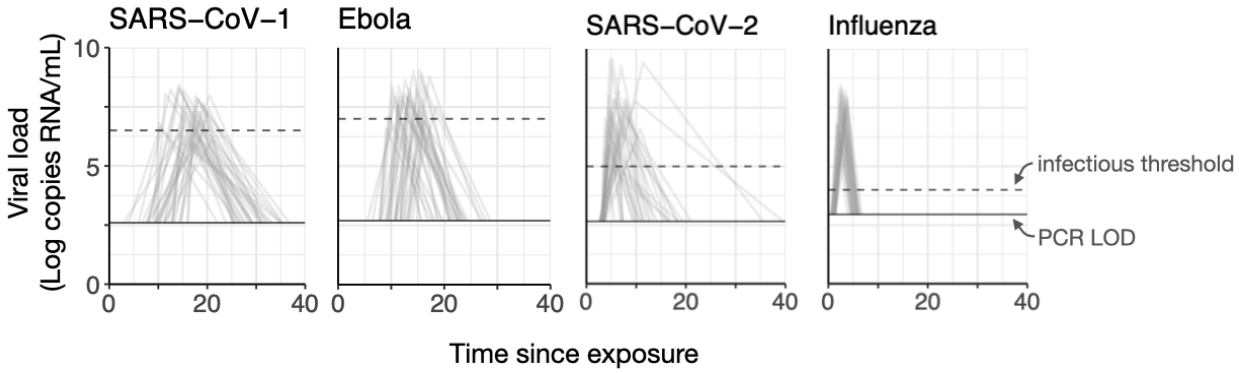

Figure A.13: **Simulated viral load trajectories for SARS-CoV-1, Ebola, SARS-CoV-2 and influenza A.** 100 stochastically drawn viral load trajectories for SARS-CoV-1, Ebola, SARS-CoV-2, and influenza A, using the control points and parameter values in Table A.2.